IS-3900

1975 ANNUAL SUMMARY REPORT

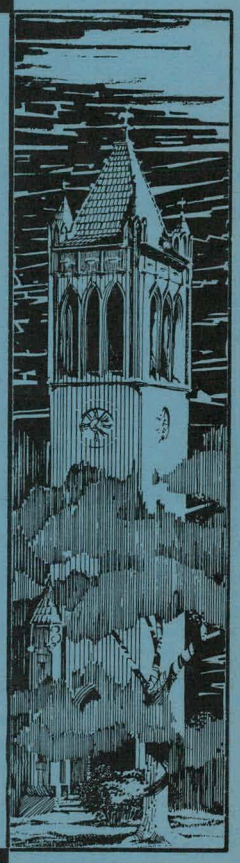

AMES LABORATORY USERDA

Iowa State University
Ames, Iowa

SEPTEMBER 1976

DISCLAIMER

Available from: National Technical Information Service
U. S. Department of Commerce
P.O. Box 1553
Springfield, VA 22161

Price: Microfiche $2.25
Paper Copy $6.00

Distribution Category UC-2

IS-3900

General, Miscellaneous, and Progress Reports (TID-4500)

1975 ANNUAL SUMMARY REPORT

HIGH ENERGY PHYSICS
NUCLEAR SCIENCES
MATERIALS SCIENCE
MOLECULAR SCIENCES

Ames Laboratory, USERDA
Iowa State University
Ames, Iowa 50011

Date Published: September 1976

Prepared for the
U. S. Energy Research and Development Administration
under Contract No. W-7405-eng-82

THIS PAGE

WAS INTENTIONALLY

LEFT BLANK

PHYSICAL RESEARCH

FOREWORD

This report consists of collections of abstracts of papers published during the previous calendar year in the areas of high energy physics, nuclear sciences, materials science and molecular sciences. These are arranged in accordance with the project titles used in the ERDA Schedule 189 Budget Proposals. The collection of abstracts therefore supplements the listing of papers published in the Schedule 189.

Recent reports in this series are:

IS-1600	IS-2600
IS-1900	IS-2800
IS-2100	IS-3300
IS-2300	IS-3500

IS-3700

CONTENTS

EC-01

HIGH ENERGY PHYSICS

Experimental

OBSERVATION OF INCREASING CHARGED MULTIPLICITY AS A FUNCTION OF TRANSVERSE MOMENTUM IN $p + p \rightarrow \pi^+ + MM$ AT 28.5 GeV/c
E. W. Anderson, T. S. Clifford, G. P. Fisher, G. P. Larson, E. Lazarus, K. M. Moy, F. Turkot, P. Schübelin, W. N. Schreiner, L. von Lindern, L. J. Gutay, A. Laasanen, G. B. Collins, J. R. Ficenec, D. R. Gilbert, B. C. Stringfellow, and W. P. Trower
Phys. Rev. Lett. 34, 294 (1975)

Abstract--We have measured the mean charged multiplicity $\bar{n}_c$ as a function of the transverse momentum $p_\perp$ of a forward π^+ meson for fixed missing mass MM in the reaction $p + p \rightarrow \pi^+ + MM$ using the multiparticle Argo spectrometer system. We observe an increase similar to that seen in $p + p \rightarrow p + MM$ at the same incident energy.

STUDY OF THE ENERGY AND CHARGED MULTIPLICITY DEPENDENCE OF INCLUSIVE π^- PRODUCTION IN $\pi^- p$ INTERACTIONS UP TO FERMILAB ENERGIES
W. Morris, B. Y. Oh, D. L. Parker, G. A. Smith, J. Whitmore, L. Voyvodic, R. Walker, R. Yaari, E. W. Anderson, H. B. Crawley, W. J. Kernan, F. Ogino, R. G. Glasser, D. G. Hill, G. McClellan, H. L. Price, B. Sechi-Zorn, G. A. Snow, F. Svrcek, W. D. Shephard, J. M. Bishop, N. N. Biswas, N. M. Cason, E. D. Fokitis and V. P. Kenney
Phys. Lett. 56B, 395 (1975)

Abstract--Using new data from 100 GeV/c $\pi^- p$ interactions, we find the energy dependence of the invariant cross-section in the target fragmentation (central) region to be consistent with an $A + Bs^{-1/2}(C + Ds^{-1/4})$ behavior. The leading particle peak near $x = +1$ exhibits a width in x which becomes smaller with increasing energy and an integrated cross section which is approximately energy independent.

TWO PARTICLE CORRELATIONS IN THE CENTRAL REGION OF pp AND π^-p INTERACTIONS AT 100-300 GeV/c

B. Y. Oh, W. Morris, D. L. Parker, G. A. Smith, J. Whitmore, R. J. Miller, J. J. Phelan, P. F. Schultz, L. Voyvodic, R. Walker, R. Yaari, E. W. Anderson, H. B. Crawley, W. J. Kernan, F. Ogino, R. G. Glasser, D. G. Hill, G. McClellan, H. L. Price, B. Sechi-Zorn, G. A. Snow and F. Svrcek

Phys. Lett. 56B, 400 (1975)

Abstract--Significant positive correlations are seen for all charge combinations of pion pairs with small rapidity separation. Joint rapidity-azimuthal correlations show that this positive correlation occurs when like (unlike) pions are produced with small (large) separation in azimuth.

CHARGED-PARTICLE MULTIPLICITY DISTRIBUTION IN pd INTERACTIONS AT 300 GeV/c

A. Sheng, A. Firestone, C. Peck, A. Dzierba, E. W. Anderson, H. B. Crawley, W. J. Kernan, J. Canter, F. T. Dao, A. Mann, J. Schneps, J. Poucher and S. Stone

Phys. Rev. D 12, 1219 (1975)

Abstract--Charged-particle multiplicity distributions in 300-GeV/c pd interactions have been determined from an exposure of the Fermi National Accelerator Laboratory 30-in. bubble chamber. The data show clear evidence for double scattering inside the deuterium nucleus. We have been able to correct for the effects of the second scatters using a simple semiempirical model. The resulting pp multiplicity distribution is in excellent agreement with the pp data obtained from a p-H_2 experiment at the same energy. The pn multiplicity distribution appears to be shifted from the pp distribution with $\langle n_c \rangle_{pn} = 7.84 \pm 0.17$.

PION DISTRIBUTIONS IN HIGHLY INELASTIC $pp \rightarrow p\pi X$ AT 28.5 GeV/c AND COMPARISONS WITH $ep \rightarrow e\pi X$

E. W. Anderson, T. S. Clifford, E. Lazarus, W. N. Schreiner, P. Schübelin, F. Turkot, L. J. Gutay, G. B. Collins, J. R. Ficenec and B. C. Stringfellow

Phys. Rev. D 12, 3375 (1975)

Abstract--We have measured the π^- yield in $pp \rightarrow p\pi^- X$ relative to the cross section for $pp \rightarrow p +$ MM at 28.5 GeV/c. The pion distributions are parameterized in terms of x, $p_\perp^2$, and ϕ in the rest frame of the missing mass, MM. The distributions are compared with the corresponding electroproduction case for $-0.1 < x < 0.6$ at the same missing mass and four-momentum transfer to the scattered beam particle. We find striking similarities: (1) The ϕ distributions are flat for the proton case as in electroproduction, (2) the slopes of the transverse-momentum distributions are the same as in electroproduction, and (3) the x distributions have the same shape as in electroproduction.

SEARCH FOR NARROW NEUTRAL-MESON RESONANCES NEAR MASS 1 GeV/c^2

M. Buttram, H. B. Crawley, D. W. Duke, R. C. Lamb, R. J. Leeper and F. C. Peterson

Phys. Rev. Lett. 35, 970 (1975)

Abstract--We examine the reaction $\pi^- p \rightarrow X^0 n$ at 2.4 GeV/c for evidence of the production of the previously reported narrow neutral mesons $M^0(940)$, $\delta(963)$, $M^0(1033)$, and $M^0(1150)$. Strong evidence against the existence of these states is presented.

SEARCH FOR BACKWARD A_1 AND A_2 PRODUCTION IN $\pi^- p \rightarrow p\pi^-\pi^+\pi^-$ AT 8GeV/c

A. Abashian, N. Beamer, A. Bross, B. Eisenstein, N. Gelfand, J. D. Hansen, W. Mollet, G. R. Morris, B. Nelson, T. O'Halloran, J. R. Orr, D. Rhines, P. Schultz, P. Sokolsky, R. G. Wagner, J. Watson and M. Buttram

Phys. Rev. Lett. 34, 691 (1975)

Abstract--Backward meson production in the reaction $\pi^- p \rightarrow p\pi^-\pi^+\pi^-$ has been studied with use of a streamer chamber triggered by the detection of a fast forward proton. For $\cos\theta^* < -0.98$ we find no evidence of A_1 or A_2 production, and we determine total backward cross-section upper limits (95% confidence) of 0.93 and 0.72 b, respectively. At $m_{3\pi} = 1.9$ GeV/c^2 we observe a broad enhancement of about 3-standard-deviation significance. Evidence for backward quasi-two-body production is seen in the $\rho^0 p\pi^-$ and $f^0 p\pi^-$ channels.

BACKWARD $\pi^- d$ ELASTIC SCATTERING FROM 496 TO 1050 MeV/c

R. Keller, D. G. Crabb, J. R. O'Fallon, T. J. Richards, L. S. Schroeder, R. J. Ott, J. Trischuk and J. Va'vra

Phys. Rev. D 11, 2389 (1975)

Abstract--Measurements of the differential cross sections for $\pi^- d$ elastic scattering in the backward angular region are presented. These measurements were made at thirteen incident-pion momenta ranging from 496 to 1050 MeV/c, over the center-of-mass angular range 148° to 177°. The experiment was performed at the LBL Bevatron. Experimental apparatus consisted of a liquid deuterium target and a double-arm spectrometer which included scintillation-counter hodoscopes. Center-of-mass differential cross sections were found to be generally smooth over the angular range covered and can be fitted with low-order polynomials. The extrapolated differential cross sections at 180° scattering angle were found to decrease

rapidly with increasing momentum, with a prominent peak near 700 MeV/c and a shoulder near 900 MeV/c. These data are discussed in terms of existing models employing "d" structures, and are compared with other similar measurements.

Theory

EXPERIMENTAL FAILURE OF SHORTEST-PATH TECHNIQUE IN INELASTIC PARTIAL WAVE ANALYSIS
N. W. Dean, T. C. Jensen, and W. F. Long
Phys. Lett. 53B, 462 (1975)

Abstract--We have conducted a feasibility test of the usual partial wave analysis procedure by generating ersatz experimental data for an inelastic reaction from a known set of partial waves, then attempting to subject them to partial-wave analysis. The presence of the ambiguous solutions proposed by Dean and Lee at all energies prevents the usual procedure from succeeding; the shortest path solutions are not the correct ones.

AMBIGUOUS SETS OF PARTIAL-WAVE AMPLITUDES CANNOT INTERSECT
N. W. Dean
Nucl. Phys. B97, 377 (1975)

Abstract--The correct set of partial-wave amplitudes can sometimes be distinguished from ambiguous ones because it joins continuously, as a function of energy, to a lower-energy set known unambiguously. If two sets intersect, however, this continuity criterion yields no unique answer. We show that such an intersection is in fact impossible in the usual experimental spin-0 spin-1/2 scattering situation.

DEEP-INELASTIC eN AND νN SCATTERING: A UNIFIED DESCRIPTION VIA DUAL REGGE POLES AND SU(3)
D. W. Duke
Phys. Rev. D 11, 43 (1975)

Abstract--The deep-inelastic scattering of electrons and neutrinos off nucleons is studied phenomenologically by means of a model that describes

the scattering of weak and electromagnetic currents off nucleons. It is found that one may impose the constraints of Regge behavior, duality, SU(3) symmetry, and current algebra in a model for the structure functions and obtain a very accurate and economical description of the data. This approach demonstrates a remarkable resemblance between the strong interactions of hadrons and their weak and electromagnetic interactions.

CAUSAL INDEPENDENCE IN ALGEBRAIC QUANTUM FIELD THEORY
B. DeFacio
Foundations of Physics 5, 229 (1975)

Abstract--Ekstein has shown that causal independence neither implies nor is implied by commutativity in an infinite-dimensional, reducible construction. DeFacio and Taylor have presented a finite-dimensional irreducible example of Ekstein's proposition. Avishai and Ekstein have shown that the original question regarding locality for algebraic quantum field theories remains open. We concur with that claim and offer additional arguments. A new denumerably infinite-dimensional, irreducible example is presented here which shows that a sort of "orthogonality" among operators is involved. Some observations on local C*- and W*-algebras are given.

HEAT CONDUCTION MODEL WITH FINITE SIGNAL SPEED
B. DeFacio
J. Math. Phys. 16, 971 (1975)

A simple physical model is derived which has a finite signal speed for a heat pulse in a linear medium. The most general E^3 invariant constitutive equation for energy flux $\mathcal{E}$ which allows the finite signal speed is given. The assumptions which are required include continuum mechanics, thermodynamics of adiabatic processes, and a generalized Fourier heat

law for the energy flux $\mathcal{E}$. Then we use singular perturbation theory with the finite signal speed u^{-1} as a parameter to reduce the hyperbolic heat equation to the usual parabolic heat conduction equation.

PHOTOPRODUCTION OF J (ψ) PARTICLES AND RISING PHOTON-NUCLEON CROSS SECTIONS
B.-L. Young and K. E. Lassila
Phys. Rev. D 12, 3424 (1975)

Abstract--The existence of vector mesons with masses above 3 GeV suggests study of their contributions to the Compton sum rule. The Compton sum rule is used to place upper limits on photoproduction cross sections for such recently discovered and yet to be found $J^P = 1^-$ particles. We are led to the result that the total proton photoabsorption cross section and forward Compton-scattering cross section will rise in the range of energies (above ~50 GeV) available for photon experiments at the Fermilab accelerator. Discussion is given on the implications of such a rising photon-proton cross section for vector-meson dominance (VMD), the quark model, generalized VMD, and the new duality, and for scaling breaking.

TRACE AND WARD-TAKAHASHI IDENTITY ANOMALIES IN AN SU(3) CURRENT MODEL WITH ENERGY-MOMENTUM TENSOR
Douglas B. Zacrep and Bing-Lin Young
Phys. Rev. D 12, 513 (1975)

Abstract--We discuss the validity of the naive Ward-Takahashi identities and trace identities for arbitrary n-point functions (n-pf's) of scalar, pseudoscalar, vector, and axial-vector currents and the improved energy-momentum tensor, thus extending the previous investigations in a unified way. We show that the validity of the naive Ward-Takahashi identities of the energy-momentum tensor implies the satisfaction of those of the

vector currents. This removes an ambiguity concerning the minimal sets of anomalous current Ward-Takahashi identities. We find that all the anomalous Ward-Takahashi identities for the broad structure of n-pf's are again restricted to the axial-vector current of n-pf's of abnormal parity in a well-defined pattern, and the trace identity anomalies occur only in normal-parity n-pf's. We give all these anomalies. Our results show that there are no new anomalies associated with the inclusion of the energy-momentum tensor in the n-pf's.

HIGH-ENERGY BEHAVIOR OF ϕ^3 THEORY IN SIX DIMENSIONS
R. W. Brown, Leon B. Gordon, T. F. Wong and B.-L. Young
Phys. Rev. D 11, 2209 (1975)

Abstract--We examine the high-energy behavior of scattering amplitudes in an asymptotically free field theory, ϕ^3 theory in six dimensions. It is seen that, as in non-Abelian gauge theories, the lack of transverse-momentum cutoff gives rise to a $1n_s^2$ expansion. Within this leading-logarithm approximation, ladder diagrams dominate in each order and their series corresponds to a fixed Regge cut. The nonleading logarithmic corrections and a (truss) bridge between our results and those for ϕ^4 in four dimensions are discussed as is the possible change in the Regge singularity if a different summation is followed.

LAGRANGIAN FORMULATION OF A GEOMETRICAL SCALAR-TENSOR THEORY OF GRAVITATION
D. K. Ross
General Relativity and Gravitation 6, 157 (1975)

Abstract--The author's geometrical theory of the scalar-tensor gravitational field is extended by formulating it in terms of a Lagrangian.

An exact solution of the coupled nonlinear field equations for a static point mass is also presented. This theory which is conformally equivalent to the empty space Einstein equations predicts the same results for experiments as the usual theory of Brans and Dicke which has a non-zero energy momentum tensor.

EC-02

NUCLEAR SCIENCE

EFFECTIVE CROSS SECTIONS FOR THE (n, 2pn), (n, 2p), AND (n, 3pn) REACTIONS USING INTERMEDIATE-ENERGY NEUTRONS
John C. Hill, D. G. Shirk, R. F. Petry and K. H. Wang
Phys. Rev. C 12, 1978 (1975).

Abstract--"Effective cross sections" for the (n, 2pn), (n, 2p), and (n, 3pn) reactions on various targets were measured relative to the $^{12}C(n, 2n)^{11}C$ reaction. The bombarding particles were the spectrum of neutrons generated in a Cu beamstop by 750-MeV protons. The cross section systematics as a function of target mass number are compared with available 14-MeV neutron cross sections for (n, ^{3}He) and (n, 2p) reactions and with results from intranuclear-cascade calculations.

DECAYS OF ^{101}Mo AND ^{101}Tc
J. F. Wright, W. L. Talbert, Jr. and A. F. Voigt
Phys. Rev. C 12, 572 (1975)

Abstract--The activities ^{101}Mo and ^{101}Tc produced from neutron capture by natural Mo were chemically separated and studied using Ge(Li) γ-ray detectors. Out of 185 transitions observed in the decay of ^{101}Mo, 170 were assigned to 44 excited levels in ^{101}Tc. For the decay of ^{101}Tc, 26 of 27 transitions were placed among 10 excited levels in ^{101}Ru. The interpretation of the ^{101}Tc level scheme using the shell-model approach is not satisfactory even for a five-particle calculation. Systematics of odd-A level structures in the region of A = 101 indicate that the level structure of ^{101}Tc could be due partly to the onset of collective effects.

γ-γ ANGULAR CORRELATIONS OF TRANSITIONS IN ^{142}Ce
G. J. Basinger, W. C. Schick, Jr. and W. L. Talbert, Jr.
Phys. Rev. C 11, 1755 (1975)

Abstract--Angular correlation measurements have been performed on 12 direct and 4 skip cascades in ^{142}Ce, all involving the 641-keV $2^+ \rightarrow 0^+$ transition. The ^{142}Ce levels were populated in the β^- decay of fission-product ^{142}La produced as a decay product of ^{142}Xe at the TRISTAN on-line isotope-separator facility. Spin-parity assignments or preferences have been made for all 13 excited levels below 3 MeV previously known to be populated in this decay. In addition, a new 0^+ level is established at 2030 keV in ^{142}Ce. These levels are described in terms of vibrations of a spherical nucleus. An alternate interpretation in terms of quasirotational bands is also presented.

INTERNAL-CONVERSION COEFFICIENT DETERMINATION OF ODD PARITY FOR THE 108.8-keV FIRST-EXCITED STATE OF ^{91}Rb
F. K. Wohn, W. L. Talbert, Jr., R. S. Weinbeck, M. D. Glascock and J. K. Halbig
Phys. Rev. C 11, 1455 (1975)

Abstract--Internal-conversion coefficients of the 108.8-keV transition in the decay of ^{91}Kr and the 93.6-keV transition in the decay of ^{91}Rb were measured by the electron-to-γ-ray ratio method using a high-resolution magnetic spectrometer and by the x-ray-to-γ-ray ratio method using a low-energy photon spectrometer. The 93.6-keV transition was found to be pure E2. The 108.8-keV transition from the first-excited state of ^{91}Rb was found to be pure M 1, which determines the parity of this state as odd, as expected from spherical shell-model considerations, and contradicts a recently reported assignment of even parity for this state.

LIFETIMES OF LEVELS IN ^{136}Xe, ^{140}Cs, AND ^{141}Cs POPULATED IN THE DECAYS OF MASS-SEPARATED ^{136}I, ^{140}Xe, AND ^{141}Xe

J. A. Morman, W. C. Schick, Jr. and W. L. Talbert, Jr.

Phys. Rev. C 11, 913 (1975)

Abstract--The decays of ^{141}Xe, ^{140}Xe, and ^{136}I were examined for the presence of energy levels in ^{141}Cs, ^{140}Cs, and ^{136}Xe, respectively, with measurable half-lives in the nsec range. Using a least-squares fitting procedure to analyze the delayed coincidence data taken with a planar Ge(Li)-plastic scintillator system, the half-lives of the following levels were measured: ^{141}Cs: 69.0 keV, 23.3 ± 0.7 nsec; 105.9 keV, 8.7 ± 0.2 nsec; ^{140}Cs: 13.9 keV, 471 ± 51 nsec; 64.7 keV, 3.7 ± 0.3 nsec; 103.1 keV, 7.3 ± 0.3 nsec (average of two measurements). In addition, upper limits for the half-lives of other levels in these two isotopes are also given, as well as for some levels in ^{136}Xe. Possible multipolarities of the transitions are discussed.

NUCLEAR DATA SHEETS FOR A = 116

G. H. Carlson, W. L. Talbert, Jr. and S. Raman

Nuclear Data Sheets 14, 247 (1975)

Abstract--The 1960 version of the Nuclear Data Sheets for A = 116 has been revised on the basis of experimental data received before August 1973, with some later modifications received via private communications. Experimental data concerning the nuclear structure of ten isotopes were compiled and used in the construction of the level schemes and J^{-}-assignments.

A SEVEN-DETECTOR ANGULAR-CORRELATION APPARATUS FOR THE STUDY OF SHORT-LIVED NUCLEI
G. J. Basinger, W. C. Schick, Jr. and W. L. Talbert, Jr.
Nucl. Instruments and Methods 124, 381 (1975)

Abstract--A seven-detector γ-γ angular-correlation apparatus has been constructed to study short-lived fission product nuclei produced by the TRISTAN on-line isotope separator system. The apparatus employs either seven NaI(Tl) detectors or six NaI(Tl) detectors and one Ge(Li) detector. A 16384-channel analyzer may be used in conjunction with a series of single-channel discriminators to measure correlations simultaneously on all cascades involving a single γ-ray transition. Alternatively, a buffer tape system may be used to record data simultaneously on all cascades in a decay scheme. The apparatus has been tested on cascades in ^{138}Ba from the decay of ^{138}Cs. The results for three direct and two skip cascades are consistent with the known spins of 2+, 4+, 4+, and 3+ for the levels at 1436, 1899, 2308, and 2446 keV in ^{138}Ba, respectively. In addition mixing ratios of 0.01 ± 0.03, $0.05^{+0.20}_{-0.12}$, and 0.10 ± 0.03 have been obtained for the transitions at 1009, 409, and 547 keV in this nucleus.

THE TRISTAN ON-LINE ISOTOPE SEPARATOR FACILITY
J. R. McConnell and W. L. Talbert, Jr.
Nucl. Instruments and Methods 128, 227 (1975)

Abstract--The TRISTAN facility consists of an isotope separator and associated nuclear spectroscopy equipment located at the Ames Laboratory Research Reactor. It is used for on-line studies of short-lived neutron-rich nuclides produced by fission of enriched ^{235}U. The facility is first described in terms of the target and neutron irradiation system

along with the associated transport line. Next, the isotope separator is described with emphasis placed on developments of components for on-line operation, and results obtained from tests for mass purity. Ion beam handling to several detector stations through the use of a switching magnet is discussed along with a description of the stations. Also included are the design considerations of a moving tape collector and its drive electronics; retention measurements on tape material; control unit for time sequencing of beam, data accumulation, and tape transport; detector station for study of delayed neutrons; and a high-resolution $\pi/2$ β-ray spectrometer. Some of the operational experiences over an eight-year period are discussed.

SYSTEMATIC STUDY OF THE PHOTODISINTEGRATION OF ^{70}Ge, ^{72}Ge, ^{74}Ge, AND ^{76}Ge

J. J. McCarthy, R. C. Morrison and H. J. Vander Molen

Phys. Rev. C 11, 772 (1975)

Abstract--Cross sections for the (γ, n), the $(\gamma, 2n)$, and the (γ, np) reactions for ^{70}Ge, ^{72}Ge, ^{74}Ge, and ^{76}Ge, and the (γ, p) reaction for ^{74}Ge have been measured from threshold to 40 MeV at the Iowa State University Synchrotron Laboratory. Cross section results were obtained by unfolding bremsstrahlung yield curves. A "total" photoabsorption cross section was obtained for each isotope by adding the partial cross sections together. Cross sections integrated to 40 MeV are given for each reaction. Giant resonance parameters obtained from the total cross sections are compared with the results of a dynamic collective model calculation. Cross section strength is found at energies above the giant dipole resonance and is discussed in terms of the integrated cross sections.

CONFIRMATION OF THE PREDICTED L DEPENDENCE IN THE RADIAL FORM FACTOR FOR NUCLEUS-NUCLEUS INELASTIC SCATTERING
P. J. Moffa, J. P. Vary, C. B. Dover, C. W. Towsley, R. G. Hanus and K. Nagatani
Phys. Rev. Lett. 35, 992 (1975)

Abstract--The multipolarity (L) dependence of the inelastic form factor for heavy-ion-induced excitations predicted by the folding model is confirmed in the analysis of the scattering of ^{14}N from ^{12}C and ^{16}O at 155 MeV. Agreement between the target deformation lengths ($\beta_L R_t$) of these measurements and those from electromagnetic and proton experiments is found when the strongly L-dependent folding-model form factor is employed.

HIGH-SPIN ANOMALIES IN Yb: CORIOLIS ANTIPAIRING VERSUS PAIR REALIGNMENT WITH A REALISTIC INTERACTION
A. L. Goodman and J. P. Vary
Phys. Rev. Lett. 35, 504 (1975)

Abstract--The Hartree-Fock-Bogoliubov cranking equations are solved for ^{168}Yb and ^{170}Yb with an effective interaction obtained from the Reid soft-core nucleon-nucleon potential. Coriolis antipairing in ^{168}Yb and pair realignment in ^{170}Yb explain their anomalous high-spin spectra.

SPIN EFFECTS IN THE SCATTERING OF 1-GeV PROTONS BY NUCLEI
E. Kujawski and J. P. Vary
Phys. Rev. C 12, 1971 (1975)

Abstract--The elastic scattering of 1-GeV protons by ^{58}Ni and ^{208}Pb is analyzed using the first-order optical potential including the spin-orbit term. These potentials are generated using realistic nucleon-nucleon scattering amplitudes and nuclear densities with full isospin dependence maintained. The sensitivity of the differential cross sections and polarizations to the spin-orbit potentials and nuclear densities is investigated.

LEVEL STRUCTURE OF ^{106}Pd FROM THE DECAY OF ^{106}Rh^{g}

S. T. Hsue, H. H. Hsu, F. K. Wohn, W. R. Western and S. A. Williams

Phys. Rev. C 12, 582 (1975)

Abstract--The low-spin level structure of ^{106}Pd was studied using high-resolution large volume Ge(Li) detectors for γ-ray singles, coincidence, and angular correlation measurements. The measurements allowed the resolution of most of the discrepancies found among previous studies. In particular, the use of two Ge(Li) detectors for coincidences and angular correlations allowed unambiguous placement of previously multiply placed γ rays and resolved discrepancies in energy level or J^{π} assignments. The experimental level structure and B(E2) ratios are compared with predictions of an anharmonic spherical vibrator model and a rotor-vibrator model; we find that the evidence strongly supports the latter of the two models.

COUNTING ALPHA PARTICLES FROM THE ^{6}Li+n REACTION BY TRACK-ETCH METHODS

Paul B. Hahn, Margaret A. Wechter and Adolf F. Voigt

Nucl. Instruments and Methods 123, 111 (1975)

Abstract--The track etch-spark counting technique using thin cellulose nitrate films has been demonstrated to be successful for measuring approximately 2 MeV alpha particles from a ^{210}Po alpha source and from the ^{6}Li(n,α)^{3}H reaction. Precision of measurement was found to approach that of counting statistics and the linearity of response extended to approximately 2000 spark counts/cm^{2} of detector film. The potential application of the technique to a surface activation analysis by the (n,α) reaction was investigated by irradiating ^{6}LiF thermoluminescence detector crystals in a neutron flux using an evacuated irradiation chamber.

EC-03
MATERIALS SCIENCE
EC-03-01
Metallurgy and Ceramics

EC-03-01-01
Structure of Materials

Multi-Technology

EFFECTS OF OXYGEN AND NITROGEN ON THE MECHANICAL PROPERTIES OF VANADIUM METAL
O. N. Carlson and D. G. Alexander
Rev. High-Temp. Mater. 2, 262 (1974)

Abstract--The state of knowledge of the solid solubilities of oxygen and nitrogen in vanadium and the effects of these solutes on the lattice parameter and mechanical properties are reviewed and evaluated. Differences in the reported limits of solid solubility of these solutes in vanadium are discussed. The effects of concentration of the individual solutes on the lattice parameter, hardness, brittle-ductile transition temperature and tensile properties are represented graphically, comparing the results of various investigators. The role of oxygen and nitrogen in both static and dynamic strain aging in vanadium is examined. The temperature dependence of the flow stress of vanadium of different interstitial impurity content is compared for both the polycrystalline material and single crystals.

INVESTIGATION OF REPORTED ANOMALIES IN THE ELECTROTRANSPORT OF INTERSTITIAL SOLUTES IN TITANIUM AND IRON
O. N. Carlson, F. A. Schmidt and R. R. Lichtenberg
Met. Trans 6A, 725 (1975)

Abstract--The electric mobilities, effective valences, and diffusivities of carbon, nitrogen, and oxygen in β-titanium were measured in the temperature range of 1335 to 1575°C. The effective valence, Z^*, of carbon was determined to be positive and nitrogen and oxygen to be negative, thus confirming a previously reported anomaly in the electrotransport behavior of carbon in titanium. A similar anomaly in the effective charge of nitrogen in γ iron was also investigated. The previously reported negative Z^* value was not supported by the results of this investigation. Positive Z^* values were obtained for nitrogen in both α and γ iron in agreement with those for carbon in these two phases. An analytical method of solving for the various transport parameters was used in this investigation. A mathematical proof of the method and the treatment of errors is described in the paper.

THE EFFECTS OF CRYSTALLOGRAPHIC ANISOTROPY ON THE GROWTH KINETICS OF WIDMANSTÄTTEN PRECIPITATES
W. P. Bosze and R. Trivedi
Acta Met. 23, 713 (1975)

Abstract--A theoretical model which emphasizes crystallographic considerations during the growth of Widmanstätten precipitates is developed. The theory predicts that the crystallographic anisotropy of interface kinetics process becomes significant under the growth conditions of small peclet numbers, viz. $p < a_1/5.5$, where a_1 is the anisotropy parameter. The results of this model are applied to the experimental data on the growth of Widmanstätten cementite plates in hypereutectoid steels.

THE KINETICS OF LATERAL GROWTH
G. J. Jones and R. Trivedi
J. Cryst. Growth 29, 155 (1975)

Abstract--A theoretical model to study the growth characteristics of a train of closely-spaced macrosteps is presented. Volume diffusion in the parent phase is assumed to be the rate controlling factor, and numerical calculations are performed to assess the effect of neighboring steps on the velocity of a given step. On the basis of the nearest neighbor step interaction, a stability analysis is presented to predict the behavior of a large train of macrosteps. The interaction analysis is extended, and discussed qualitatively, to the case of microsteps which advance either by volume or by surface diffusion mechanism.

THEORY OF CAPILLARITY
R. Trivedi
Lectures on the Theory of Phase Transformations, ed. H. I. Aaronson
(New York: Metallurgical Society of AIME, 1975) pp. 51-81

Abstract-- The term capillarity refers to the macroscopic motion of fluid under the influence of its own surface and interfacial forces. The theory of capillarity therefore deals with phenomena which occur due to the surface tension forces. In general, all surface effects in solids and liquids are referred to as capillarity effects. Because surface effects in solids are complex most of the literature is concerned with surface effects in incompressible fluids only. We shall therefore develop major concepts of surface effects in incompressible fluids, and then briefly discuss the concepts which must be modified when solid systems are considered.

COEXISTENCE OF SUPERCONDUCTIVITY AND THE KONDO EFFECT IN PbCe AND InCe QUENCH-CONDENSED FILMS
R. J. Delfs, B. J. Beaudry and D. K. Finnemore
Phys. Rev. B 11, 4212 (1975)

See abstract under Experimental Physics III: Superconductivity, page

DERIVATION, EXTRACTION, AND PREPARATION
K. A. Gschneidner, Jr.
Scandium--Its Occurrence, Chemistry, Physics, Metallurgy, Biology and Technology, eds. C. T. Horovitz, K. A. Gschneidner, Jr., G. A. Melson, D. H. Youngblood and H. H. Schock (London: Academic Press, 1975) pp. 66-75

No abstract available.

PURIFICATION OF RARE-EARTH METALS BY ELECTROTRANSPORT
O. N. Carlson, F. A. Schmidt and D. T. Peterson
J. Less-Common Metals 39, 277 (1975)

Abstract--The principles of the electrotransport purification process are described, together with those variables that affect the degree of purity attainable. Experiments on the purification of yttrium, lutetium, and gadolinium with respect to carbon, nitrogen, and oxygen are described and the results compared with those predicted from theory. Metal purities were evaluated by resistance ratio measurements and chemical analyses.

THE SOLUBILITY OF RH_{2-x} IN Gd, Er, Tm, Lu AND Y FROM AMBIENT TO 850°C
B. J. Beaudry and F. H. Spedding
Met. Trans. 6B, 419 (1975)

Abstract--The solubility of hydrogen in Gd, Er, Tm, Lu and Y was determined from 25 to 850°C when the metal was in equilibrium with RH_{2-x}

(x varies between 0.1 and 0.2 depending on the rare earth metal). The room temperature solubilities determined by the lattice parametric method were found to be <0.1, 3.6, 7.7, 20.6 and 19.0 at. pct H in Gd, Er, Tm, Lu and Y, respectively. The change in unit cell volume for each atomic percent hydrogen added was nearly the same for all metals. The solubility of hydrogen increases more rapidly with temperature in those metals with low solubility at room temperature. Thus the solubility of hydrogen at 850°C is nearly the same in all five of the metals studied, that is, 35.0, 36.2, 36.0, 36.0 and 37.3 at. pct H in Gd, Er, Tm, Lu and Y, respectively. The equilibrium pressure of H_2 in these studies was the equilibrium pressure of hydrogen in contact with RH_{2-x} at the temperature concerned. A change in slope was observed in the solubility curves of the Gd-, Er-, Tm- and Lu-H systems. The log C (at. pct H in R) was plotted vs $1/T$ for each system. Straight lines were obtained at temperatures above and below the changes in slope of the solubility curves. A calculation of the approximate ΔH of solution of RH_{2-x} in the metals from the slope of the lines gave 4.35, 1.88, 1.28, 0.61 and 0.55 kcal/mole for Gd, Er, Tm, Lu and Y, respectively in the low temperature portion. The change in slope which occurs at some point between 350°C and 650°C, depending on the metal, indicates a lower heat of solution of RH_{2-x} in these metals at the higher temperatures. In Lu there appears to be yet another change in slope in the neighborhood of 250°C.

Mechanical Properties

Multi-Technology

DISCONTINUOUS YIELDING IN PURE NICKEL-COPPER ALLOYS
R. P. Zerwekh and T. E. Scott
Scripta Met. 9, 407 (1975)

Abstract--Discontinuous yielding was observed in high purity nickel-copper alloys. The phenomenon of discontinuous yielding is not expected for the nickel-copper system because short-range order does not occur and dislocation pinning by the Cottrell mechanism requires larger atomic mismatches than exist in this system. It appears that a specific grain boundary structure combined with a mechanism for segregation of solute atoms to the grain boundaries are the necessary conditions for discontinuous yielding. Two potential mechanisms for grain boundary segregation are suggested; namely, non-equilibrium segregation with the vacancy flux and phase separation within the apparent miscibility gap.

MECHANICAL PROPERTIES OF POLYCRYSTALLINE NEODYMIUM FROM 78 TO 600 K
C. V. Owen and T. E. Scott
J. Less-Common Metals 41, 303 (1975)

Abstract--The flow-stress temperature dependence, strain-rate sensitivity, strain-hardening exponent and ductility of neodymium were

determined from 78 to 600 K at strain rates of 0.005, 0.01, 0.1 and 1.0 min^{-1}. The results are presented, and comparisons of the properties of neodymium with those of some rare-earth metals and other h.c.p. materials are discussed.

EFFECT OF NITROGEN ON THE STRENGTH OF THORIUM
D. T. Peterson and D. R. McLachlan
Met. Trans 6A, 1359 (1975)

Abstract--The effect of nitrogen in solid solution on the plastic deformation of polycrystalline thorium was studied by measuring the flow stress from 4.2 K to 773 K at several strain rates. Nitrogen was found to behave similarly to carbon in thorium and increased the thermally activated component of the flow stress. The activation energy was 1.3 eV for overcoming nitrogen atoms in solution. Aging the higher nitrogen alloys produced an age hardening contribution to the flow stress which was a thermally activated component at about 600 K but became an athermal component at lower temperatures.

Physical Properties

Solar Energy

REPRODUCIBILITIES OF SOME PHYSICAL PROPERTIES OF MgF_2

D. M. Bailey, F. W. Calderwood, J. D. Greiner, O. Hunter, Jr., J. F. Smith and R. J. Schiltz, Jr.

J. Am. Ceram. Soc. 58, 489 (1975)

Abstract--Optical-quality MgF_2 specimens selected to represent varying levels of fabrication stresses and impurities were examined to determine their elastic moduli, thermal expansions, and thermal conductivities. These properties proved to be insensitive to the variations in impurities among the samples. The elastic moduli were also insensitive to the variations in residual strain. Any sensitivity to residual strain was masked, in the case of thermal conductivity measurements, by the fracture of highly strained specimens during sample manipulation and, in the case of thermal expansion measurements, by crushing the specimens to powder before measurement.

Conversion, Storage and Transmission

INTERDIFFUSION IN THE CaF_2-YF_3 SYSTEM

R. G. Visser, W. F. Schiavi and M. F. Berard

J. Am. Ceram. Soc. 58, 438 (1975)

Abstract--An electron microprobe interdiffusion study was made in single crystals between 1200° and 1331 °C over the solid-solution

compositional range 0 to 20 mol%YF_3 in CaF_2. At constant temperature, the value of $\tilde{D}$, the interdiffusion coefficient, increased approximately exponentially with increasing YF_3 content. As YF_3 content increased, the temperature dependence of $\tilde{D}$ decreased. Extrapolation of $\tilde{D}$ to 0%YF_3 combined with consideration of the defect formation mechanism at infinite dilution allowed estimation of the impurity diffusion coefficient for Y in essentially pure CaF_2.

THE DIFFUSION COEFFICIENT OF Bi IN DILUTE LIQUID ALLOYS OF Bi IN Sn
J. D. Verhoeven, E. D. Gibson and M. B. Beardsley
Met. Trans. 6B, 349 (1975)

Abstract--A radioisotope technique was used to measure the diffusion coefficient of Bi in liquid Sn over a temperature range of 237 to 525°C. Data on dilute alloys in the 240-350°C range had previously been available only by extrapolation, and the present results show that these extrapolated values were in significant error.

THE EFFECT OF SOLUTE CONVECTION UPON MACROSEGREGATION IN OFF-EUTECTIC COMPOSITE GROWTH
J. D. Verhoeven, K. Kurtz Kingery and R. Hofer
Met. Trans. 6B, 647 (1975)

Abstract--Vertical solidification experiments have been carried out on Pb-Sn and Pb-Cd alloys at hypereutectic compositions where solute convection was present. A significant amount of macrosegregation was observed due to the convection, and the macrosegregation was found to be independent of tube diameter for those diameters studied, 3 to 6 mm. The resulting macrosegregation correlated well with existing theories. The experiments employed a temperature gradient of 360°C/cm and it was

found that thermotransport made a significant contribution to the observed macrosegregation at growth rates below around 5 μm/s.

MEASUREMENT OF LIQUID METAL DIFFUSION COEFFICIENTS FROM STEADY-STATE SOLIDIFICATION EXPERIMENTS
J. D. Verhoeven, E. D. Gibson and R. I. Griffith
Met. Trans. 6B, 475 (1975)

Abstract--Steady state solidification experiments were carried out on Sn-Bi alloys of compositions from zero to 3.5 at. pct Bi with tube diameters from 1.9 to 5 mm. Solute profiles were determined utilizing a radioisotope, Bi^{207}, and a microtome slicing technique. Results indicate the technique offers a relatively precise method for determining liquid metal diffusion coefficients at the solidus temperature. Convection does not appear to be a problem for tube diameters under 3 mm. It is shown that neglect of thermal transport may give errors in the measured diffusion coefficients as high as 10 to 30 pct.

THE PREPARATION OF SINGLE CRYSTAL LaB_6 CATHODES FOR ELECTRON MICROSCOPES
E. D. Gibson and J. D. Verhoeven
J. Phys. E: Sci. Instr. 8, 1003 (1975)

Abstract--Experimental techniques are presented for (i) a very simple zone melting technique employing a floating zone maintained by an arc which allows preparation of high purity single crystal cathodes, and (ii) a grinding device which allows the LaB_6 tips to be ground to a radius of curvature of less than 3 μm using a metallurgical polishing wheel.

ROTATION BETWEEN SEM MICROGRAPH AND ELECTRON CHANNELLING PATTERNS

J. D. Verhoeven and E. D. Gibson

J. Phys. E: Sci. Instr. 8, 15 (1975)

Abstract--This work describes a 180° rotation effect which occurs between the scanning electron microscope (SEM) micrograph and the corresponding electron channelling pattern (ECP). The effect occurs in both the normal double deflection mode used for large area ECPS and the deflection focusing technique used for selected area ECPS. The cause of the effect is explained.

Nuclear Energy

ON LOWER VALENT THORIUM CHLORIDES IN FUSED CHLORIDE SALTS

P. Chiotti and C. H. Dock

J. Less-Common Metals 41, 225 (1975)

Abstract--Emf data on cells of the types

$Th/KCl-LiCl-ThCl_4/KCl-LiCl-AgCl/Ag$

and $Th/KCl-LiCl-ThCl_4/ThZn_{8.5},Zn$

have been obtained in order to evaluate the valence state of thorium chloride in the fused salts. These data show that the valence of thorium is 4+. Literature data on the thermodynamic properties of $ThOCl_2$ are summarized, and a relationship developed for the standard free energy of formation for this compound. It is shown that some of the literature data on the existence of lower valent thorium chlorides in fused salt can be explained on the basis

of contamination by ThO_2 whilst other evidence, based on the slope of emf data composition plots, can be misleading if the composition dependence of the activity coefficient of $ThCl_4$ is not taken into account.

PHASE DIAGRAM AND THERMODYNAMIC PROPERTIES OF THE URANIUM-ZINC SYSTEM
P. Chiotti and J. T. Mason
J. Less-Common Metals 40, 39 (1975)

Abstract--Literature data on the uranium-zinc system have been reviewed and combined with new data to establish the phase relations and thermodynamic properties. The existence of two compounds, U_2Zn_{17} and UZn_{12}, has been firmly established. The first compound undergoes a transformation at 724 ± 3°C on the uranium-rich side of the compound, at 824 ± 10°C on the zinc-rich side and melts congruently at 970 ± 5°C. UZn_{12} has a defect structure with a stoichiometry which ranges from $UZn_{9.4}$ to $UZn_{11.5}$. It undergoes a peritectic reaction at 768 ± 10°C. Other features of the phase relations are as originally reported.

The standard free energies of formation (in calories) of the compounds are given by the relations

$$\Delta G^\circ\ (UZn_{8.5}) = -46.530 + 30.87T\ (420 - 668°C)$$

$$\Delta G^\circ\ (UZn_{8.5}) = -47,200 + 31.58T\ (668 - 724°C)$$

$$\Delta G^\circ\ (UZn_{8.5}) = -45,395 + 29.78T\ (744 - 775°C)$$

$$\Delta G^\circ\ (UZn_{8.5}) = -46,530 + 30.87T\ (775 - 970°C)$$

$$\Delta G^\circ\ (UZn_{12}) = -52,750 + 36.73T\ (420 - 668°C)$$

$$\Delta G^\circ\ (UZn_{12}) = -53,415 + 37.44T\ (668 - 775°C)$$

REACTION OF THORIUM AND $ThCl_4$ WITH UO_2 AND $(Th,U)O_2$ IN FUSED CHLORIDE SALTS

P. Chiotti, M. C. Jha and M. J. Tschetter

J. Less-Common Metals 42, 141 (1975)

Abstract--An experimental and theoretical investigation of the reactions of thorium and $ThCl_4$ with UO_2 and $(Th,U)O_2$ in fused KCl-LiCl and NaCl-$MgCl_2$ eutectic salts has been carried out. The equilibrium $ThCl_4 + ThO_2 \rightleftharpoons 2ThOCl_2$ has been considered in some detail and the maximum solubility of $ThOCl_2$ as a function of the $ThCl_4$ concentration in KCl-LiCl calculated. The activity coefficient of $ThOCl_2$ was estimated from experimental data. Similar calculations were made for the solubility of $UOCl_2$. The reaction of $ThCl_4$ with UO_2 involves three independent reactions. The equilibrium concentration of components in KCl-LiCl salt for the overall reaction $Th + UO_2 \rightarrow ThO_2 + U$ can be described in terms of two independent reactions, and the experimental data are consistent with available thermodynamic data. The reduction of UO_2 and $(Th,U)O_2$ to produce uranium and ThO_2 has been demonstrated. Methods for separating the uranium from the ThO_2 precipitate are considered briefly.

THERMODYNAMICS OF FORMATION OF Th-Cu ALLOYS

D. M. Bailey and J. F. Smith

Thermodynamics of Nuclear Materials, 1974 Vol. 2, (Vienna, Austria: IAEA, 1975) pp. 355-365)

Abstract--Electromotive force cells have been used to determine the Gibbs free energies, enthalpies and entropies of formation for $ThCu_6$, $ThCu_{3.6}$, $ThCu_2$ and Th_2Cu over the temperature range 729-1219 K. Solid CaF_2 was used as the electrolyte. Comparison of the present measurements

with earlier measurements on the most copper-rich phase shows that the free energies are reproducible by this technique to ~4%. The magnitudes of the entropies of formation were all measured as less than 1 cal/g-atom·K and are therefore physically reasonable. The values for the entropies of formation of $ThCu_6$ and $ThCu_{3.6}$ were found to be positive, that of $ThCu_2$ to be essentially zero, and that of Th_2Cu to be negative. Comparison with data from other thorium systems shows that positive entropies of formation are atypical for binary intermetallic phases of thorium. The free energies of formation of the Th-Cu phases were found to be roughly one-half as negative as values reported for Zr-Cu phases at comparable temperatures and stoichiometries.

THE YTTRIA-HAFNIA SYSTEM
D. W. Stacy and D. R. Wilder
J. Am. Ceram. Soc. 58, 285 (1975)

Abstract--Phase equilibria in the yttria-hafnia system were investigated by high-temperature and room-temperature x-ray diffraction. The HfO_2 transformation, solid solution limits, and liquidus temperatures are given. A tentative phase diagram is proposed.

Multi-Technology

MAGNETIC PROPERTIES OF MnPt AND CoPt
C. W. Chen and R. W. Buttry
Proceedings of the 20th Annual Magnetism and Magnetic Materials - 1974 Conference, AIP Conference Proceedings No. 24, eds. C. D. Graham, Jr., G. H. Lander and J. J. Rhyne (New York: American Institute of Physics, 1975) pp. 437-438

Abstract--Magnetization measurements were conducted on ordered and disordered polycrystalline specimens of MnPt and three Co-Pt alloys

between 4.2 and 293°K. The magnetic data, while confirming the onset of antiferromagnetism in the ordered MnPt, reveal the presence of ferromagnetic regions in the disordered MnPt. Chemical order tends to exert a pronounced (~80%) adverse effect on saturation magnetization ($M_{s,0}$) of the Co-Pt alloys at 0°K near the equiatomic composition. Meanwhile, the effect of Co concentration on $M_{s,0}$ of the Co-Pt alloys is shown to be appreciable only when the Co content exceeds 50%.

ENTROPIES OF TRANSFORMATION AND FUSION OF THE METALLIC ELEMENTS
K. A. Gschneidner, Jr.
J. Less-Common Metals 43, 179 (1975)

Abstract--The entropy of transformation of metals which possess two or more of the common metallic structures and the entropy of fusion of metals which have one of these structures prior to melting were analyzed. It is concluded that both entropies are dependent upon the crystalline structure of the phases involved and the number of valence electrons, except for transitions between the close-packed structures, h.c.p. → f.c.c. and d.h.c.p. → f.c.c., for which the entropy of transformation is apparently only structure dependent. Application of these correlations enabled the prediction of the entropies of fusion for 16 metals and the entropies of transformation for 5 metals for which no reliable experimental data exist.

HEAT CAPACITY AND MAGNETIC SUSCEPTIBILITY OF SINGLE-PHASE α-CERIUM
D. C. Koskimaki and K. A. Gschneidner, Jr.
Phys. Rev. B 11, 4463 (1975)

Abstract--The heat capacity of single-phase α-cerium has been measured from 1.6 to 22 K and the magnetic susceptibility from 1.6 to

150 K. The electronic-specific-heat constant was found to be 12.8 ± 0.2 mJ(g atom)$^{-1}$K^{-2} and the Debye temperature at zero degrees was found to be 179 ± 2 K. The susceptibility results show a skewed U type of temperature behavior with minimum of 3.77 x 10^{-6} emu g^{-1} near 50 K and a rapid rise of about 20% below 20 K. The results are interpreted according to various models for the nature of α-cerium and the $\alpha \rightleftarrows \gamma$ transition.

MAGNETIC EXCITATIONS AND MAGNETIC ORDERING IN PRASEODYMIUM
J. G. Houmann, M. Chapellier, A. R. Mackintosh, P. Bak, O. D. McMasters and K. A. Gschneidner, Jr.
Phys. Rev. Lett. 34, 587 (1975)

Abstract--The dispersion relations for magnetic excitons propagating on the hexagonal sites of double-hcp Pr provide clear evidence for a pronounced anisotropy in the exchange. The energy of the excitations decreases rapidly as the temperature is lowered, but becomes almost constant below about 7 K, in agreement with a random-phase-approximation calculation. No evidence of magnetic ordering has been observed above 0.4 K, although the exchange is close to the critical value necessary for an antiferromagnetic state.

NEUTRON SCATTERING AND MAGNETIZATION MEASUREMENTS ON THE KONDO COMPOUND $CeAl_3$
A. S. Edelstein, T. O. Brun, G. H. Lander, O. D. McMasters and K. A. Gschneidner, Jr.
Proceedings of the 20th Annual Magnetism and Magnetic Materials - 1974 Conference, AIP Conference Proceedings No. 24, eds. C. D. Graham, Jr., G. H. Lander and J. J. Rhyne (New York: American Institute of Physics, 1974) pp. 428-429

Abstract--Previous measurements on the Kondo compound, $CeAl_3$ (hexagonal DO_{19}), indicate that with decreasing temperature it transforms

gradually into a singlet state and does not magnetically order above 0.6 K. To determine the spatial extent of the magnetic moment we have measured the spin-dependent cross section of neutrons diffracted from the (201) planes of a polycrystalline sample in 50 kOe at 5, 19 and 81 K. At 50 kOe and these temperatures the total moment from magnetization measurements on the same sample is only 5–15% lower than the moment determined by the neutrons if one assumes a 4f form factor. This approximate agreement supports the hypothesis that the moment decreases without changing its spatial distribution. A similar spatially uniform reduction of the moment occurs also in dilute Kondo systems. From the field dependence of the magnetization M, the characteristic or Kondo temperature is estimated to be 5.1 K.

THE RARE EARTH INDUSTRY--THE 1976-1977 OUTLOOK
K. A. Gschneidner, Jr.
Ceramic Industry 104, 28 (1975)

No abstract available.

PHYSICAL PROPERTIES--Chapter 5 pp. 76-110
K. A. Gschneidner, Jr.
INORGANIC COMPOUNDS--Chapter 8 pp. 152-251
K. A. Gschneidner, Jr.
ALLOYS AND INTERMETALLIC COMPOUNDS--Chapter 9 pp. 252-322
K. A. Gschneidner, Jr.
TECHNOLOGY, APPLICATION AND ECONOMY--Chapter 12 pp. 489-496
D. H. Youngblood and K. A. Gschneidner, Jr.

The previous four chapters are all in SCANDIUM--Its Occurrence, Chemistry, Physics, Metallurgy, Biology and Technology, eds. C. T. Horovitz, K. A. Gschneidner, Jr., G. A. Melson, D. H. Youngblood and H. H. Schock (London: Academic Press, 1975)

No abstracts available.

THERMODYNAMIC STABILITY AND PHYSICAL PROPERTIES OF METALLIC SULFIDES AND OXYSULFIDES
K. A. Gschneidner, Jr.
Sulfide Inclusions in Steel, eds. J. J. de Barbadillo and E. Snape (Metals Park, Ohio: American Society for Metals, 1975) pp. 159-177

No abstract available.

THE DENSITIES OF HIGH-PURITY IRON-CARBON ALLOYS IN THE SPHEROIDIZED CONDITION
F. X. Kayser, A. Litwinchuk and G. L. Stowe
Met. Trans. 6A, 55 (1975)

Abstract--The densities were determined for a series of spheroidized then slowly cooled, high-purity iron-carbon alloy specimens containing from 0 to 4.17 pct C. They were found to follow the relationship ρ^{-1} (cc/g at 23°C) = $0.12698_8 + (5.03_6 \times 10^{-4})$ (wt pct C). Whereas the intercept value coincided with the x-ray specific volume of iron, the extrapolated value at the Fe_3C composition was slightly greater than published x-ray specific volumes for Fe_3C. The results suggested that the cementite phase in these specimens was slightly iron-rich with respect to Fe_3C. Assuming a vacancy-defect structure for the cementite, we were able to roughly estimate its composition. This appears to be a promising method for determining the cementite/(cementite + ferrite) saturation boundary.

ORDERING TEMPERATURE FOR $Cu_{79}Au_{21}$
J. W. Brophy and F. X. Kayser
Phys. Stat. Sol. (a) 30, K33 (1975)

Abstract--The room temperature lattice parameters were recently determined for a series of well-annealed, high-purity, copper-gold alloys containing from 0 to 29 at% gold. These data provide, among other things, information relative to the position of the long-range order boundary in

this system at room temperature. The purpose of the present investigation was to determine the ordering temperature for a 20.9 at% gold alloy by measuring the room temperature lattice parameters of samples that had been rapidly quenched from various annealing temperatures.

RELATIONSHIP BETWEEN ATOMIC ORDERING AND FRACTURE IN Fe-Al ALLOYS
M. J. Marcinkowski, M. E. Taylor and F. X. Kayser
J. Materials Sci. 10, 406 (1975)

Abstract--The fracture surfaces of slowly cooled Fe-Al alloys containing up to 28 at.% Al were examined using scanning electron microscopy techniques. It was found that the fracture modes changed from void coalescence to transgranular and finally, to intergranular as the Al concentration increased. The latter two modes of fracture were of the brittle type and were associated with the onset of long range order in these alloys. In particular, it has been postulated that atomic ordering leads to markedly reduced cross-slip, in turn reducing the degree to which void coalescence, with accompanying ductility, can occur.

INTERACTION PARAMETERS IN THE Zn-Pb-Sn SYSTEM AT LOW ZINC CONCENTRATIONS
Z. Moser and W. Zakulski
J. Electrochem. Soc. Solid State Sci. Tech. 122, 691 (1975)

Abstract--The thermodynamic properties of liquid dilute zinc solutions at a lead concentration of $\underline{X}_{Pb}$ = 0.01-0.7 molar fraction were determined by means of emf measurements of concentration cells. These investigations combined with previous analogical experiments at a tin concentration of $\underline{X}_{Sn}$ = 0.01-0.1 molar fraction enabled the calculation of ternary interaction parameters ϵ_{Zn}^{Pb} and ϵ_{Zn}^{Sn} from plots $(\ln\gamma_{Zn})_{X_{Zn}} \rightarrow$

$_0$ vs. X_{Pb}. For the binary end-points on the plots $\ln \gamma_{Zn}$ vs. X_{Pb} and $(\ln \gamma_{Zn})_{X_{Zn} \to 0}$ vs. X_{Pb} separate measurements were carried out for Zn-Sn and Zn-Pb systems at concentrations up to 0.1 molar fraction of zinc. Experimental results were interpreted by means of Krupkowski's formalism and attempts were made to calculate ϵ_{Zn}^{Pb} and ϵ_{Zn}^{Sn} on the basis of limiting values of activity coefficients of components of binary systems Zn-Sn, Zn-Pb, and Pb-Sn.

QUANTITATIVE NON-DESTRUCTIVE MAGNETIC ANALYSIS OF OXYGEN IN A SCANDIUM SINGLE CRYSTAL
J. D. Greiner and J. F. Smith
J. Less-Common Metals 41, 129 (1975)

Abstract--The Faraday technique was employed to determine the principal magnetic susceptibilities of a scandium single crystal at room temperature, with several field strengths in the range 6 - 11 kOe. The field-dependence of the experimental data was quite weak, and it was deduced that only about 15% of the 60 ppm of iron, indicated by chemical analysis to be present in the starting material, was clustered to a sufficient extent to couple ferromagnetically. Bulk paramagnetic susceptibilities were obtained in the standard manner from reciprocal-field plots up to infinite-field values. The bulk susceptibilities were interpreted as indicating an oxygen content of 1.8 ± 0.3 at.% in the crystal. This interpretation used the extensive data of Spedding and Croat as a standard for the magnetic susceptibilities of pure scandium, and used their results for the effects, on the susceptibility, of various impurities. The validity of the oxygen analysis was substantiated by vacuum-fusion analysis on an equivalent piece of scandium metal.

THERMODYNAMIC PROPERTIES OF MAGNESIUM LEAD ALLOYS
Z. Moser and J. F. Smith
Met. Trans. 6B, 457 (1975)

Abstract--Magnesium activities in liquid magnesium-lead alloys have been measured with electromotive force cells over the temperature range 745 to 868 K and over the mole fraction range $0.03 < X_{Mg} < 0.50$. The experimental data were used to evaluate the parameters in the empirical temperature-composition relationship proposed by Krupkowski for describing the activity coefficients. Values generated from the Krupkowski formulae were utilized with data for liquidus compositions to evaluate the free energies of formation of the solid intermediate phases and compared with available experimental data for Mg_2Pb.

THERMODYNAMIC STUDIES OF DILUTE ZINC SOLUTIONS IN THE Zn-Sn-Cd-Pb SYSTEM AT HIGH LEAD CONCENTRATIONS
Z. Moser and W. Zakulski
J. Electrochem. Soc. 122, 232 (1975)

Abstract--The activity coefficients of zinc were measured in the concentration range $0.03 < X_{Zn} < 0.1$ at temperatures in the range 714°-877°K for lead-rich alloys in the quaternary system Zn-Sn-Cd-Pb with tin and cadmium mole fractions limited to $0.01 < X_{Sn} < 0.1$ and $0.01 < X_{Cd} < 0.1$. Measurements were of emf of concentration cells. Experimental values of $\ln \gamma Zn$ were compared with values obtained from the Krupkowski formalism and from the Wagner formalism. In the latter instance two sets of values were generated, one set considering first-order interactions only and the other set considering both first- and second-order interactions. The comparisons show that the experimental data are reasonably described by both the Krupkowski approach and the Wagner approach with first-order interactions

only. However, less satisfactory accord is obtained after inclusion of second-order interactions in the Wagner equations. The present results show that in the quaternary system strong negative self-interaction parameters, ϵ^{Zn}_{Zn} which lead to marked positive deviations from Raoult's law in the Zn-Pb binary system also lead to negative zinc-cadmium and zinc-tin interaction parameters in the quaternary system. This is in accord with earlier results on ternary systems.

SINGLE-CRYSTAL ELASTIC CONSTANTS OF Zr_2Ni
F. R. Eshelman and J. F. Smith
J. Appl. Phys. 46, 5080 (1975)

Abstract--The ultrasonic pulse-echo-overlap technique has been used to determine the six independent elastic constants of tetragonal Zr_2Ni over the temperature range 4.2-300 K. The temperature dependence of the shear constants, particularly C_{66}, are atypical and indicate a significant degree of mode softening at low temperatures. The results correlate with the recent calculation of Sinha and Harmon in that Zr_2Ni satisfies their conditions for the development of charge density waves with attendant mode softening and support the view that mode softening and superconductivity are correlated.

Radiation Effects

EVIDENCE FOR THE SUPPRESSION OF VOID FORMATION BY A DYNAMIC TRAPPING MECHANISM IN NICKEL
S. M. Sorensen, Jr. and C. W. Chen
J. Nucl. Mater. 58, 119 (1975)

Abstract--Irradiation experiments conducted on Ni-C alloys to a fluence of 9×10^{19} n/cm^2 (E > 0.1 MeV) at 710°C in the fast-flux facility of the Ames Laboratory Research Reactor revealed a pronounced effect of carbon on void formation. Typically, as the concentration of carbon dissolved in the matrix of nickel was increased from 4 to 84 ppm by weight, the density of voids induced decreased from 10.3×10^{13} to 0.3×10^{13} voids/cm^3, whereas the mean void diameter increased from 204 to 390 Å. Consequently the associated swelling decreased from 0.046% to 0.009%. Specimens containing 600 ppm C showed complete absence of voids. This suppressing effect of carbon is attributed to a trapping mechanism, whereby nongaseous atoms of the interstitial solute act as efficient traps for radiation-produced vacancies, thus inhibiting the nucleation of voids. Because solitary carbon atoms are capable of moving rapidly through the lattice at the irradiation temperature, the present mechanism is considered to be dynamic in nature in contrast to other mechanisms that rely on stationary defects, such as substitutional solute atoms, coherent precipitates, and grain boundaries, for trapping.

TRANSMISSION ELECTRON MICROSCOPY EVIDENCE FOR DISLOCATION DISSOCIATION AND STACKING FAULTS IN NIOBIUM

C. P. Chang and C. W. Chen

Scripta Met. 9, 349 (1975)

Abstract--New evidence has been obtained for the dissociation of glissile dislocations in Nb by transmission electron microscopy. Micrographs prepared from many Nb specimens of different contents of interstitial impurities (the total varied from 26 to 300 wt. ppm) persistently reveal the dissociation of screw dislocations on {211} slip planes according to the Crussard mechanism:

$$(a/2)[\bar{1}11]_{(211)} \rightarrow (a/3)[\bar{1}11](211) + (a/6)[\bar{1}11]_{(211)}.$$

Both the partial dislocations and the enclosed stacking faults are clearly visible in strong-beam bright-field and weak-beam dark-field micrographs, respectively. The extended dislocations were observed to exhibit high mobility, thus ruling out the likelihood of impurity segregation in the faulted regions. The present results not only demonstrate the important role played by the dissociated screw dislocations in slip in body-centered cubic metals, but also imply a less than expected effect of dissolved interstitial impurities on the morphology of dislocations.

EC-03-02

Solid State Physics

EC-03-02-01

Neutron Scattering

FIELD-INDUCED-MAGNETIC-MOMENT FORM FACTOR OF METALLIC CHROMIUM
C. Stassis, G. R. Kline and S. K. Sinha
Phys. Rev. B 11, 2171 (1975)

Abstract--Polarized-neutron techniques have been used to study the spatial distribution and temperature dependence of the field-induced magnetic moment in metallic chromium. It is demonstrated that the coherent magnetic scattering of neutrons by the induced magnetic moment in chromium may be described in terms of free-ion form factors. The angular distribution of the magnetic scattering is best fitted by having a 60% 3d orbital-40% 3d spin contribution to the induced moment both above and below the antiferromagnetic transition temperature of the sample. The orbital and spin contribution to the static susceptibility were found to be $(98 \pm 3) \times 10^{-6}$ emu/mol and $(65 \pm 2) \times 10^{-6}$ emu/mol, respectively; the gyromagnetic ratio is 1.25 ± 0.04. These results are in good agreement with bulk-susceptibility measurements performed on the same sample, as well as with independent measurements of the gyromagnetic ratio of chromium. The magnitude of the localized induced moment has been found to be

temperature independent in the (27–200)°C temperature region. This result implies the absence of any well-defined local moment above the antiferromagnetic transition temperature of the sample.

LATTICE DYNAMICS OF GaSb
Marvin K. Farr, Joseph G. Traylor and S. K. Sinha
Phys. Rev. B 11, 1587 (1975)

Abstract--The lattice dynamics of gallium antimonide has been investigated experimentally using the method of coherent inelastic scattering of thermal neutrons. The frequencies for phonons propagating in the [001], [111], and [110] symmetry directions in an undoped gallium antimonide crystal at 300 K have been determined with an estimated precision of 2%. The sample had a carrier concentration of 4.85×10^{17} holes/cm^3 (upper limit) at 300 K. Both second-neighbor and first-neighbor shell models (SM) were fitted to the measured phonon dispersion curves. Some systematic trends among the fitted parameters for the first-neighbor SM for the gallium group-V compounds (GaP, GaAs, and GaSb) are discussed. The fitted second-neighbor SM parameters have been used to generate a phonon frequency distribution, which in turn has been used in the calculation of the temperature dependence of the specific heat at constant volume and the Debye Θ.

MAGNETIC SCATTERING OF NEUTRONS
C. Stassis and H. W. Deckman
Phys. Rev. B 12, 1885 (1975)

Abstract--The magnetic scattering of neutrons by an arbitrary system of particles has been examined by exploiting its similarity to the

radiation problem in spectroscopy. It has been shown, in fact, that the magnetic scattering amplitude can be expressed in terms of the multipole moments of the scattering system. The number of multipoles, which contribute to the scattering amplitude, is limited by selection rules based on the symmetry properties of the states of the system, in particular, parity and angular momentum conservation. The formalism has been applied to the magnetic scattering of neutrons by an atom in the $\underline{l}^{\underline{n}}$ electronic configuration. If the spin-other-orbit and orbit-orbit interactions in the atomic Hamiltonian can be neglected, only even-order electric and odd-order magnetic multipoles, whose order of multipolarity is less than or equal to $2\underline{l} + 1$, contribute to the scattering amplitude. In this case the calculation of the magnetic scattering amplitude is reduced to evaluating matrix elements of the Racah double tensors $\underline{W}^{(0,\underline{k})}$ and $\underline{W}^{(1,\underline{k}')}$ ($\underline{k}'$ even). The former tensors are associated with the convection current and the latter with the spin magnetization contribution to the magnetic scattering amplitude. The calculation of the matrix elements of these tensors is simplified by selection rules based on the groups $Sp(4\underline{l} + 2)$, $R(2\underline{l} + 1)$, $R(3)$, G_2 used in the classification of the atomic states. The contribution to the magnetic scattering amplitude of the convection current, associated with the spin-orbit and mass correction terms of the atomic Hamiltonian, has been examined in some detail.

EC-03-02-02
Experimental Physics

I. Electronic Structure and Magnetic Properties of Solids

ELECTRICAL RESISTIVITY AND MAGNETO-RESISTANCE OF VERY DILUTE Cu-Cr ALLOYS
S. Legvold, T. A. Vyrostek, J. A. Schaefer, P. Burgardt and D. T. Peterson
Solid State Comm. 16, 477 (1975)

Abstract--Measurements of the electrical resistivity from 1.5-80 K and the longitudinal magnetoresistivity from 0-95 kOe at 1.9, 4.2 and 25 K for very dilute Cr in Cu alloys are reported.

FERMI SURFACE "NESTING" IN Tb ALLOYS
P. Burgardt and S. Legvold
Proceedings of the 20th Annual Magnetism and Magnetic Materials - 1974 Conference, AIP Conference Proceedings No. 24, eds. C. D. Graham, Jr., G. H. Lander and J. J. Rhyne (New York: American Institute of Physics, 1975) pp. 418-419

Abstract--Magnetization and electrical resistivity measurements from 4.2 to 300 K have been made on alloys of Tb with Th, Mg, and Yb in order to test valency effects on magnetic ordering in Tb. Tetravalent Th raises E_F and promotes ferromagnetism by reducing the "nesting" feature in the Tb Fermi surface. Divalent Mg and Yb lower E_F to enhance the "nesting" feature and promote the helical structure. The results are understood in terms of valency effects on the Fermi surface and impurity size effects.

II. Nuclear Resonance in Solids

HYPERFINE FIELDS AND CRITICAL POINT EXPONENTS OF SOME TWO-DIMENSIONALLY LAYERED Fe(2+) SALTS

J. L. Schurter, R. G. Barnes and R. D. Willett

Proceedings of the 20th Annual Magnetism and Magnetic Materials - 1974 Conference, AIP Conference Proceedings No. 24, eds. C. D. Graham, Jr., G. H. Lander and J. J. Rhyne (New York: American Institute of Physics, 1975) pp. 307-308

Abstract--The nuclear hyperfine properties of the two-dimensionally layered antiferromagnetic ferrous chloride complexes, methylammonium ferrous chloride (MA_2FeCl_4) and benzylammonium ferrous chloride (BA_2FeCl_4), have been studied by (57)Fe Mössbauer spectroscopy. Temperature dependence of the effective magnetic hyperfine fields, as well as isomer shifts and quadrupole couplings, were determined by transmission experiments on powders. Saturation hyperfine fields and Neel temperatures were found to be: for MA_2FeCl_4, $H(0) = 280$ kOe and $T_N = 95.5$ K, and for BA_2FeCl_4, $H(0) = 265$ Oe and $T_N = 75.6$ K. Analysis of the hyperfine fields in terms of critical point behavior, $H(T)/H(0) = B(1 - T/T_N)^{\beta}$ yields for MA_2FeCl_4, $B = 1.10$ and $\beta = 0.23$, and for BA_2FeCl_4, $B = 1.04$ and $\beta = 0.28$. These values are compared with the predictions of the two-dimensional Ising model, $B = 1.22$ and $\beta = 0.125$, and with the exponents γ and γ' obtained previously from susceptibility measurements.

A MÖSSBAUER EFFECT STUDY OF ^{57}Fe IN TRANSITION METAL MONOBORIDES

D. B. DeYoung and R. G. Barnes

J. Chem. Phys. 62, 1726 (1975)

Abstract--The phase characteristics and nuclear hyperfine properties of 45 transition metal monoborides $M_{1-x}Fe_xB$ were studied by Mössbauer

effect spectroscopy of ^{57}Fe. Transmission measurements with powders were completed in the temperature range 4.2–1000 K; additional scattering and 18 kOe applied field data were collected at 300 K. Measured ^{57}Fe nuclear hyperfine parameters are discussed in terms of atomic bonding, charge transfer, and spontaneous magnetism in the borides. Within the context of the rigid band model, the isomer shift data for all boride phases indicate an electron transfer from boron to the metal 3d band. Similarly, the effective magnetic hyperfine field in ferromagnetic monoborides is proportional to the magnetization and also reveals a possible charge transfer from boron to metal. Quadrupole coupling constant results show a strong ionic contribution to the electric field gradient at the ^{57}Fe site in the monoborides. Measurements on FeB confirm the existence of two distinct structural modifications possessing different magnetic hyperfine fields but the same Curie temperatures. The defect (α) phase of FeB appears to be stabilized by the addition of manganese.

METHYL GROUP DEUTERON QUADRUPOLE COUPLING PARAMETERS IN SOLID TOLUENE-d_8, ortho- AND para-XYLENE-d_{10}

R. G. Barnes, W. C. Harper and D. R. Torgeson
J. Chem. Phys. 62, 4572 (1975)

Abstract--Quadrupole coupling constants and asymmetry parameters have been determined for the methyl group deuterons in toluene-d_8, $C_6D_5CD_3$ and in ortho- and para-xylene, o-$C_6D_4(CD_3)_2$ and p-$C_6D_4(CD_3)_2$ in polycrystalline samples at 77 K. The coupling constants e^2qQ/h for the three materials have an average value of 51.9 ± 1.5 kHz and are equal with experimental uncertainty. The asymmetry values η are non zero and are not

equal, presumably resulting from small differences in nearest neighbor environments of the methyl group deuteron sites, determined by details of the molecular packing in the solid phase.

NMR STUDY OF $CuAl_2$: ^{27}Al, ^{63}Cu, AND ^{65}Cu QUADRUPOLE AND ANISOTROPIC SHIFT INTERACTIONS

D. R. Torgeson and R. G. Barnes

J. Chem. Phys. 62, 3968 (1975)

Abstract--The nuclear magnetic resonance spectra of ^{27}Al, ^{63}Cu, and ^{65}Cu have been studied in a polycrystalline specimen of the intermetallic compound $CuAl_2$ of the C16 structure type at room temperature between 3 and 40 MHz. The ^{27}Al spectra yield to interpretation in terms of a completely anisotropic Knight shift and an asymmetric nuclear electric quadrupole interaction. The observed field separations of the several ^{27}Al quadrupole satellite spectral features at fixed frequencies yield values of the lowest quadrupole frequency ν_Q = 420.2(8) kHz and asymmetry paramcter η = 0.413(9). The ^{27}Al satellite features also yield the three Knight shift parameters K_x = 0.159(1)%, K_y = 0.153(2)%, and K_z = 0.148(10)%. Excellent agreement has also been obtained between the observed ^{27}Al central line shape and the theoretical shapes of J. F. Baugher, H. M. Kriz, P. C. Taylor, and P. J. Bray, J. Mag. Reson. 3, 415 (1970). The ^{63}Cu and ^{65}Cu central lines exhibit a strong second and a fourth order quadrupole splitting with $\nu_Q(^{63}Cu)$ = 7.54(17) MHz and $\nu_Q(^{65}Cu)$ = 7.05(18) MHz. An analysis of the copper Knight shifts is also presented.

TEMPERATURE INDEPENDENT ^{55}Mn MAGNETIC HYPERFINE FIELDS IN $ErMn_2$ AND $TmMn_2$

R. G. Barnes and B. K. Lunde

Proceedings of the 20th Annual Magnetism and Magnetic Materials - 1974 Conference, AIP Conference Proceedings No. 24, eds. C. D. Graham, Jr., G. H. Lander and J. J. Rhyne (New York: American Institute of Physics, 1975) pp. 217-218

Abstract--Analysis of the complex NMR spectra of ^{55}Mn in the hexagonal Laves phase compounds $ErMn_2$ and $TmMn_2$ reveals only a very slight temperature dependence of the ^{55}Mn Knight shift K at either of the two inequivalent lattice sites, in contrast to the Curie-Weiss behavior of the susceptibility of these compounds and their known ferromagnetic ordering properties. In addition, K differs negligibly from that in isostructural $ScMn_2$ which does not order magnetically. Both neutron diffraction and NMR data indicate that Mn carries no local moment, and the Knight shift measurements suggest that K results essentially entirely from the orbital contribution, K_{orb}. Unlike the case of the $LnAl_2$ cubic Laves phase compounds, for example, the net contribution to K resulting from indirect interaction between ^{55}Mn and the rare-earth moments is relatively small.

III. Superconductivity

COEXISTENCE OF SUPERCONDUCTIVITY AND THE KONDO EFFECT IN PbCe AND InCe QUENCH-CONDENSED FILMS

R. J. Delfs, B. J. Beaudry and D. K. Finnemore

Phys. Rev. B 11, 4212 (1975)

Abstract--The coexistence of superconductivity and the Kondo effect have been studied in quench-condensed films of PbCe and InCe. Both systems

show a Kondo effect and a regular depression of the superconducting transition temperature. Results show that the onset of superconductivity causes major changes in the formation of the Kondo state.

MEAN-FREE-PATH DEPENDENCE OF K_2 IN CLEAN SUPERCONDUCTORS
J. E. Ostenson and D. K. Finnemore
Phys. Rev. B 12, 114 (1975)

Abstract--The slope of the magnetization curve near the upper critical field H_{c2} has been measured for NbTa alloys in order to study systematically the deviations from the Eilenberger theory in the clean limit. K values determined from these slopes, K_2, agree well with the theory for K greater than 1.0, but the measurements lie well above the theory for $K < 1.0$. A study of pure V, as well as these alloys, shows that λ/ξ rather than ξ/l_{tr} is the important parameter governing the magnitude of the deviation.

ELECTRON PHONON INTERACTION IN THE PROXIMITY EFFECT REGIME
J. R. Toplicar and D. K. Finnemore
Proceedings of the 14th International Conference on Low Temperature Physics, Vol. 2., eds. M. Krusius and M. Vuorio (Amsterdam: North Holland Publishing Co., 1975) pp. 415-416

Abstract--Lifetime broadening is shown to be the major factor governing the transition temperature of superconducting proximity effect sandwiches.

IV. Thermodynamic and Transport Properties of Solids

THE ANNEALING OF DEFORMED POTASSIUM III. LENGTH-CHANGE MEASUREMENTS
D. Gugan
The Phil. Mag. 31, 453 (1975)

Abstract--Measurements of length-change have been used to study the recovery of high-purity potassium deformed by compression at 1·2K. There is a large annealing band between 1·2 and about 20 K, the relative length-recovery rate being roughly constant at about $2 \times 10^{-5} K^{-1}$, the total length-increase being about 1% of the original plastic compression. The recovery spectrum is quite different from the 15 K point-defect stage observed in resistivity studies on cold-worked potassium. It is shown that the point-defect recovery stage is not affected by dislocation movement involved in the length recovery, which itself reflects a strong temperature dependence of internal stress due to thermal activation over some obstacle to dislocation motion, perhaps the Peierls-Nabarro stress.

LOCAL CHARACTER OF MANY-BODY EFFECTS IN X-RAY PHOTO-EMISSION FROM TRANSITION-METAL COMPOUNDS: Na_xWO_3
M. Campagna, G. K. Wertheim, H. R. Shanks, F. Zumsteg and E. Banks
Phys. Rev. Lett. 34, 738 (1975)

Abstract--X-ray photoemission spectra of W core levels in metallic sodium tungsten bronzes, Na_xWO_3, clearly show asymmetries due to many-body effects. Na and O core levels show only the expected plasmon satellite, demonstrating the importance of the local density of states in the screening of the core hole.

SEARCH FOR CRYSTALLOGRAPHIC INSTABILITY IN HEXAGONAL TUNGSTEN BRONZES
A. C. Lawson, Z. Fisk and H. R. Shanks
Phys. Rev. B 11, 4054 (1975)

Abstract--X-ray powder diffraction at 6 K shows no evidence of crystallographic instability in $K_{0.3}WO_3$ and $Rb_{0.3}WO_3$.

THRESHOLD SWITCHING IN MELANIN
C. H. Culp, D. E. Eckels and P. H. Sidles
J. Appl. Phys. 46, 3658 (1975)

Abstract--Threshold-switching measurements of synthetic melanin confirm that this organic semiconductor switches to a low-resistance state in low electric fields as reported by McGinness et al. Time-dependent current-vs-voltage curves show that the time to traverse the negative-differential-resistance (NDR) segment is much slower than would be expected from electronic-switching mechanisms. Double-pulse measurements add to the evidence that thermal effects dominate electronic effects in melanin. A pseudomemory effect was found in melanin.

VARIABLE COMPOSITION THIN FILMS IN TERNARY CHALCOGENIDE SYSTEMS BY rf COSPUTTERING
B. F. T. Bolker, P. H. Sidles and G. C. Danielson
J. Vac. Sci. Tech. 12, 114 (1975)

Abstract--A combination of rf cosputtering and control of film temperature and film bias conditions have been investigated to determine the feasibility of obtaining films of many different compositions from a single main sputtering target. In the low Ge region of the Te-As-Ge ternary system each of these techniques was found to be effective. Tellurium was found to have a lower sticking coefficient than As and Ge and to preferrentially resputter.

EXPERIMENTAL EQUATIONS OF STATE FOR THE RARE GAS SOLIDS
M. S. Anderson and C. A. Swenson
J. Phys. Chem. Solids 36, 145 (1975)

Abstract--Piston-displacement equations of state (EOS) for the rare gas solids neon, argon, krypton and xenon have been determined to 20 kbar at temperatures from 4.2 K to the triple point in each case, with $\underline{V}(\underline{P}, \underline{T})$ relations which are believed to be accurate to roughly 0.1 per cent. The present paper describes the results for the three heavier solids, argon, krypton and xenon, and indicates consistency between these results and other low pressure experiments at all temperatures. In particular, the individual isotherms can be represented by $\underline{P}(\underline{V})$ relations which are suggested by the form of the Lennard-Jones potential, the bulk moduli are only slightly temperature dependent at constant volume, and the data for the three solids appear to obey a reduced EOS both at $\underline{T} = 0$ and near the triple point.

EXPERIMENTAL THERMAL EXPANSIONS FOR SOLID NEON, 2-14 K
J. C. Holste and C. A. Swenson
J. Low Temp. Phys. 18, 477 (1975)

Abstract--Linear thermal expansion measurements are reported for free-standing samples of solid neon at temperatures from 2 to 14 K. After normalization, the results agree well with x-ray data in an overlap region between 8 and 14 K. The $\underline{T} = 0$ Grüneisen parameter $\gamma_0 = 2.58$ ($\pm$ 0.05) is in excellent agreement with the results obtained from high-pressure equation of state data. Smoothed thermodynamic functions for solid neon at saturated vapor pressure are tabulated, and inconsistencies in published high-temperature bulk modulus results are discussed.

SENSITIVE APPARATUS FOR OBTAINING FREEZING CURVES. PURITY OF 4-AMINOPYRIDINE
Frederick R. Kroeger, C. A. Swenson, William C. Hoyle and Harvey Diehl
Talanta 22, 641 (1975)

Abstract--Freezing curves of highly-purified 4-aminopyridine have been obtained with an instrument of new design employing a gold crucible, a platinum resistance thermometer, electrical heating elements on crucible and heat shield, and accessory electrical control devices such that the temperature difference between crucible and shield could be maintained constant within 0.005° while the temperature of the 4-amino-pyridine and crucible dropped through the freezing range. No stirring was used. Methods were devised for handling the data as the derivative of temperature with respect to time and of correcting the freezing curve for the heat capacity of the crucible and charge. Although interpretation of the freezing curves obtained on the 4-aminopyridine was confused by attack on the gold by the molten 4-aminopyridine, the initial impurity in the 4-aminopyridine was probably less than the detection limit, 0.001 mole %.

V. Optical and Spectroscopic Properties of Solids

ANISOTROPIC INTERBAND EFFECTS IN ELECTROREFLECTANCE OF Ag
T. E. Furtak and D. W. Lynch
Phys. Rev. Lett. 35, 960 (1975)

Abstract--Measurements of the normal-incidence electroreflectance of clean, strain-free single crystals of Ag and Au with use of a novel drop-electrolyte technique show an anisotropy on the (110) face of Ag which is not present on Au. It can be explained by field-induced indirect interband

transitions which are observed in Ag but not in Au. This work shows that part of the electroreflectance spectrum of Ag arises from electrons which interact with the periodic crystal potential.

ANISOTROPIC OPTICAL PROPERTIES OF HEAVY-RARE-EARTH SINGLE CRYSTALS
J. H. Weaver and D. W. Lynch
Phys. Rev. Lett. 34, 1324 (1975)

Abstract--The optical absorptivities of oriented single crystals of hcp Gd, Tb, Dy, Ho, Er, Tm, and Lu were measured at 4.2 K between 0.2 and 4.4 eV. Polarized radiation was used to reveal the optical anisotropy. Systematic movement of structures in the absorptivity and optical conductivity was observed as a result of trends within sp and d bands. Low-energy structures were related to effects of s-f exchange interaction, but were more complicated than previously thought.

ELECTROREFLECTANCE OF GaAs AND GaP TO 27 eV USING SYNCHROTRON RADIATION
D. E. Aspnes, C. G. Olson and D. W. Lynch
Phys. Rev. B 12, 2527 (1975)

Abstract--Electroreflectance (ER) spectra of GaAs and GaP, taken with the Schottky-barrier method, exhibit to 27 eV the strong structural enhancement and high resolution characteristic of similar measurements below 6 eV. Above 20 eV, a new set of critical points are observed between the flat valence bands derived from the Ga 3d core levels and the local extrema of the sp^3 conduction bands. The attained resolution, of the order of 100 meV, enables us to resolve clearly the spin-orbit splitting of 0.50 eV of the 3d-derived valence bands. The following critical point energies have been determined in GaAs and GaP, respectively: sp^3

valence-conduction: E_1': 6.63 ± .05 eV and 6.80 ± .05 eV; $E_1' + \Delta_1'$: 6.97 ± .05 eV (GaAs only); E_0'' ($\Gamma_{15}^v \rightarrow \Gamma_{12}^c$): 10.53 eV and 9.38 ± .1 eV; E_0''' ($\Gamma_{15}^v \rightarrow \Gamma_1^c$): 8.33 ± .1 eV and 10.27 ± .1 eV; E_1'': 9.4 ± .2 eV and 10.7 ± .2 eV. E_5, E_6, and E_7 structures are observed at 15.1, 16.7, and 17.9 eV in GaAs, and at 14.7, 16.1, 18.6 eV in GaP. We have also determined energies of a number of conduction band states relative to the top of the valence band in both materials from ER spectra from the flat 3d valence bands. We find that the $L_{4,5}^v$ state is 0.95 ± .1 eV below Γ_8^v in both materials. The excitonic energy shift between the conduction states and the localized core hole in 3d valence band transitions is shown to be 0.4 eV in GaAs and 0.7 eV in GaP. Spectral features with initial structure less than 100 meV in width are observed above 20 eV, showing that broadening effects are much smaller in this energy range than previously believed.

INFRARED ABSORPTION OF CHROMIUM-RICH Cr-Fe, Cr-Co, AND Cr-Ni ALLOYS AT 4.2 K
D. W. Lynch, R. Rosei and J. H. Weaver
Phys. Stat. Sol. (a) 27, 515 (1975)

Abstract--The absorptivity of dilute Cr-based alloys with Fe, Co, Ni, and Ru has been measured at 4.2 K in the range of 0.08 to 1 eV (to 4.5 eV for some samples). Peaks indicating the occurrence of the incommensurate and commensurate antiferromagnetic phases are used to compare these alloys with those having Mn and V as solutes. Except for Cr-Ru, the peaks are much broader than when Mn is used as solute. As expected from neutron scattering and magnetic data on incommensurately ordered alloys, Fe and Co behave like Mn except that the formation of a virtual

bound state makes them less effective than Mn in raising the Fermi level; Ni probably behaves like V. When 2 to 7% Fe or 4% Co is present, the order is commensurate with the lattice, but the details of the absorptivity depend on the solute and its concentration. More than 7% Fe alters the Cr band structure sufficiently that the infrared peak characteristic of antiferromagnetic ordering is not present. Such band structure changes make the interpretation of magnetic data difficult.

LOW-ENERGY INTERBAND ABSORPTION IN Pd
J. H. Weaver and R. L. Benbow
Phys. Rev. B 12, 3509 (1975)

Abstract--The optical absorptivity of crystalline Pd was measured at 4.2 K between 0.15 and 4.4 eV. The data were Kramers-Kronig analyzed to determine the dielectric functions and the optical conductivity, σ. A strong maximum was observed in σ at 0.46 eV followed by a broad shoulder near 1.25 eV. These are interpreted in terms of transitions involving the bands near L in the Brillouin zone.

MULTIPLET STRUCTURE BELOW "THRESHOLD" IN APPEARANCE-POTENTIAL SPECTRA--LANTHANUM $N_{4,5}$
R. J. Smith, M. Piacentini and D. W. Lynch
Phys. Rev. Lett. 34, 476 (1975)

Abstract--We present the $N_{4,5}$ appearance-potential spectrum of La. Structure exists at energies lower than the threshold energy for transitions terminating at the Fermi level. Several similarities between optical absorption spectra and our results are discussed. These results contradict the simple model usually used to interpret appearance-potential spectra and emphasize the need for a new theory.

A NEW INTERPRETATION OF THE FUNDAMENTAL EXCITON REGION IN LiF

M. Piacentini

Solid State Comm. 17, 697 (1975)

Abstract--We have reanalyzed LiF optical data between 12 and 15 eV. We show that the conductivity spectrum can be fitted using effective mass theory for excitons with asymmetric Lorentzian lineshapes. We find the band gap is about 14.5 eV. The determination of the effective rydberg is not accurate enough to give the short-range correction to the hydrogenic energy for the $n = 1$ state.

OPTICAL ABSORPTION IN Al AND DILUTE ALLOYS OF Mg AND Li IN Al AT 4.2 K

R. L. Benbow and D. W. Lynch

Phys. Rev. B 12, 5615 (1975)

Abstract--The absorptances of Al and alloys of up to 5.5 at.% of Li and Mg in Al were measured at 4.2 K in the 0.2-3.0 eV range. The theory of Ashcroft and Sturm was fitted to the data. The fit obtained is reasonably good, provided three relaxation times are used, one for the Drude term and one for each type of transition between parallel bands. The fit is slightly better for the more concentrated alloys. In all cases the discrepancy between the fit and the data is greatest in the region between the two interband peaks in the optical conductivity, and known extensions to the theory do not qualitatively improve the fit. Pseudopotential Fourier coefficients $\underline{U}_{200}$ and $\underline{U}_{111}$ obtained from the fits vary with solute type and concentration. The variation can be explained semiquantitatively with a virtual-crystal pseudopotential.

OPTICAL PROPERTIES OF CRYSTALLINE TUNGSTEN
J. H. Weaver, C. G. Olson and D. W. Lynch
Phys. Rev. B 12, 1293 (1975)

Abstract--The optical properties of W are presented between 0.15 and 33 eV. The optical absorptivity or reflectivity was measured at near-normal incidence, and the data were Kramers-Kronig analyzed to determine the dielectric functions. Drude parameters were determined at low energy and were used to separate interband and intraband contributions to ϵ_2. Structures in ϵ_2 were apparent at 0.42, 0.97, 1.82, 2.35, 3.42, 5.25, 8.8, 11.3, 16.5, 22.5, and 31.5 eV. These features were discussed in terms of recent calculations of Christensen and Feuerbacher and by analogy to other transition metals studied. The loss functions were shown to have three volume plasmons (25.3, 15.2, and 10.0 eV) and three surface plasmons (20.8, 14.8, and 9.7 eV). Structure near 31.5 eV was interpreted as due to N_{VII} core transitions.

OPTICAL PROPERTIES OF Ti, Zr, AND Hf FROM 0.15 TO 30 eV
D. W. Lynch, C. G. Olson and J. H. Weaver
Phys. Rev. B 11, 3617 (1975)

The absorptivity or reflectivity of polycrystalline samples of Ti, Zr, and Hf was measured from 0.15 to ~30 eV. The data were Kramers-Kronig analyzed to determine the dielectric functions. Between ~0.2 and ~7 eV, each metal showed five structures in the absorptivity and ϵ_2. These were interpreted as interband transitions within the d bands. The ϵ_2 spectra had minima near 7 eV similar to that observed in the bcc transition metals. Additional structures at higher energy could be related to transitions involving highlying bands and the core levels. The electron-energy-loss functions were calculated and discussed in terms of volume and

surface plasmons. These metals, like the other transition metals studied, exhibited two volume and two surface plasmons.

TEMPERATURE MODULATION OF THE OPTICAL TRANSITIONS INVOLVING THE FERMI SURFACE IN Ag: THEORY
R. Rosei
Phys. Rev. B 10, 474 (1974)

Abstract--The thermomodulation mechanism for optical transitions originating or terminating near the Fermi surface in noble metals has been investigated. Detailed thermoderivative line shapes of $\Delta\epsilon_2$ for both inter-conduction-band transitions and transitions from the d bands to the Fermi surface have been calculated for Ag. The calculation also gives the temperature dependence of the joint density of states for these transitions.

THERMOMODULATION STUDY OF PLASMONS AND LONGITUDINAL EXCITONS IN ALKALI HALIDES
M. Piacentini, C. G. Olson and D. W. Lynch
Phys. Rev. Lett. 35, 1658 (1975)

Abstract--Thermoreflectance measurements on LiF and KCl were made from 10 to 30 eV using synchrotron radiation. Analysis of the differential dielectric and electron-energy-loss functions shows that the energy-loss peak generally attributed to the valence plasmon actually arises from the plasmon and overlapping longitudinal-exciton-like peak(s).

THERMOREFLECTANCE OF Mo FROM 0.5 TO 35 eV
J. H. Weaver, C. G. Olson, D. W. Lynch and M. Piacentini
Solid State Comm. 16, 163 (1975)

Abstract--The thermoderivative spectrum, $\Delta R/R$, is presented for Mo from 0.5 to 35 eV. Much of the observed structure is interpreted in terms of transitions involving states at the Fermi level. Spin-orbit splitting of the Δ_5 band is observed and is estimated to be 0.24 eV.

Structures at 10.3 and 24.2 eV are identified as thermally modulated volume plasmons. A large feature at 11.5 eV corresponds to transitions from the occupied d bands to high lying bands. Structure is observed at 33.7 eV which can be related to modulation of core state transitions.

THE SOLUBILITY OF RH_{2-x} IN Gd, Er, Tm, Lu AND Y FROM AMBIENT TO 850°C

B. J. Beaudry and F. H. Spedding

Met. Trans. B 6B, 419 (1975)

Abstract--The solubility of hydrogen in Gd, Er, Tm, Lu and Y was determined from 25 to 850°C when the metal was in equilibrium with RH_{2-x} (x varies between 0.1 and 0.2 depending on the rare earth metal). The room temperature solubilities determined by the lattice parametric method were found to be < 0.1, 3.6, 7.7, 20.6 and 19.0 at. pct H in Gd, Er, Tm, Lu and Y, respectively. The change in unit cell volume for each atomic percent hydrogen added was nearly the same for all metals. The solubility of hydrogen increases more rapidly with temperature in those metals with low solubility at room temperature. Thus the solubility of hydrogen at 850°C is nearly the same in all five of the metals studied, that is, 35.0, 36.2, 36.0, 36.0 and 37.3 at. pct H in Gd, Er, Tm, Lu and Y, respectively. The equilibrium pressure of H_2 in these studies was the equilibrium pressure of hydrogen in contact with RH_{2-x} at the temperature concerned. A change in slope was observed in the solubility curves of the Gd-, Er-, Tm- and Lu-H systems. The log C (at. pct H in R) was plotted vs $1/T$ for each system. Straight lines were obtained at temperatures above and below the changes in slope of the solubility curves. A calculation of the approximate

$\Delta\underline{H}$ of solution of $\underline{RH}_{2-\underline{x}}$ in the metals from the slope of the lines gave 4.35, 1.88, 1.28, 0.61 and 0.55 kcal/mole for Gd, Er, Tm, Lu and Y, respectively in the low temperature portion. The change in slope which occurs at some point between 350°C and 650°C, depending on the metal, indicates a lower heat of solution of $\underline{RH}_{2-\underline{x}}$ in these metals at the higher temperatures. In Lu there appears to be yet another change in slope in the neighborhood of 250°C.

THE USE OF INERT ATMOSPHERES IN THE PREPARATION AND HANDLING OF HIGH PURITY RARE EARTH METALS
B. J. Beaudry and P. E. Palmer
Proceedings of the 11th Rare Earth Research Conference, eds. John M. Haschke and Harry A. Eick (Traverse City, Michigan: USERDA, 1975) pp. 612

Abstract--The results of studies on the preparation of the rare earth metals by the calcium reduction of the rare earth fluorides under various conditions will be presented. It was shown that the major role of an inert atmosphere during the room temperature handling operations is to keep the calcium from oxidizing and to protect the as-reduced metal from the air. The effect of the reactants' purity on the purity of the final product is also discussed.

Data on the contamination of rare earth metals during cold working and heat treating procedures are presented. Methods to minimize contamination from the various mechanical operations and heat treating are described.

EC-03-02-03

Theoretical Physics

I. Optical and Surface Physics

THEORY OF THE OPTICAL PROPERTIES OF IONIC CRYSTAL CUBES
R. Fuchs
Phys. Rev. B 11, 1732 (1975)

Abstract--A theory is developed for the optical properties of particles of arbitrary shape, composed of a homogeneous isotropic material with a dielectric constant $\epsilon(\omega)$. The particles are so small that retardation can be neglected. An expression is obtained for the average dielectric constant of a medium containing a small fractional volume of particles. Calculations for a cube show that six resonances contribute to the optical absorption. They span a frequency range such that $\epsilon'(\omega)$, the real part of the dielectric constant, lies between -3.68 and -0.42, as contrasted with the single resonance for a sphere at $\epsilon'(\omega) = -2$. A comparison of the theory with experiments on the optical absorption of NaCl and MgO cubes shows that the width of the absorption peak can be explained by the frequency range of the cube resonances. Previous theories which assumed spherical particles required an unphysically high damping in $\epsilon(\omega)$ to account for the width.

p-POLARIZED OPTICAL PROPERTIES OF A METAL WITH A DIFFUSELY SCATTERING SURFACE
J. M. Keller, Ronald Fuchs and K. L. Kliewer
Phys. Rev. B 12, 2012 (1975)

Abstract--A theory is developed for the p-polarized optical properties of a semi-infinite electron gas with a surface that scatters the electrons

diffusely. The electron gas response is described by the Boltzmann equation. An important ingredient of the theory is the use of a legitimate distribution function for electrons leaving the surface, one which permits the normal component of the current density to vanish at the surface. It is found that the optical absorptance below the plasma frequency is an order of magnitude too large if this boundary condition on the normal component of the current is ignored by simply using the unperturbed distribution function for electrons leaving the surface. The calculated absorptance is compared for diffusely and specularly scattering surfaces. Below the plasma frequency the absorptance is higher for diffuse scattering, as is also true for s polarization, while above the plasma frequency the absorptance is essentially the same for diffuse and specular scattering. Interesting structure occurs in the vicinity of the plasma frequency.

PHOTOEMISSION STUDIES OF SILVER WITH LOW-ENERGY (3 TO 5 eV), OBLIQUELY INCIDENT LIGHT
J. K. Sass, H. Laucht and K. L. Kliewer
Phys. Rev. Lett. 35, 1461 (1975)

Abstract--By use of the photoemission-into-electrolyte technique, the photoyields of silver have been measured for p- and s-polarized light in the energy range 3 to 5 eV with a wide range of incident angles. Pronounced structure, providing striking evidence for the validity of the nonlocal theory of the surface photoeffect, is obtained.

LOCAL-FIELD EFFECTS, X-RAY DIFFRACTION, AND THE POSSIBILITY OF OBSERVING THE OPTICAL BORRMANN EFFECT: SOLUTIONS TO MAXWELL'S EQUATIONS IN PERFECT CRYSTALS
David Linton Johnson
Phys. Rev. B 12, 3428 (1975)

Abstract--The electromagnetic normal-mode solutions to Maxwell's equations in perfect crystals are investigated including local-field effects

by means of the dielectric-response matrix. The dynamical theory of x-ray diffraction is seen to be a special case thereof. At optical frequencies, a perturbation-theory expansion in q, the reduced wave vector, is solved and used to investigate the possibility that a microscopically varying component of the normal mode, $\underline{e}^{i(\vec{q} + \vec{K}).\vec{r}}$ ($\vec{K}$ is a reciprocal-lattice vector), can transmit into the vacuum. The optimal efficiency for this process is estimated to be 2.6×10^{-10} for $\hbar\omega = 1.5$ eV in diamond. However, this process may be affected by the intrinsic irregularities, on an atomic scale, of the crystal-vacuum interface.

II. Superconductivity

ON THE BREAKDOWN OF FORCE-FREE CONFIGURATIONS IN TYPE-II SUPERCONDUCTORS
J. R. Clem
Phys. Lett. 54A, 452 (1975)

Abstract--The steady-state time-averaged voltage produced along a current-carrying type-II superconductor in a longitudinal magnetic field cannot be described as a flux-flow voltage generated by an inward-collapsing array of helical vortices.

GUIDED FLUX MOTION AND FARADAY INDUCTION IN HOLLOW SUPERCONDUCTING CYLINDERS
S. M. Khanna, John R. Clem and M. A. R. LeBlanc
Low Temperature Physics - LT14, Vol. 2, eds. M. Krusius and M. Vuorio (Amsterdam: North Holland, 1975) pp. 461-464

Abstract--Experiments are reported which show that, when magnetic flux threading the hole and wall of a hollow superconducting Nb cylinder collapses after application of a heat pulse, the time-dependent and time-

integrated voltage pulses observed across contact points on the cylinder surface depend dramatically upon the spatial configuration of the voltage measuring leads relative to the direction of flux motion. Our theoretically calculated results are in good agreement with these observations.

MAGNETIC COUPLING FORCE OF THE SUPERCONDUCTING dc TRANSFORMER

J. W. Ekin and John R. Clem

Phys. Rev. B 12, 1753 (1975)

Abstract--The temperature dependence and magnetic field dependence of the coupling force have been measured in two transformer systems, one with primary and secondary film thicknesses d_p and d_s comparable with the superconducting penetration depth λ ($d_p/\lambda_p \sim d_s/\lambda_s \sim 1$) and one with film thicknesses small compared with the penetration depth ($d_p/\lambda_p \sim d_s/\lambda_s \sim 10^{-1}$). The results show that (i) the coupling force is nearly two orders of magnitude greater in the thick-film transformer than in the thin-film transformer; (ii) there exists a transition field above which the coupling force decreases very rapidly, typical values for the transition field being quite low (~0.5 G); and (iii) the temperature dependence of the coupling force over much of the range investigated is simply proportional to the temperature dependence of $\lambda_p^{-2}\lambda_s^{-2}$. A Gibbs-free-energy theory describing the coupling force has been numerically evaluated and compared with these data. The results show that the theory can be used to predict accurately both the absolute magnitude and the field and temperature dependences of the coupling force for wide-ranging values of the operating parameters.

SIMPLE MODEL FOR THE VORTEX CORE IN A TYPE II SUPERCONDUCTOR
John R. Clem
J. Low Temp. Phys. 18, 427 (1975)

Abstract--In order to model the core of an isolated vortex in a type II superconductor, a variational trial function for the magnitude of the normalized order parameter of the form $f = \rho/R$ is assumed, where ρ is the radial coordinate, $R = (\rho^2 + \zeta_v^2)^{1/2}$, and ζ_v is a variational core radius parameter. Remarkably simple analytic expressions for the magnetic flux density and supercurrent density that solve Ampere's law and the second Ginzburg-Landau equation are obtained. An analytic result for the free energy of the isolated vortex is then derived by integrating the Ginzburg-Landau free energy functional. The value of ζ_v that minimizes the free energy is calculated as a function of the Ginzburg-Landau parameter $\kappa = \lambda/\zeta$ and is found to range from $\zeta_v = 0.935\zeta$ for $\kappa = 0.707$ to $\zeta_v \simeq 1.414\zeta$ for $\kappa \gg 1$. A simple expression for the form factor or the Fourier transform of the flux density is obtained, which may be useful in the analysis of neutron diffraction experiments.

THEORY OF THE COUPLING FORCE IN MAGNETICALLY COUPLED TYPE-II SUPERCONDUCTING FILMS
John R. Clem
Phys. Rev. B 12, 1742 (1975)

Abstract--A pair of infinite type-II superconducting films with thicknesses d_p and d_s and penetration depths λ_p and λ_s separated by an insulating layer of thickness d_i is assumed to contain in the primary film a triangular vortex lattice, initially in perfect registry directly below an identical lattice in the secondary film. A theory is developed for the coupling force exerted upon a secondary vortex by the primary-vortex

lattice as a function of the displacement of the primary lattice relative to the secondary lattice. The theory is based upon a London model of the vortex line, modified to account for vortex-core effects. The theoretical maximum coupling force is largest at low flux density, where it has a value of order $\varphi_0^2/8\pi^2\rho_{eff}^2$, where $\varphi_0 = hc/2e$ and $\rho_{eff} = d_i + \lambda_p \coth(d_p/\lambda_p) + \lambda_s \coth(d_s/\lambda_s)$.

PHENOMENOLOGICAL THEORY OF THE LOCAL MAGNETIC FIELD IN TYPE-II SUPERCONDUCTORS
John R. Clem
Low Temperature Physics - LT14, Vol. 2, eds. M. Krusius and M. Vuorio (Amsterdam: North Holland, 1975) pp. 285-288

Abstract--Within the framework of the Ginzburg-Landau theory, the procedure of obtaining the local magnetic field by a linear superposition of contributions of individual flux lines is shown to be valid for all flux-line spacings, provided these contributions are calculated using the correct spatially-dependent magnitude of the order parameter that is appropriate for the given flux line spacing. The field contribution of an individual flux line can be approximated by a simple model involving two parameters, a core radius parameter, which is of the order of the Ginzburg-Landau coherence length, and a field-dependent penetration depth, which reduces to the weak-field penetration depth at low average flux density, increases with increasing flux density, and diverges at the upper critical field. This model, using only a single fitting parameter, is shown to give a good semi-quantitative overall description of the neutron diffraction form factors and the corresponding magnetic field distribution in niobium at 4.2 K.

ELECTRONICALLY DRIVEN LATTICE INSTABILITIES

S. K. Sinha and B. N. Harmon
Phys. Rev. Lett. 35, 1515 (1975)

Abstract--A general and physically simple model based on rigorous formulations of the dielectric function is presented and used to explain the phonon anomalies in niobium and niobium carbide. The model contains the explicit q dependence of both the electron-phonon and electron-electron interactions for localized states near the Fermi energy and appears quite useful for explaining the q dependence of phonon anomalies and lattice instabilities in various systems.

ENERGY BANDS, ELECTRONIC PROPERTIES, AND MAGNETIC ORDERING OF CrB_2

S. H. Liu, L. Kopp, W. B. England and H. W. Myron
Phys. Rev. B 11, 3463 (1975)

Abstract--The energy bands of the compound CrB_2 have been calculated by using the Korringa-Kohn-Rostoker method in the muffin-tin-potential approximation. The bands near the Fermi level have mostly Cr d character, and one of the bands gives rise to a very flat piece of Fermi surface perpendicular to the hexagonal axis. We propose that this piece of Fermi surface stabilizes a spin-density-wave state which manifests itself as antiferromagnetic ordering of the compound below 85 K. We also interpret the excess specific heat and electronic-spin susceptibility as due to exchange enhancement.

STATISTICAL THEORY OF MAGNETIC EXCITATIONS IN HEISENBERG PARAMAGNETS

S. H. Liu and P. A. Swanson

Proceedings of the 20th Annual Magnetism and Magnetic Materials - 1974 Conference, AIP Conference Proceedings No. 24, eds. C. D. Graham, Jr., G. H. Lander and J. J. Rhyne (New York: American Institute of Physics, 1975) pp. 163

Abstract--We propose a statistical method to calculate the dynamical correlation function $G(\vec{q}, t) = \langle \vec{S}_{\vec{q}}(t) \cdot \vec{S}_{-\vec{q}}(0) \rangle$ for the Heisenberg model above the ordering temperature. The function may be expanded into a power series of the time and the coefficients are expressed in terms of static multi-spin correlation functions. In the limit $\lambda > q^{-1} > r$, where λ is the spin correlation length and r is the range of interaction, the dominant contributions to the coefficients come from spins within correlated clusters. Therefore, we treat the dynamics of such a cluster by the spin-wave theory for an infinite crystal, then weigh the contribution of each cluster to $G(\vec{q}, t)$ according to its probability. The result is that the excitations in the range $q\lambda > !$ are magnon-like modes broadened by a mean-free-path measured by λ. In addition, there is a central peak at zero frequency, which is the diffused remnant of the magnetic Bragg peak. The theory compares favorably with the neutron scattering data on TMMC and nickel.

THEORETICAL DETERMINATION OF THE INDUCED MAGNETIZATION DENSITY AND FORM FACTOR OF PALLADIUM

A. J. Freeman, B. N. Harmon and T. J. Watson-Yang

Phys. Rev. Lett. 34, 281 (1975)

Abstract--Induced magnetization densities determined from an *ab initio* augmented-plane-wave wave-function study of Pd metal including local density-of-states effects on the Fermi surface were found to yield

a neutron magnetic form factor in excellent agreement with the recent experiments of Cable et al. A remarkable feature of these solid-state spin densities is their spatial localization which is greater than even the very contracted Hartee-Fock density of the free Pd^{2+} ion.

THEORETICAL MAGNON DISPERSION CURVES FOR Gd
P.-A. Lindgård, B. N. Harmon and A. J. Freeman
Phys. Rev. Lett. 35, 383 (1975)

Abstract--The magnon dispersion curve of Gd metal has been determined from first principles by use of augmented-plane-wave energy bands and wave functions. The exchange matrix elements $\underline{I}(\vec{k},\vec{k}')$ between the 4f electrons and the conduction electrons from the first six energy bands were calculated under the assumption of an unscreened Coulomb interaction. The results are in good overall agreement with experiment provided the $\underline{I}(\vec{k},\vec{k}')$ are diminished by a constant scale factor of about 2 which may be caused by screening.

EC-03-03

Materials Chemistry

EC-03-03-01

Chemical Structures

I. X-Ray and Neutron Crystallography

DODECAMETHYL CYCLOHEXAGERMANE, $C_{12}H_{36}Ge_6$
W. Jensen, R. Jacobson and J. Benson
Cryst. Struct. Comm. 4, 299 (1975)

Abstract-- Compounds of the type $Ge_xSi_{6-x}(CH_3)_{12}$ where $1 \leq X \leq 6$ have similar x-ray diffraction powder patterns. The single crystal x-ray diffraction study of $Ge_6(CH_3)_{12}$ was undertaken to establish the structural similarities of these compounds.

PROPELLANES. VII. BRIDGEHEAD OLEFINS VIA ACETOLYSIS
Philip Warner, Shih-Lai Lu, Elaine Myers, Patrick W. DeHaven and Robert A. Jacobson
Tet. Lett. 4449 (1975)

Abstract--In recent studies of the chemistry involved in the Ag^+-assisted solvolysis of tricyclic cyclopropyl halides, evidence has accumulated for the protic capture of bridgehead olefin intermediates. Product studies which also implicate bridgehead olefins are now reported.

THE CRYSTAL AND MOLECULAR STRUCTURE OF THE β-PICOLINE-N-OXIDE-FUMARIC ACID ADDUCT

B. T. Gorres, E. Ray McAfee and R. A. Jacobson

Acta Cryst. B31, 158 (1975)

Abstract--The crystal structure of the β-picoline-N-oxide-fumaric acid adduct, $2(C_6H_7NO) \cdot C_4H_4O_4$, has been determined by three-dimensional x-ray analysis. The crystals were monoclinic, space group $P2_{1/c}$, $a = 3.888 \pm 0.003$, $b = 14.194 \pm 0.010$, $c = 14.663 \pm 0.011$ Å, $\beta = 98.85 \pm 0.01°$, and $Z = 2$. The structure was solved by a symmetry-map frequency-check procedure in conjunction with a roving molecular fragment. A full-matrix weighted least-squares refinement modified to include a secondary extinction parameter gave a final conventional discrepancy index of $R = 0.052$ and a weighted discrepancy index of $wR = 0.037$ for 533 reflections $[I_N > 3\sigma(I)]$ recorded by a scintillation counter method. The β-picoline-N-oxide and the fumaric acid moieties are held together by hydrogen-bonding forces and are planar to within 0.020 and 0.001 Å, respectively. A strong hydrogen bond between the OH group of the acid and the oxygen of the β-picoline-N-oxide ring appears to hold the adduct together. This short O···O distance of 2.517 ± 0.006 Å lies within a range characteristic of a symmetric hydrogen bond.

AN X-RAY INVESTIGATION OF DL-(ETHYLVALINATE-N,N-DIACETATO)-DIAQUOCOPPER(II)

J. Rodgers and R. A. Jacobson

Inorg. Chim. Acta 13, 163 (1975)

Abstract--A single-crystal x-ray structure investigation of the DL form of (ethylvalinate-N,N-diacetato)diaquocopper(II) has been carried out. The compound crystallizes in the monoclinic space group $P2_1/n$, with

a = 7.50 ± 0.01, b = 28.60 ± 0.01, c = 7.50 ± 0.01 Å, β = 91.27 ± 0.01°, and Z = 4. Least-squares refinement on 1252 reflections with $|F_o| > 3\sigma(F)$ resulted in a final discrepancy factor of 0.130. The stereochemistry around the copper is distorted octahedral, the equatorial co-ordination consisting of the tertiary nitrogen, the two acetate oxygens, and a water molecule. Here, the bonding distances to the metal range from 1.94(1) to 2.04(1) Å. The second water molecule occupies an axial position at a greater distance from the metal (2.32(1) Å), while the ether oxygen of the ester linkage occupies an opposite axial position, lying at 2.84(2) Å from the metal. The ester carbonyl group is not co-ordinated. The ester chain is partially disordered, corresponding to a randomness of the two isomers.

CRYSTAL AND MOLECULAR STRUCTURE OF ORGANOPHOSPHORUS INSECTICIDES. I. RONNEL
Russell G. Baughman and Robert A. Jacobson
Agri. Food Chem. 23, 811 (1975)

Abstract--The crystal and molecular structure of ronnel (O,O-dimethyl O-2,4,5-trichlorophenyl phosphorothioate, $(H_3CO)_2PSOC_6H_2Cl_3$, monoclinic, $P2_1/c$, a = 12.162 (9), b = 9.990 (8), and c = 11.98 (1) Å, β = 113.61 (4)°, Z = 4, Mo Kα radiation) has been determined by three-dimensional x-ray analysis. The structure was solved by direct methods and refined by full-matrix least-squares procedures to a final discrepancy index R = 0.061 for 1905 observed reflections ($F_o > 2.5\sigma(F_o)$). The structure displays a hydrogen-sulfur intermolecular bond in the b direction and a phosphorus which is readily accessible for phosphorylation of acetylcholinesterase. The phosphorus-"ring center" distance of 4.05 Å corresponds quite well to the 4.10-Å nitrogen-carboxyl carbon distance in acetylcholine.

MOLECULAR STRUCTURE OF THE CARCINOSTAT ISOPHOSPHAMIDE
H. A. Brassfield, R. A. Jacobson and J. G. Verkade
J. Am. Chem. Soc. 97, 4143 (1975)

Abstract--A crystal and molecular structure determination of isophosphamide, a potent carcinostat has been carried out. The space group is Pbca and the unit cell parameters are a = 13.29(1), b = 21.16(1) and c = 8.78(1) Å. The P=O group is in an axial rather than equitorial position.

POTASSIUM TETRABROMOPALLADATE(II)
Don S. Martin Jr., John L. Bonte, Rhonda M. Rush and Robert A. Jacobson
Acta Cryst. B31, 2538 (1975)

Abstract--Tetragonal, P4/mmm, a=b=7.409(12), c = 4.309(7) Å; K_2PdBr_4, Z = 1, D_x = 3.54 g cm^{-3}. The dark brown crystals were grown from the aqueous solution by evaporation. The structure, refined to R = 0.040, is isomorphous with K_2PtCl_4 with a Pd-Br distance of 2.444(3) Å.

II. Low Oxidation States

RARE EARTH METAL-METAL HALIDE SYSTEMS. XVIII. HOLMIUM-HOLMIUM(III) CHLORIDE SYSTEM. HOLMIUM IN THE DIVALENT STATE
Ulrich Löchner and John D. Corbett
Inorg. Chem. 14, 426 (1975)

Abstract--The phase study of the system $HoCl_3$-Ho is reported. The only reduced chloride formed therein, $HoCl_{2.14\pm0.01}$, melts incongruently at 551 (±1)°, only slightly higher than the temperature of the system eutectic, 543° (at 17.1% Ho). The limited stability of this phase and the apparent absence of any reduced bromide or iodide of holmium is interpreted and generalized in terms of systematics expected for the phase relationships. The formation of a reduced holmium chloride phase is in good accord with expectations from Born-Haber calculations.

POLYIODINE CATIONS AS CHLOROMETALATE SALTS. SYNTHESIS AND NUCLEAR QUADRUPOLE RESONANCE CHARACTERIZATION OF TRIIODINIUM, PENTAIODINIUM, AND CHLORODIIODINIUM TETRACHLOROALUMINATES, I_3AlCl_4, I_5AlCl_4 AND $I_2ClAlCl_4$

Don J. Merryman, John D. Corbett and Paul A. Edwards

Inorg. Chem. 14, 428 (1975)

Abstract--Reactions of I_2 with $ICl-AlCl_3$ mixtures have been investigated by thermal, microscopic, and x-ray analysis. The system contains only the phases I_3AlCl_4, I_5AlCl_4, and $2ICl \cdot AlCl_3$ ($=I_2ClAlCl_4$) which melt at 45, 50–50.5, and 53°, respectively. Comparable polyhalogen derivatives of the anions $FeCl_4^-$, $HfCl_6^{2-}$, and $TaCl_6^-$ do not exist and neither do any compounds with compositions corresponding to I_4Cl^+, $I_3Cl_2^+$, I_2^+, or Br_3^+ with $AlCl_4^-$ or $SbCl_6^-$ anions or the phase $ICl \cdot TaCl_5$. Unfavorable physical characteristics of the three new phases preclude many normal methods of characterization but the ^{35}Cl and ^{127}I nqr and ^{27}Al nmr spectra for these and the compound ICl_2AlCl_4 provide substantial information, indicating that the compounds contain normal "ionic" $AlCl_4^-$ groups and therefore the cations I_3^+, I_5^+, I_2Cl^+, and ICl_2^+. A bonding angle of 97° is obtained from the observed ^{127}I data in I_3^+; I_2Cl^+ and ICl_2^+ appear closely analogous. Bond populations and atom charges inferred from the nqr data for these cations are given. Properties of chlorometalate anions which appear important for the stabilization of these cations are considered. The published estimation of the chloride ion affinity of $FeCl_3(g)$ is corrected to a value of about 85 kcal/mol.

STABLE HOMOPOLYATOMIC ANIONS: THE CRYSTAL STRUCTURES OF SALTS OF THE ANIONS PENTAPLUMBIDE(2-) AND ENNEASTANNIDE(4-)
John D. Corbett and Paul A. Edwards
J. Chem. Soc. Chem. Comm. 984 (1975)

Abstract--The unique trigonal bipyramidal Pb_5^{2-} and unicapped antiprismatic Sn_9^{4-} anions have been discovered by x-ray structural studies on their salts with Na^+(2,2,2-crypt).

SYNTHESIS OF STABLE HOMOPOLYATOMIC ANIONS OF ANTIMONY, BISMUTH, TIN, AND LEAD. THE CRYSTAL STRUCTURE OF A SALT CONTAINING THE HEPTAANTIMONIDE(3-) ANION
John D. Corbett, Douglas G. Adolphson, Don J. Merryman, Paul A. Edwards, Frank J. Armatis
J. Am. Chem. Soc. 97, 6267 (1975)

Abstract--The heavy post-transition metals have long been claimed to form homopolyatomic anions in liquid ammonia. However, no isolation and characterization has heretofore been possible. A general solution of this problem is described. Synthesis of polyanions of tin, lead, antimony and bismuth is achieved through the reaction of the strong complexing agent 'crypt' with the respective alkali metal intermetallic phases. The crystal structure of such a salt of the Sb_7^{3-} ion is described.

III. Chemistry of the Heavy Transition Metals

SYNTHESIS AND STRUCTURE OF DINUCLEAR NIOBIUM AND TANTALUM COMPLEXES CONTAINING AN UNUSUAL BRIDGING LIGAND DERIVED FROM ACETONITRILE
Patricia A. Finn, Margaret Schaefer King, Peter A. Kilty and Robert E. McCarley
J. Am. Chem. Soc. 97, 220 (1975)

Abstract--Reactions of $TaCl_4$ or $TaBr_4$ with neat acetonitrile were found to provide low yields of compounds having composition $TaX_3(CH_3CN)_3$,

X = Cl or Br. Zinc metal added to these solutions provided increased yields, and added to a solution of $NbCl_5$ provided $NbCl_3(CH_3CN)_3$. Subsequent chemical and spectroscopic studies revealed that one of the nitrile ligands L was modified in the reactions as indicated by the formulation $MCl_3(CH_3CN)_2L$, M = Nb or Ta. Reaction of the niobium compound with bis(triphenylphosphine)-iminium chloride in acetonitrile, followed by addition of chlorobenzene provided crystals for x-ray structure determination. Solution and refinement of the structure showed that the compound was correctly formulated as $\{[(C_6H_5)_3P]_2N\}_2[Nb_2Cl_8(CH_3CN)_2(C_4H_6N_2)]\cdot 2C_6H_5Cl$, monoclinic space group $P2_1/n$, a = 14.95(1), b = 20.96(1), c = 15.09(1)Å, β = 105.9(1)°, Z = 2. In the anion $[Nb_2Cl_8(CH_3CN)_2(C_2H_6N_2)]^{2-}$ the two Nb-atoms are bound to the N-atoms of the unique planar bridging ligand $NC(CH_3)C(CH_3)N$, which evidently is formed by reductive coupling of two acetonitrile molecules through the C-atoms of the nitrile functionality. Bond distances and angles within the chain Nb-N-C-C-N-Nb suggest extensive π-electron delocalization over all atoms of the chain, with double or triple bond character in the Nb-N bonds.

SPECIES WITH STRONG HETERONUCLEAR METAL-METAL BONDS. DIMERS WITH TUNGSTEN-MOLYBDENUM BONDS OF ORDER 3.5 AND 4.0
V. Katović, J. L. Templeton, R. J. Hoxmeier, R. E. McCarley
J. Am. Chem. Soc. 97, 5300 (1975)

Abstract--The first heteronuclear metal-metal bonded dimer of bond order 3.5 has been prepared by selective oxidation of $MoW(O_2CC(CH_3)_3)_4$-$Mo_2(O_2CC(CH_3)_3)_4$ mixtures in benzene solution with iodine. The resulting product was precipitated as $[MoW(O_2CC(CH_3)_3)_4]I$ and subsequently recrystallized from acetonitrile to provide the acetonitrile adduct $[MoW(O_2CC(CH_3)_3)_4]$

CH_3CN. Red brown crystals of the latter were orthorhombic with a = 35.59(3), b = 36.22(3), c = 10.01(1) Å, space group Fdd2, $\rho_{calc.}$ = 1.76 g cm^{-3} for 16 formula units per unit cell. Solution and refinement of the structure revealed a molecular unit with the I-atom bound to W, d(W-I) = 3.054(2)Å, and the N-atom of acetonitrile weakly bonded to Mo, d(Mo-N) = 2.71(2)Å. Other features of the structure were entirely analogous to those of $Mo_2(O_2CCH_3)_4$, with d(Mo-W) = 2.194(2), d(Mo-O, ave.) = 2.081(13), d(W-O, ave.) = 2.064(13)Å. The very short Mo-W bond of order 3.5 is considered to be polarized with a higher formal charge residing on tungsten. Reduction of the iodide derivative with zinc in acetonitrile is shown to provide $MoW(O_2CC(CH_3)_3)_4$, the first pure heteronuclear dimer with metal-metal bond order of 4.0.

EC-03-03-02

Engineering Chemistry

I. Liquid Metals

THE HIGH-TEMPERATURE ENTHALPY OF LIQUID LANTHANUM BY LEVITATION CALORIMETRY
Lawrence A. Stretz and Renato G. Bautista
J. Chem. Thermodynamics 7, 83 (1975)

Abstract--A levitation calorimetry technique was used to measure the enthalpy of liquid lanthanum from 1250 to 2420 K. Lanthanum samples ranging from 0.5 to 2 g were levitated and melted in an inert atmosphere using a 15 KV A, 450 kHz radio-frequency generator. The results, in the temperature range 1250 to 2420 K, were fitted by the following equation

where the indicated errors were obtained from the average deviation of the results from the values predicted by the equation:

$$\{\underline{H}(\underline{T})-\underline{H}(298.15\ K)\}/J\ mol^{-1} = (32.77 \pm 0.18)(\underline{T}/\underline{K})-(2289\pm343).$$

Convection and radiation heat losses during the fall of the sample from the levitation chamber into the calorimeter amounted to 0.5 to 2.0 per cent and 2 to 5 per cent of the total enthalpy respectively. The levitation calorimetry method is estimated to have a maximum error of ±2.5 per cent.

THE THERMODYNAMIC PROPERTIES OF LIQUID NEODYMIUM BY LEVITATION CALORIMETRY
Lawrence A. Stretz and Renato G. Bautista
High Temp. Sci. 7, 197 (1975)

Abstract--A radio-frequency generator, providing sample levitation and heating, was used in combination with a conventional copper block drop calorimeter to experimentally measure the enthalpy of molten neodymium samples. An inert atmosphere consisting of an argon-helium mixture was utilized to prevent sample oxidation and aid in temperature control. Sample sizes ranged from 0.5 to 1.5 grams. The data were fitted by the following equation where the indicated error represents the average deviation of the experimental values from the values predicted by the equation:

$$\underline{H}_{\underline{T}} - \underline{H}_{298.15} = \{44.04 \pm 0.38\}\ (\underline{T} - 1297) \times \{47,049 \pm 251\}\ J/mol$$

$$1446\ K < \underline{T} < 2246\ K.$$

The maximum estimated error for the heat content, including corrections for convection and radiation heat losses during the drop, is ± 2.5 per cent.

II. Fluid Dynamics

SIMULATION FOR CONTROL SYNTHESIS OF A PLUTONIUM-URANIUM EXTRACTION COLUMN
E. B. McCutcheon, L. E. Burkhart and R. E. Felt
Trans. Am. Nucl. Soc. 22, 317 (1975)

Abstract--Simulation of an extraction column for separating uranium and plutonium in a plutonium recycle extraction flowsheet was undertaken to determine the mechanism of partition failure which had been experienced in plant operations. A careful study of the mechanisms and rate constants for the competing reactions in the column showed that five principal reactions involving plutonium, nitric acid, nitrous acid, hydroxylamine and hydrazine were sufficient to simulate the primary transient behavior of the system. Subsequent work with the simulation model revealed that control of the nitrous acid catalyst, produced by the autocatalytic oxidation of Pu(III) with nitric acid was responsible for the dominant mode of partition failure under conditions encountered in the plant. The overriding importance of this reaction was a result of the high plutonium concentrations maintained in a system employing plutonium recycle.

EC-03-03-03

High Temperature and Surfaces Chemistry

I. High Temperature Chemistry

FIRST PERIOD TRANSITION METAL SULFIDE GASEOUS MOLECULES: MATRIX SPECTRA, OXIDE-SULFIDE CORRELATION, AND TRENDS
T. C. DeVore and H. F. Franzen
High Temp. Sci. 7, 220 (1975)

Abstract--Infrared spectra for the gaseous monosulfides of Ti, V, Cr, Mn, Fe, and Ni and electronic transitions for the gaseous monosulfides

of V, Cr, and Fe have been observed in Ar and OCS matrices. All infrared frequencies were observed between 500 and 600 cm^{-1}. The sulfide force constants ($\underline{K}_{ms}$) were found to be related to those of the isoelectronic oxide ($\underline{K}_{mo}$) by the equation

$$\frac{\underline{D}_{mo}\underline{K}_{ms}}{\underline{D}_{ms}\underline{K}_{mo}} \approx 0.769,$$

where $\underline{D}$ is the dissociation energy. A schematic MO diagram is presented which explains the observed trends in the dissociation energies and the force constants.

THE NiAs-MnP PHASE TRANSITION IN VS
H. F. Franzen and G. A. Wiegers
J. Solid State Chem. 13, 114 (1975)

Abstract--Results of measurements of the lattice parameters, magnetic susceptibility, and electrical resistivity of stoichiometric VS as functions of temperature through the MnP-NiAs transition region are reported and discussed. The properties are found to be consistent with a metallic solid in which the Fermi energy passes through a marked change in the density of states with the concurrent formation of zigzag metal chain in the a-b plane.

SPECTRUM OF VANADIUM IN RARE GAS MATRICES
T. C. DeVore
J. Chem. Phys. 62, 520 (1975)

Abstract--The spectrum of V isolated in Ar and Kr matrices at 10 K has been correlated with the gas phase spectrum. The electron configuration was found to be a major factor in determining the direction and the magnitude of the matrix shift for this system. A model calculation was performed using extended Hückel theory. A plausible explanation for the origin of the matrix

shifts and the altered intensity relationships observed in the matrix has been developed.

VARIATION OF LATTICE PARAMETERS IN TiS-VS SOLID SOLUTIONS
H. F. Franzen, D. H. Leebrick and F. Laabs
J. Solid State Chem. 13, 307 (1975)

Abstract--Results of measurements of lattice parameters and densities in nonstoichiometric solid solutions of titanium and vanadium monosulfide are reported and discussed. The results indicate that a second-order phase transition from the NiAs-type of MnP-type structure occurs at an intermediate composition, and that the phase transition is accompanied by a marked change in the rate of change of the metal-metal distances in the c-axis direction.

THE VISIBLE ABSORPTION SPECTRA OF Mn_2, Fe_2, AND Ni_2 IN ARGON MATRICES
T. C. DeVore, A. Ewing, H. F. Franzen and V. Calder
Chem. Phys. Lett. 35, 78 (1975)

Abstract--Electronic absorption bands in the visible spectral region have been observed for Mn_2, Fe_2 and Ni_2 in argon matrices at 10 K.

AN X-RAY PHOTOELECTRON STUDY OF $V_{0.92}S$ WITH THE NiAs-TYPE STRUCTURE
H. F. Franzen and G. A. Sawatzky
J. Solid State Chem. 15, 229 (1975)

Abstract--An x-ray photoelectron study of defect vanadium monosulfide reveals that this compound can be thought of as an intermetallic compound with relatively little charge transfer between vanadium and sulfur atoms. This conclusion is reached from a study of the core electron binding energies, as well as from the strong band mixing found for the conduction and valence bands.

II. Surface Chemistry and Catalysis

A MOLECULAR ORBITAL INVESTIGATION OF CHEMISORPTION. II. NITROGEN ON TUNGSTEN (100) SURFACE

Leon W. Anders, Robert S. Hansen and L. S. Bartell
J. Chem. Phys. 62, 1641 (1975)

Abstract--The relative bonding energies of nitrogen chemisorbed at three symmetric sites on a W(100) surface, represented by finite arrays of tungsten atoms were obtained by means of the extended Hückel molecular orbital theory (EHMO). The preferred site for nitrogen chemisorption was found to be the five coordination number (5 CN) site or the fourfold site with a tungsten atom below four tungsten atoms surrounding the nitrogen atom. The 5p orbital repulsive energy, in the case of hydrogen chemisorption, could be adequately approximated by the sum over pairs of empirical exponential repulsive terms; in the case of nitrogen chemisorption, this same method was approximately 10% in error at the equilibrium bond distance, and repulsive energies were therefore obtained from calculations including tungsten 5p orbitals but with smaller arrays.

MIXED ADSORPTION OF CARBON MONOXIDE AND OXYGEN ON TUNGSTEN (100), (110), AND (111) SINGLE CRYSTAL FACES

Leon W. Anders and Robert S. Hansen
J. Chem. Phys. 62, 4652 (1975)

Abstract--Flash desorption spectra of $C^{16}O$ and $C^{18}O$ were measured for $C^{16}O$ dosed on tungsten (100), (110), and (111) at 300 K with varying $^{18}O_2$ predoses and postdoses. Heavy doses of $C^{16}O$ resulted in flash desorption spectra characterized by a single α peak and two β peaks on each of W(100) and W(110) crystal faces, and single sharp α and β peaks on the W(111) crystal face. Predoses or postdoses of $^{18}O_2$ resulted in extensive

isotope exchange in all β peaks, and slight exchange in all α peaks. Postdosing of a $C^{16}O$ monolayer by $^{18}O_2$ resulted in no change in total CO on the surface, although in cases where two β peaks occurred, that state desorbing at lower temperature was enhanced at the expense of that desorbing at higher temperature. With increasing predose of $^{18}O_2$ the total β-CO resulting from a fixed $C^{16}O$ dose steadily decreased, and the amount of α-CO at first increased, then decreased. The results are broadly in accord with the Goymour-King model, according to which β states arise from dissociatively chemisorbed CO, α states from CO associatively adsorbed on isolated single sites. Isotopic exchange at low $C^{16}O$ doses followed by heavy $^{18}O_2$ doses appears best interpreted in terms of random selection of oxygen from immediate neighbors in an immobile monolayer, rather than in terms of random mixing of oxygen isotopes over the entire monolayer.

COAGULATION KINETICS AND BIMOLECULAR REACTION KINETICS
R. S. Hansen
H. van Olphen and Karol J. Mysels, eds. Physical Chemistry: Enriching Topics from Colloid and Surface Science Chapter 13 IUPAC Commission (LaJolla, Cal.: Theorex, 1975) pp. 201-218

Abstract--The frequency with which two kinetic units, be they molecules or ions or colloidal particles, meet each other is basic to the rate at which a homogeneous reaction between them can occur. The fundamentals of a broadly based unified view of this process are presented in this chapter beginning with elementary considerations and ending with an alternative point of view.

AN ELECTROCAPILLARY STUDY TO TEST THE APPLICABILITY OF THE FLORY-HUGGINS ISOTHERM

K. G. Baikerikar and Robert S. Hansen

Surface Sci. 50, 527 (1975)

Abstract--The Flory-Huggins isotherm with interaction parameter has been tested using accurate electrocapillary data for four aliphatic compounds at the mercury-electrolytic solution interface. When surface coverages derived by differentiation of surface pressure-activity data were tested in the Flory-Huggins isotherm and when all parameters were freely optimized, the equation fit the data very well in all cases, but the size ratio parameter thus obtained was about 0.5. When parameters of the Flory-Huggins isotherm were fixed by limiting properties of surface pressure-activity data directly (with no differentiations performed), the size parameter was about 1.0. The size parameter expected physically is about 3.0. The Flory-Huggins isotherm with realistic size parameters did not fit the data as well as the simpler Frumkin equation in any of the cases considered. The physical basis underlying both models is weak for interaction parameters as large as encountered in aqueous-organic solute systems.

ELECTROSORPTION OF SOME ALIPHATIC COMPOUNDS AT THE MERCURY-SOLUTION INTERFACE

K. G. Baikerikar and Robert S. Hansen

J. Colloid Interface Sci. 52, 277 (1975)

Abstract--The electrochemical adsorption of four aliphatic compounds, i.e., n butanol, isopentanol, n-pentanoic acid, and n-hexanoic acid has been investigated by employing a capillary electrometer of greatly improved sensitivity.

8

As observed by previous workers from this laboratory, for each adsorbate, π versus ln $\underline{a}$ curves at different polarizations were found to be superimposable by abscissa translation implying thereby that the adsorbate-adsorbate interactions in the surface layer are independent of the electrical nature of the interface and that the surface charge density varies linearly with surface excess at fixed polarization. The improved precision attained in the measurements of interfacial tension permitted construction of well-documented $\ln(\pi/\underline{a})$ versus π curves; such plots do not appear to have been published before. These curves resemble parabolas and for a given adsorbate, the family of these curves obtained at different polarizations were superimposable by ordinate translation.

The Frumkin equation was used to fit the data for each absorbate. Three further methods that can be used to determine the parameters of the Frumkin equations are discussed. These are based on the analysis of $\ln(\pi/\underline{a})$-π, $\ln \underline{a}$-θ, and π-$\ln \underline{a}$ data. The free energies of adsorption referred to specified standard states have been calculated on the basis of the Frumkin equation. The model evolved in the previous work correlating the standard free energies of adsorption with polarizations of the adsorbate molecules has been successfully tested.

MAGNETIC SUSCEPTIBILITY OF ONE-DIMENSIONAL LINEAR CHAINS OF FERROMAGNETICALLY COUPLED $Cu_2X_6^{2-}$ DIMERS

Chee Chow, R. D. Willett and B. C. Gerstein
Inorg. Chem. 14, 205 (1975)

Abstract--The study of copper dimers with triplet ground states has been of much current interest. In particular, it has been shown that the

$Cu_2Cl_6^{2-}$ ion in $Ph_4AsCuCl_3$ existed with a triplet ground state with a singlet excited state at approximately 40 cm^{-1}. The esr spectra of single crystals of the corresponding bromide salt and a mixed bromo-chloro salt are anomalous and suggest the possibility of interdimer interactions. To investigate this possibility, as well as to determine the magnitude of the singlet-triplet splitting, a susceptibility study of $Ph_4AsCuBr_3$ and $Ph_4AsCuBrCl_2$ was initiated.

THERMAL AND MAGNETIC BEHAVIOR OF ONE-DIMENSIONAL MAGNETS
Bernard C. Gerstein
H. J. Keller, ed. Low-Dimensional Cooperative Phenomena (New York: Plenum Publishing Corp., 1975) pp. 125-146

Abstract--A theory of the behavior of lower dimensional magnets is developed. The concepts of exchange, superexchange and the transfer matrix are developed, and used to predict behavior of solids in which one dimensional magnetic interactions are large compared to those in two and three dimensions.

MAGNETIC TRANSITIONS IN TWO DIMENSIONAL SYSTEMS AS A FUNCTION OF INTERLAYER SEPARATION: BIS-PROPYLAMMONIUM TETRACHLOROMANGANATE(II) AND BIS-PENTADECYLAMMONIUM TETRACHLOROMANGANATE(II)
B. C. Gerstein, Chee Chow, Ruth Capulo and Roger Willett
Proceedings of the 20th Annual Magnetism and Magnetic Materials - 1974 Conference, AIP Conference Proceedings No. 24, eds. C. D. Graham, Jr., G. H. Lander and J. J. Rhyne (New York: American Institute of Physics, 1975) pp. 361-362

Abstract--The initial susceptibilities of the two dimensional systems $(C_3H_7NH_3)_2MnCl_4$ ($PrAMnCl_4$) and $(C_{15}H_{31}NH_3)_2MnCl_4$ ($PDAMnCl_4$) have been measured from 4 - 200 K. Both salts exhibit sharp transitions in the neighborhood of 42 K. In the latter case, the transition is found to be field dependent, with the magnitude of the real and imaginary susceptibilities

increasing with decreasing fields, with ac fields in the range 13-30 oe. This behavior is similar to that found in the 2-D system $(CH_3NH_3)_2MnCl_4$ which exhibits ordering at 45.3 K. The magnetic losses are found to be as sensitive an indicator of the transitions as are the dispersion for both salts. The fact that the transition temperatures for all three salts are in the neighborhood of 40 K indicates that the transition is independent of interlayer separation.

EC-04

MOLECULAR SCIENCES

EC-04-01

Radiation and Separation Research

EC-04-01-01

Radiation Sciences

I. Photochemistry and Spectroscopy

MEDIUM INDEPENDENT DUSCHINSKY ROTATION IN THE $\underline{S}_1$ STATE OF THE AZAAZULENES AND AZULENE
F. P. Burke, D. R. Eslinger and G. J. Small
J. Chem. Phys. 63, 1309 (1975)

Abstract--The 7000 Å $^1\underline{B}_1(\underline{S}_1) \leftarrow {}^1\underline{A}_1$ and 3500 Å $^1\underline{A}_1(\underline{S}_2) \leftarrow {}^1\underline{A}_1$ azulene absorption systems have been the subject of many studies. The latter absorption system exhibits extensive $\underline{a}_1$ vibronic activity, is strongly medium dependent, and does not mirror the $\underline{S}_2$ fluorescence spectrum (essentially medium independent). The mirror symmetry breakdown (MSB) is symptomatic of the Duschinsky effect (DE). Two DE mechanisms exist: one medium dependent and the other medium independent (vide infra). The former has been used to explain, in part, the dependence of $\underline{S}_2$'s absorption spectrum on the medium. We demonstrate here that the $\underline{S}_1$ states of certain azaazulenes and azulene, itself, are subject to the medium independent DE. Some implications of this finding for $\underline{S}_2$ of azulene are discussed.

NONADIABATIC EFFECTS ON VIBRONIC INTENSITIES OF LARGER POLYATOMIC MOLECULES IN THE PRERESONANCE REGIME
Gerald J. Small
J. Chem. Phys. 62, 4661 (1975)

Abstract--The approximations used to simplify the perturbation based theory of nonadiabatic interactions and their effects on vibronic intensities in the preresonance regime are examined for the larger polyatomic molecules. They include employment of a crude adiabatic basis set and certain approximate sum rules.

NON-ADIABATIC VIBRONIC INTERACTIONS AND THE RAMAN EFFECT
Gerald J. Small and E. S. Yeung
Chem. Phys. 9, 379 (1975)

Abstract--The role of non-adiabatic interactions in vibronically induced Raman scattering processes is examined for both the preresonance and resonance regimes. Attention is focused on the class of molecules whose linear electron-vibration coupling strengths are characteristic of the larger poly-atomics, e.g., the benzenoid aromatics. Various approximations are introduced to simplify the general theory and the applicability of each is discussed. It is shown that for randomly oriented scatterers the non-adiabatic contribution to induced scattering in the pre-resonance regime is of minor importance relative to the adiabatic contribution. For oriented scatterers, e.g., molecular crystals, some control over the non-adiabatic contribution can be achieved through choice of polarization conditions. For resonance Raman scattering it is shown that the non-adiabaticity can play an important role in vibronically induced scattering processes.

PRE-RESONANCE RAMAN INTENSITIES

Edward S. Yeung, Michael Heiling and Gerald J. Small

Spectrochim. Acta 31A, 1921 (1975)

Abstract--A series expansion for the sum over the vibrational levels of an intermediate electronic state, which occurs in the dispersion theory of the Raman effect, is presented. The convergence properties of the series, as a function of electron-vibration coupling strength and exciting photon energy, have been studied for many model systems which span the range between rigid and diatomic-like molecules. Both Condon type fundamental and overtone transitions and vibronically induced transitions are considered. The single most important result is that the leading term of the above series represents a good approximation to the exact sum up to ca. 3000 cm^{-1} from resonance with the intermediate electronic state for Raman fundamentals. It should be possible, therefore, to study excited state geometries by pre-resonance Raman spectroscopy. The theory also shows that the Condon and vibronic coupling mechanisms exhibit very different dependences on the exciting photon frequency. The corresponding series for Raman overtones has poorer convergence properties. In particular, it is shown that for the general case frequency changes in excited states are as important as geometry changes in inducing overtone intensities.

II. Radiation and Solid State Spectroscopy

ISOTOPIC EXCHANGE OF BROMINE IN AQUEOUS SYSTEM: CIS-DIBROMODIAMMINEPLATINUM(II), TETRABROMOPLATINATE(II), BROMIDE

G. F. Vandegrift, III and D. S. Martin, Jr.
Inorg. Chim. Acta 12, 179 (1975)

Abstract--The aquation equilibria for cis-dibromodiammineplatinum(II) have been measured. For the first and second aquations at 25° C: K_1 = 1.13 mM. $\Delta H°$ = 3.9 ± .7 kcal/mol, K_2 = 0.042 mM, $\Delta H°$ = 10 ± 3 kcal/mol. Some isotopic exchange of ^{82}Br between c-$Pt(NH_3)_2Br_2$ and $PtBr_4^{2-}$ occurs without the formation of a free bromide ion and with a rate expression: Rate Exchange = $(k_{ac}' + k_{ac}''/[Br^-])[Pt(NH_3)_2Br_2]\,[PtBr_4^{2-}]$. It has been shown that the presence of c-$Pt(NH_3)_2Br(H_2O)^+$ serves to catalyze the aquation of $PtBr_4^{2-}$, but that the catalysis step does not account for all the bromide dependent exchange.

POLARIZED CRYSTAL SPECTRA OF POTASSIUM TETRACHLOROPALLADATE(II) AND POTASSIUM TETRABROMOPALLADATE(II)

Rhonda M. Rush, Don S. Martin, Jr., and Roger G. LeGrand
Inorg. Chem. 14, 2543 (1975)

Abstract--Absorption spectra have been recorded for aqueous solutions and single crystals of K_2PdCl_4 and K_2PdBr_4. For both compounds $^1A_{2g}$ and ^1E_g peaks are not resolved in a polarization although the $^1A_{2g}$ peak has the much stronger vibrational structure at 15°K. For K_2PdCl_4 the $^1A_{2g}$ and ^1E_g states are assigned at 21,700 and 23,200 cm^{-1}, respectively, and for K_2PdBr_4 they are at 20,200 and 21,700 cm^{-1}. The $^1A_{2u} \leftarrow {}^1A_{1g}$ ($M \leftarrow L\pi$) charge-transfer bands have surprisingly low intensity and are observed at 37,400 and 30,900 cm^{-1} for K_2PdCl_4 and K_2PdBr_4.

The $^1B_{1g}$ transition appears to be hidden by the $^1A_{2u}$ transition in the c polarization. Weak spin-forbidden bands were observed in both polarizations for both compounds. For K_2PdBr_4 exceptional vibrational structure has been recorded at 15°K. Also, in K_2PdBr_4 two weak transitions at 37,000 and 43,200 cm^{-1} have been assigned as forbidden charge-transfer transitions.

POTASSIUM TETRABROMOPALLADATE(II)
Don S. Martin, Jr., John L. Bonte, Rhonda M. Rush and Robert A. Jacobson
Acta Cryst. B 31, 2538 (1975)

Abstract--Tetragonal, P4/mmm, a = b = 7·409(12), c = 4·309(7) Å; K_2PdBr_4, Z = 1, D_x = 3·54 g cm^{-3}. The dark brown crystals were grown from the aqueous solution by evaporation. The structure, refined to R = 0·040, is isomorphous with K_2PtCl_4 with a Pd-Br distance of 2·444(3) Å.

EC-04-01-02

Separations Research

I. Separations Research

APPLICATION OF ION-EXCLUSION AND ION-EXCHANGE TECHNIQUES IN PREPARING α,β,β'-TRIHYDROXYISOBUTYRAMIDE AND α,β,β'-TRIHYDROXYISOBUTYRIC ACID FROM 1,3-DIHYDROXY-2-PROPANONE VIA THE CYANOHYDRIN SYNTHESIS
J. E. Powell and S. Kulprathipanja
J. Chromatog. 107, 167 (1975)

Abstract--α,β,β'-Trihydroxyisobutyramide (2,3-dihydroxy-2-hydroxymethylpropanamide) melting point 107.5-108°, has been prepared from 1,3-dihydroxy-2-propanone via formation and partial hydrolysis of its cyanohydrin. After isolation by ion-exclusion techniques and crystallization from water and ethanol-water mixtures, the amide was converted

nearly quantitatively to α, β, β'-trihydroxyisobutyric acid (2,3-dihydroxy-2-hydroxymethylpropanoic acid), melting point 117–117.5°, by boiling with excess aqueous NaOH followed by cation-exchange elimination of Na^+ and any unevolved NH_3 on H^+-form Dowex 50. Proton NMR spectra for both amide and acid were recorded.

FORMATION CONSTANTS OF 2,3-DIHYDROXY-2-METHYLPROPANOATO AND 2,3-DIHYDROXY-2-METHYLBUTANOATO RARE EARTH CHELATE SPECIES
J. E. Powell, J. L. Farrell and S. Kulprathipanja
Inorg. Chem. 14, 786 (1975)

Abstract--The consecutive step formation constants of the 1:1, 2:1, and 3:1 chelate species formed by interaction of 2,3-dihydroxy-2-methylpropanoate and 2,3-dihydroxy-2-methylbutanoate anions (separately) with the tripositive lanthanon and yttrium cations were determined potentiometrically at an ionic strength of 0.100 (KNO_3) and 25.0°. The results indicate that these dihydroxycarboxylate ligands exhibit a tridentate character in bonding to the lighter (larger) lanthanons (La-Sm) but bond only bidentately to the heavier (smaller) lanthanons (Ho-Lu) and to yttrium. The dentate character appears to change gradually from tridentate to bidentate as the lanthanon radius diminishes from that of samarium to that of holmium.

THE PREPARATION OF METASTABLE SOLID NEODYMIUM NITRATE
William G. O'Brien and Renato G. Bautista
J. Less-Common Metals 41, 191 (1975)

Abstract--A metastable, solid form of neodymium nitrate, with a clear, glossy appearance has been prepared while crystallizing neodymium nitrate solution. It is readily soluble in water, can be drawn into fine

strands, deforms readily under slight pressure and decays with the passage of time.

EC-04-02
Chemical and Geophysical Energy

EC-04-02-01
Chemical Energy

I. Reaction Mechanisms of Inorganic and Bioinorganic Systems

ACIDOLYSIS AND OXIDATIVE CLEAVAGE REACTIONS OF BENZYL-CHROMIUM CATIONS
Ronald S. Nohr and James H. Espenson
J. Am. Chem. Soc. 97, 3392 (1975)

Abstract--The organometallic complex $[(H_2O)_5CrCH_2C_6H_5]^{2+}$ is oxidized in aqueous perchloric acid by Fe^{3+}, Cu^{2+}, $[Co(NH_3)_5Cl^{2+}]$, $[Co(NH_3)_5Br^{2+}]$, O_2 and H_2O_2 at an identical rate, independent of the nature and concentration of the oxidizing agent. The first-order rate constant is $10^3 k_1$ (sec^{-1}) = 2.63 ± 0.21 (25.0°, μ = 1.00 M). The organic products and Cr(III) products were determined. In certain instances, the reaction initiates polymerization of acrylonitrile but in other instances it does not. The rates of para-substituted derivatives correlate with the Hammett σ_μ parameter, giving ρ = -1.01. The reactions are discussed in terms of a unimolecular homolysis of the Cr-C bond by the SH1 mechanism, followed by rapid oxidation of one or both of the fragments so formed.

KINETIC STUDY OF THE TRANSFER OF METHYL GROUPS TO MERCURY(II) FROM A SERIES OF METHYLCOBALT(III)-CHELATE COMPLEXES
James H. Espenson, William R. Bushey and Michael E. Chmielewski
Inorg. Chem. 14, 1302 (1975)

Abstract—Kinetics studies of the electrophilic cleavage of the Co-C σ bond in a series of six $CH_3Co(chelate)H_2O$ complexes by Hg^{2+}

were carried out. The kinetic data support an electrophilic (SE2 mechanism, in that changes in electron density at the cobalt center which accompany the variation in chelate structure are transmitted to the transition state for the heterolytic cleavage of the $Co-CH_3$ bond. The values of $\underline{k}/\underline{M}^{-1}sec^{-1}$ at 25.0° and μ 1.0 M in aqueous solution are as follows: saloph, (3.3 ± 0.3) x 10^4; salen, (2.6 ± 0.4) x 10^4; Me_2salen, (2.1 ± 0.1 x 10^4; $(dmgH)_2$, 65 ± 2; dpnH, 1.77 ± 0.03; tim (at μ 1.60 M), (4.5 ± 0.5) x 10^{-4}. For the first four members, the reaction rate is lowered by $[H^+]$, attributed to the protonation of the cobalt complex to an unreactive form; the equilibrium constants for these interactions were also evaluated.

RAPID REACTION OF DIMETHYL SULFOXIDE WITH NITRATOPENTAAQUOCHROMIUM(III) ION

Mike L. Mitchell, Theresa Montag, James H. Espenson and Edward L. King

Inorg. Chem. 14, 2862 (1975)

Abstract--The deaquation and $\underline{NO_3}^-$ substitution reactions of $\underline{Cr}(H_2O)_5NO_3^{2+}$ in aq. Me_2SO were studied. The deaquation rate constant at 25° was ~8 x 10^{-2} sec^{-1}, several orders of magnitude larger than the deaquation rate constant for $Cr(H_2O)_6^{3+}$, with a nitrate loss rate constant of 8.8 x 10^{-6} sec^{-1} at 25°. The nitrate ligand labilizes all 5 H_2O ligands, presumably via transient bidentate species.

II. Properties of Rare Earth Electrolytes

APPARENT AND PARTIAL MOLAL HEAT CAPACITIES OF SOME AQUEOUS RARE EARTH CHLORIDE SOLUTIONS AT 25°C
Frank H. Spedding, John P. Walters and James L. Baker
J. Chem. Eng. Data 20, 438 (1975)

Abstract--Specific heats of aqueous solutions of the stoichiometric trivalent Pr, Sm, Eu, Gd, Tb, Ho, Tm, and Lu chlorides were measured over the concentration range of 0.1m to saturation at 25°C. Apparent molal heat capacities, ϕ_{cp}, were calculated for these solutions, and empirical polynomial equations were obtained which expressed ϕ_{cp}, within experimental accuracy, as a function of $m^{1/2}$ for each salt. From these equations the partial molal heat capacities of the solvent $\bar{C}_{p1}$, and the solute, $\bar{C}_{p2}$, were calculated. Together with earlier reported data on five other rare earth chlorides, the $\bar{C}_{p1}$ data at even molalities exhibited a two series effect across the rare earth series over the whole concentration range, similar to the rare earth perchlorate data. The differences in the concentration dependence of the heat capacity properties between rare earth chloride and rare earth perchlorate solutions are discussed in terms of ion-ion and ion-solvent interactions.

APPARENT AND PARTIAL MOLAL HEAT CAPACITIES OF AQUEOUS RARE EARTH PERCHLORATE SOLUTIONS AT 25°C
Frank H. Spedding, James L. Baker and John P. Walters
J. Chem. Eng. Data 20, 189 (1975)

Abstract--Specific heats of aqueous solutions of the stoichiometric trivalent rare earth perchlorates (La, Pr, Nd, Sm, Gd, Eu, Tb, Dy, Ho, Er, Tm, Yb, and Lu) were measured over the concentration range of

0.1$\underline{m}$ to saturation at 25°C. Apparent molal heat capacities, $\phi_{\underline{cp}}$, were calculated for these solutions, and empirical polynomial equations were obtained which expressed $\phi_{\underline{cp}}$ as a function of $\underline{m}^{1.2}$ for each salt. From these equations the partial molal heat capacities of the solvent, $\bar{C}_{\underline{p1}}$, and solute, $\bar{C}_{\underline{p2}}$, were calculated. The $\bar{C}_{\underline{p1}}$ data at given molalities exhibit a two-series effect across the rare earth series over the whole concentration range. For the lighter rare earths through Gd, $\phi_{\underline{cp}}$ increases almost linearly with molality above 2.5$\underline{m}$, whereas for the heavier rare earths, $\partial\phi/\partial\underline{m}$ decreases with increasing concentration.

DENSITIES AND APPARENT MOLAL VOLUMES OF SOME AQUEOUS RARE EARTH SOLUTIONS AT 25°C. I. RARE EARTH CHLORIDES
Frank H. Spedding, Victor W. Saeger, Karen A. Gray, Phyllis K. Boneau, Mary A. Brown, Carroll W. DeKock, James L. Baker, Loren E. Shiers, Herman O. Weber, and Anton Habenschuss
J. Chem. Eng. Data 20, 72 (1975)

Abstract--The densities of aqueous solutions of $LaCl_3$, $PrCl_3$, $NdCl_3$, $SmCl_3$, $EuCl_3$, $GdCl_3$, $TbCl_3$, $DyCl_3$, $HoCl_3$, $ErCl_3$, $TmCl_3$, $YbCl_3$, $LuCl_3$, and YCl_3 were determined from approximately 0.02$\underline{m}$ to saturation at 25°C with an accuracy of $\pm 1 \times 10^{-5}$ g/ml by a pycnometric method. The densities of YCl_3 were also determined at 0°C. Empirical equations representing the densities were obtained. Apparent molal volumes calculated from the experimental densities were fitted to semiempirical equations. Available dilute solution data (less than 0.2$\underline{m}$) were included in these fits. The partial molal volumes of the salt and water were discussed in terms of the ion-water and ion-ion interactions. A two-series effect in the partial molal volumes of the salt across the rare earth chloride series reported earlier was confirmed in dilute solutions, and this effect persists to high concentrations.

DENSITIES AND APPARENT MOLAL VOLUMES OF SOME AQUEOUS RARE EARTH SOLUTIONS AT 25°C. II. RARE EARTH PERCHLORATES
Frank H. Spedding, Loren E. Shiers, Mary A. Brown, John L. Derer, Douglas L. Swanson and Anton Habenschuss
J. Chem. Eng. Data 20, 81 (1975)

Abstract--The densities of aqueous solutions of La, Pr, Nd, Sm, Eu, Gd, Tb, Dy, Ho, Er, Tm, Yb, and Lu perchlorate were determined from approximately 0.05m to saturation at 25°C with an accuracy of ± 5 x 10^{-5} g/ml by a pycnometric method. The apparent molal volumes calculated from the experimental densities were fitted to semiempirical equations. Dilute apparent molal volume data (less than 0.2m) available in the literature for La, Nd, Gd, and Lu perchlorate were included in these fits. Apparent molal volumes at infinite dilution for the remaining perchlorates were obtained from the additivity relationships. A two-series effect in the partial molal volumes across the rare earth series, similar to the one found for the chlorides, persists to high concentrations in the perchlorates. This two-series effect is discussed in terms of a change in the inner sphere water coordination of the cations in the rare earth series.

DENSITIES AND APPARENT MOLAL VOLUMES OF SOME AQUEOUS RARE EARTH SOLUTIONS AT 25°. III. RARE EARTH NITRATES
F. H. Spedding, L. E. Shiers, M. A. Brown, J. L. Baker, L. Gutiérrez, L. S. McDowell and A. Habenschuss
J. Phys. Chem. 79, 1087 (1975)

Abstract--The densities of aqueous solutions of $La(NO_3)_3$, $Pr(NO_3)_3$, $Nd(NO_3)_3$, $Sm(NO_3)_3$, $Gd(NO_3)_3$, $Tb(NO_3)_3$, $Dy(NO_3)_3$, $Ho(NO_3)_3$, $Er(NO_3)_3$, $Yb(NO_3)_3$, and $Lu(NO_3)_3$ were determined from approximately 0.03 m to saturation at 25° with an accuracy of ±3 x 10^{-5} g/ml by a pycnometric method. The densities are represented with empirical equations. The apparent

molal volumes were fitted to semiempirical equations and partial molal volumes were calculated. The partial molal volume data for the nitrate solutions are compared to the rare earth chloride and perchlorate data. The two-series effect in the partial molal volumes of the rare earth nitrates at infinite dilution, attributed to a decrease in the inner-sphere water coordination of the cation, disappears by 0.5 m. Above this concentration, the partial molal volumes of the rare earth nitrates generally decrease from $La(NO_3)_3$ to $Lu(NO_3)_3$. These results are interpreted in terms of inner-sphere nitrate complex formation.

DENSITIES AND THERMAL EXPANSION OF SOME AQUEOUS RARE EARTH CHLORIDE SOLUTIONS BETWEEN 5° AND 80°C. I. $LaCl_3$, $PrCl_3$, AND $NdCl_3$

Wayne M. Gildseth, Anton Habenschuss and Frank H. Spedding

J. Chem. Eng. Data 20, 292 (1975)

Abstract--A dilatometric method is used to measure densities of aqueous $LaCl_3$, $PrCl_3$, and $NdCl_3$ solutions from approximately 0.1 to 3.5 molal, and from 20° to 80°C for $LaCl_3$ and 5° to 80°C for $PrCl_3$ and $NdCl_3$, at 5° intervals. Equations representing the apparent molal volumes as a function of temperature and concentration are given. Partial molal volumes, coefficients of thermal expansion, and apparent and partial molal expansibilities calculated from these fits are discussed in terms of ion-ion and ion-solvent interactions, as well as in terms of solvent structure. Water appears to undergo greater electrostriction with decreasing rare earth ionic radii, resulting in decreasing apparent and partial molal volumes at all temperatures. However, the apparent and partial molal expansibilities increase with decreasing rare earth ionic radii. The existence of an

inversion temperature below which the solution is more expansible than pure water and above which the reverse is true is verified.

ELECTRICAL CONDUCTANCES OF SOME AQUEOUS RARE EARTH ELECTROLYTE SOLUTIONS AT 25°. III. THE RARE EARTH NITRATES
J. A. Rard and F. H. Spedding
J. Phys. Chem. 79, 257 (1975)

Abstract--The electrical conductances of the aqueous trinitrates of La, Pr, Nd, Sm, Gd, Tb, Dy, Ho, Er, Yb, and Lu were measured over the concentration range of approximately 0.004 m to saturation at 25°. Below 0.9 m the equivalent conductances, at constant molality, decrease from La to Sm and then rise to Lu. Above 0.9 m, the equivalent conductances increase from La to Lu. These results imply that in dilute solutions the amount of complex formation increases from La to Sm and then decreases to Lu while, at higher concentrations, the amount of complex formation decreases from La to Lu. The trends in the aqueous rare earth nitrate series are discussed in terms of changes in inner- and outer-sphere coordination across the rare earth series.

RELATIVE VISCOSITIES OF SOME AQUEOUS RARE EARTH NITRATE SOLUTIONS AT 25°C
Frank H. Spedding, Loren E. Shiers and Joseph A. Rard
J. Chem. Eng. Data 20, 88 (1975)

Abstract--The relative viscosities of aqueous solutions of the trivalent nitrates of La, Pr, Nd, Sm, Gd, Tb, Dy, Ho, Er, Yb, and Lu were measured over the concentration range of approximately 0.05m to saturation at 25°C. The relative viscosities of the aqueous rare earth chlorides and perchlorates were reported previously. The rare earth nitrate relative viscosities at constant molal concentrations increased

regularly from La to Lu. The nitrate viscosity data are briefly compared to the chloride and perchlorate viscosities, and the trends in the nitrate viscosities are briefly discussed in terms of complexation between the rare earth and nitrate ions and in terms of hydration changes across the rare earth series.

RELATIVE VISCOSITIES OF SOME AQUEOUS RARE EARTH PERCHLORATE SOLUTIONS AT 25°C
Frank H. Spedding, Loren E. Shiers and Joseph A. Rard
J. Chem. Eng. Data 20, 66 (1975)

Abstract--The relative viscosities of aqueous solutions of the trivalent perchlorates of La, Pr, Nd, Sm, Eu, Gd, Tb, Dy, Ho, Er, Tm, Yb, and Lu were measured over the concentration range of 0.05m to saturation at 25°C. The relative viscosities of the aqueous rare earth chlorides were reported previously. With the perchlorate and chloride viscosity data, a best set of rare earth ionic Jones-Dole B-coefficients was calculated. A distinct two-series effect appears in the viscosities, across the rare earth series, from about 3.0m to saturation. The concentration dependence of the relative viscosities and trends across the rare earth series are discussed in terms of a change in the inner sphere cation hydration number, changes in overall hydration, and in terms of water sharing between the various ions.

EC-04-03

Molecular and Atomic Sciences

EC-04-03-01

Chemical Physics

I. Crystallography of Organic and Biological Materials

ALKOXALYL COMPLEXES OF PALLADIUM(II) AND PLATINUM(II)
Edward D. Dobrzynski and Robert J. Angelici
Inorg. Chem. 14, 59 (1975)

Abstract--Alkoxalyl complexes of the general formula trans-$MCl(COCO_2R)L_2$, where M = Pt or Pd, R = CH_3 or C_2H_5, and L = $P(C_6H_5)_3$, $P(CH_3)(C_6H_5)_2$ or $P(C_2H_5)_3$, were prepared by oxidative-addition reactions of ML_4 with $ClCOCO_2R$. The C=O groups of the planar alkoxalyl ligand have an s-trans conformation in the solid state, but in solution $PtCl(COCO_2CH_3)L_2$ exists as two conformers as indicated by infrared studies. With Cl_2, $PtCl(COCO_2CH_3)[P(C_6H_5)_3]_2$ rapidly yields $ClCOCO_2CH_3$ and $PtCl_2[P(C_6H_5)_3]_2$. With C_2H_5OH and a trace of $C_2H_5O^-$, $PtCl(COCO_2CH_3)[P(C_6H_5)_3]_2$ is transesterified to give $PtCl(COCO_2C_2H_5)[P(C_6H_5)_3]_2$. While the platinum-alkoxalyl complexes are stable in solution, the palladium analogs readily undergo decarbonylation in solution to give the corresponding alkoxycarbonyl complexes ($PdCl(CO_2R)L_2$). This decarbonylation is greatly inhibited by adding phosphines (L) to the solutions. Attempts to prepare alkoxalyl complexes by CO insertion into alkoxycarbonyl complexes are also briefly described.

THE ABSOLUTE CONFIGURATION OF VINCOSIDE
K. C. Mattes, C. R. Hutchinson, James P. Springer and Jon Clardy
J. Am. Chem. Soc. 97, 6270 (1975)

Abstract--The absolute configuration of vincoside (I, R = H) was determined by x-ray analysis of N_b-(p-bromobenzyl)vincoside tetraacetate. Chemical correlation of I (R = H) to its lactam (II) and its synthesis via the use of I (R = $Cl_3CCH_2O_2C$) was described. Isovincoside (strictosidine), the C-3 epimer of I (R = H), was prepared.

CRYSTAL AND MOLECULAR STRUCTURE OF $[Ag(P(OMe)_3)_2NO_3]_2$.
A CASE OF SYMMETRIC NITRATE-OXYGEN BRIDGING
J. H. Meiners, J. C. Clardy and J. G. Verkade
Inorg. Chem. 14, 633 (1975)

Abstract--The crystal and molecular structure of tetrakis(trimethyl phosphite)-di-μ-nitrato-disilver(I), $[Ag(P(OMe)_3)_2NO_3]_2$, has been determined by single-crystal x-ray diffraction methods. The compound crystallizes in the orthorhombic P_{bca} space group with four molecules per unit cell of which the dimensions are a = 9.146(3), b = 16.769(4), and c = 20.689(6) Å. The structure was solved by the heavy-atom method and refined by least-squares calculations to a final R of 0.048 with 1233 independent reflections. While the molecule is a centrosymmetric dimer in the crystalline state with an Ag-Ag bond distance of 4.095(2) Å, molecular weight determinations indicate the presence of extensive dissociation in solution. The geometry around the silver atom in the solid state is a greatly distorted tetrahedron with an OAgO angle of 67.0(3)° and a PAgP angle of 133.8(1)°. The bridging oxygens are equidistant (2.456(8) and 2.454(8) Å) from both silvers.

CRYSTAL AND MOLECULAR STRUCTURE OF BICYCLIC THIOPHOSPHATE $SP(OCH_2)_3P$

J. C. Clardy, D. C. Dow and J. G. Verkade
Phosphorus 5, 85 (1975)

Abstract--The structure of 1-sulfo-2,6,7-trioxa-1,4-diphosphabicyclo-[2.2.2] octane, $SP(OCH_2)_3P$ has been determined by the single crystal x-ray diffraction technique. The crystals belong to the orthorhombic space group Pnma with four molecules per unit cell. The unit cell parameters are a = 11.483(5) Å, b = 7.753(5) Å, c = 7.797(5) Å. The final R and ωR factors were 0.073 and 0.123 for the 456 observed reflections, respectively. The terminal P=S bond distance is 1.902(3) Å and the P-O, O-C and P-C distances average 1.555(6), 1.493(8) and 1.838(9) Å, respectively. The average bond angles are Sap-O, 112.7(3)°; O-P-O, 106.1(2)°; C-P-C, 97.60(3)°; P-C-O 113.4(4)° and P-O-C, 118.9(4)°. These parameters are compared to those found in related phosphorus polycycles and some of the unusual Lewis base properties of the parent compound $P(OCH_2)_3P$ are partially rationalized on hybridizational constraints imposed by the polycyclic structure.

CRYSTAL AND MOLECULAR STRUCTURE OF BROMOTETRAKIS(TRIMETHYL PHOSPHITO)NICKEL(II) TETRAFLUOROBORATE, $\{Ni[P(OCH_3)_3]_4Br\}BF_4$

D. S. Milbrath, J. P. Springer, J. C. Clardy and J. G. Verkade
Inorg. Chem. 14, 2665 (1975)

Abstract--The crystal and molecular structure of the five-coordinate nickel complex $\{NiBr[P(OCH_3)_3]_4\}BF_4$ has been determined from three-dimensional single-crystal x-ray data. The compound crystallizes in the monoclinic space group $P2_1/n$, with a = 13.333 (4), b = 18.195 (5), c = 11.731 (2) Å, and β = 93.61 (2)°. The structure was determined by Patterson

and conventional least-squares methods using 2894 independent nonzero reflections to give a final R factor of 0.060. The coordination geometry around Ni is essentially trigonal bipyramidal with Br in an equatorial position. Axial Ni-P distances are 2.181 (2) and 2.180 (2) Å while the equatorial Ni-P bonds are 2.187 (2) and 2.239 (2) Å and the Ni-Br distance is 2.456 (2) Å. The equatorial plane angles are Br-Ni-P = 123.44 (7) and 112.24 (7)°, and the P-Ni-P angle is 124.31 (9)°. The axial phosphorus ligands are bent toward the bromine with an average angle of 86.12°. Qualitative bonding considerations are used in comparing the present structure to others in the low-spin NiL_5^{2+}, NiL_4X^+, and NiL_3X_2 series.

CRYSTAL AND MOLECULAR STRUCTURE OF DIIODOTRIS(TRIMETHYL PHOSPHITE)NICKEL(II), $NiI_2[P(OCH_3)_3]_3$

L. J. Vande Griend, J. C. Clardy, and J. G. Verkade
Inorg. Chem. 14, 710 (1975)

Abstract--The crystal and molecular structure of the five-coordinate title complex has been determined from three-dimensional single-crystal x-ray data. The compound crystallizes in the monoclinic space group $P2_1/n$, with a = 9.711 (2) Å, b = 19.054 (5) Å, c = 12.267 (3) Å, and β = 94.75 (1)°. The structure was determined by Patterson and conventional least-squares methods with 2812 nonzero reflections to give a final R factor of 0.034. The geometry around the Ni atom is nearly trigonal bipyramidal. The two axial Ni-P bond distances are 2.180 (2) and 2.183 (2) Å while the slightly shorter equatorial Ni-P length is 2.169 (2) Å. The two equatorial Ni-I bond distances are 2.664 (1) and 2.657 (1) Å and the I-Ni-I bond angle is compressed from the ideal equatorial angle of 120° to 112.11 (3)°.

EUCOSTEROL, A NOVEL SPIROCYCLIC NORTRITERPENE ISOLATED FROM BULBS OF EUCOMIS SPECIES
William T. L. Sidwell, Christoph Tamm, Réne Ziegler, Janet Finer and Jon Clardy
J. Am. Chem. Soc. 97, 3518 (1975)

Abstract--Eucosterol (I) was isolated from the neutral extracts of the bulbs of E. autumnalis, E. punctata and a botanically undefined E. sp., and

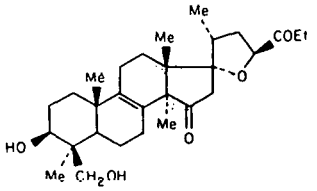

its structure determined by chemical, spectroscopic and x-ray diffraction studies. The final crystallographic residual index was 0.061 for the 1823 observed reflections using a model in which H atoms were fixed, nonhydrogen atoms were varied anisotropically and Br and S anomalous scattering corrections were used.

IRIEOL A AND IRIEDIOL, DIBROMODITERPENES OF A NEW SKELETAL CLASS FROM LAURENCIA
William Fenical, Bruce Howard, Kirsten B. Gifkins and Jon Clardy
Tet. Lett. 3983 (1975)

Abstract--Red seaweeds of the genus Laurencia possess a wide variety of biosynthetic pathways for both terpenoid and nonterpenoid compounds. This paper reports two new diterpenes related to the antibiotic sesquiterpene oppositol. A rigorous proof of structure is presented and the absolute stereochemistries are discussed.

9-ISOCYANOPUPUKEANANE, A MARINE INVERTEBRATE ALLOMONE WITH A NEW SESQUITERPENE SKELETON
B. Jay Burreson, Paul J. Scheur, Janet Finer and Jon Clardy
J. Am. Chem. Soc. 97, 4763 (1975)

Abstract--9-Isocyanopupukeanane was isolated from the opisthobranch mollusk Phyllidia varicosa as well as from its prey the sponge Hymeniacidon sp.

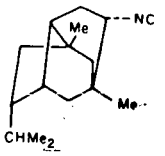

I

and by chemical, spectroscopic and x-ray diffraction techniques it had structure I.

A PLATINUM(II) COMPLEX CONTAINING A METALLODITHIOCARBOXYLATE LIGAND
James M. Lisy, Edward D. Dobrzynski, Robert J. Angelici and Jon Clardy
J. Am. Chem. Soc. 97, 656 (1975)

Abstract--The reaction of trans-$(Ph_3P)_2Pt(Cl)[C(=S)OMe]$ with BF_3 in CH_2Cl_2 initially produces a reactive compound which is assigned the thiocarbonyl structure, $[(Ph_3P)_2Pt(Cl)(CS)]BF_4$, based on its spectroscopic properties. It reacts readily with MeOH to give trans-$(Ph_3P)_2Pt(Cl)[C(=S)OMe]$ and with Me_2NH in CH_2Cl_2 to give trans-$(Ph_3P)_2Pt(Cl)[C(=S)NMe_2]$. With H_2O, the complex reacts to exchange the S atom with O yielding trans-$[(Ph_3P)_2Pt(Cl)(CO)]BF_4$. On standing in solution, the compound slowly is converted to the very stable $[(Ph_3P)_2(Cl)Pt(CS_2)Pt(PPh_3)_2]BF_4$. The x-ray crystallographic investigation of this compound shows it to contain the novel $(Ph_3P)_2(Cl)Pt(CS_2^-)$ metallo-dithiocarboxylate ligand bound to the 2nd Pt(II) atom.

PREPARATION, PROPERTIES, AND CRYSTAL STRUCTURE OF A CATIONIC NICKEL NITROSYL BICYCLIC PHOSPHITE COMPLEX
J. H. Meiners, C. J. Rix, J. C. Clardy and J. G. Verkade
Inorg. Chem. 14, 705 (1975)

Abstract--Nitrosonium tris(1,3,7-trioxa-2-phospha-5-methylbicyclo-[2.2.2]octane)nickel(0) tetrafluoroborate, $[Ni(P(OCH_2)_3CCH_3)_3NO]BF_4$,

was synthesized by direct reaction of $NOBF_4$ with the zerovalent $Ni[P(OCH_2)_3CCH_3]_4$. The complex exhibited a strong absorbance at 1867 cm^{-1} in its infrared spectrum, and a conductivity measurement indicated it to be a uni-univalent electrolyte. The crystal structure of this salt has been determined by three-dimensional single-crystal x-ray analysis. The compound crystallizes in the monoclinic space group C2/c with a = 27.29 (3) Å, b = 12.63 (1) Å, c = 24.84 (3) Å, and β = 135.55 (2)°. The structure was solved by conventional heavy-atom techniques and refined by least-squares methods to weighted and unweighted R factors of 0.085 and 0.090, respectively, for 2000 independent reflections which had intensities greater than 2σ above background. The density of 1.60 g/cm^3 computed from the unit cell volume of 6048 $Å^3$ on the basis of eight $[Ni(P(OCH_2)_3CCH_3)_3NO]BF_4 \cdot CHCl_3$ molecules per unit cell agrees well with the 1.61 g/cm^3 determined by flotation methods. The coordination geometry around the nickel is a slightly distorted tetrahedron with an average P-Ni-P angle of 104.2° and an average P-Ni-N angle of 114.3 (2)°. The nitrosyl is nearly linear with the Ni-N-O angle equal to 176.8 (18)°. One chloroform molecule per molecule of complex was found in the lattice.

PROPELLANES. X. THE DIMERIZATION OF 9,9-DICHLOROTRICYCLO-[4.2.1.$0^{1,6}$]NON-3-ENE

Philip M. Warner, Richard C. LaRose, Richard F. Palmer, Chee-man Lee, David O. Ross and Jon C. Clardy

J. Am. Chem. Soc. 97, 5507 (1975)

Abstract--The syntheses and subsequent dimerization of 9,9-dichloro-tricyclo[4.2.1.$0^{1,6}$]non-3-ene and 9,9-dichlorotricyclo[4.2.1.$0^{1,6}$]-nonane are reported. Both dimerizations occur via the intermediacy of a bridgehead olefin (comparable to a trans-cycloheptene). In the former case,

this olefin has been trapped as a Diels-Alder adduct with furan. The double bond of the first above-mentioned dichloride exerts a retarding effect on the ring-opening (leading to dimerization) reaction, either via a rather large inductive effect, or a bishomoantiaromatic (electronic) effect.

A REVISED STRUCTURE FOR THE ANTIBIOTIC PILLAROMYCIN A
John O. Pezzanite, Jon Clardy, Pui-Yan Lau, Gordon Wood, David Louis Walker and Bert Fraser-Reid
J. Am. Chem. Soc. 97, 6250 (1975)

Abstract--The single crystal x-ray diffraction of the antibiotic Pillaromycin A showed that the sugar component is a 2,3,6-trideoxy-aldohexose bearing a $-O:C-CH_2OH$ substituent at C-4, and not a 2,3,6-trideoxy-4-keto-aldohexose bearing a $-O:C-CH_2OH$ moiety at C-2 as was previously suggested. Spectral studies indicate a 542 (instead of 540) for the antibiotic, and 173 for the pillarosyl nucleus.

THE STRUCTURE OF CROTOFOLIN A, A DITERPENE WITH A NEW SKELETON
W. R. Chan, E. C. Prince, P. S. Manchand, J. P. Springer and Jon Clardy
J. Am. Chem. Soc. 97, 4437 (1975)

Abstract--Crotofolin A (I) was isolated from Croton corylifolius and

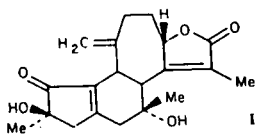

I

its structure was determined by x-ray crystallography. A possible biogenesis of this skeleton is suggested to occur via a bicyclic precursor.

THE STRUCTURE OF FUMITREMORGIN A
Nancy Eickman, Jon Clardy, R. J. Cole and Jerry W. Kirksey
Tet. Lett. 83, 1051 (1975)

Abstract--The structure of fumitremorgin A, isolated from Aspergillus fumigatus, was determined by x-ray analysis. Crystals were orthorhombic, space group $P2_12_12_1$, a 26.862, b 15.718, c 7.472 Å, and Z = 4. The structure was solved by direct methods and refined to R 7.6%.

THE STRUCTURE OF A NEW TYPE OF PLANT GROWTH INHIBITOR EXTRACTED FROM IMMATURE TOBACCO LEAVES
James P. Springer, Jon Clardy, Richard H. Cox, Horace G. Cutler and Richard J. Cole
Tet. Lett. 2737 (1975)

Abstract--The structure and absolute configuration of 4, 8, 13-duvatriene-1,2-diol (I), the more active component of young tobacco leaves, was determined from spectral data and by x-ray analysis. Crystals of I were trigonal, space

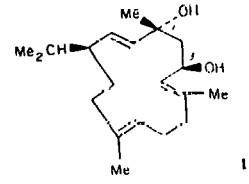

I

group $P3_12_1$, a 16.980, c 11.83 Å. The structure was solved by a 'multi'-solution weighted tangent formula approach and refined by least squares to R 0.109. A second less active growth inhibitor isolated from the young leaves was epimeric with I at C-3 and C-1.

THE STRUCTURE OF PAXILLINE, A TREMORGENIC METABOLITE OF PENICILLIUM PAXILLI BAINIER
James P. Springer, Jon Clardy, John M. Wells, Richard J. Cole and Jerry W. Kirksey
Tet. Lett. 2531 (1975)

Abstract--Crystals of paxilline (I) were orthorhombic, space group $P2_12_12_1$, with a 31.009, b 11.522, and c 7.707 Å; R was 0.04 from 1840

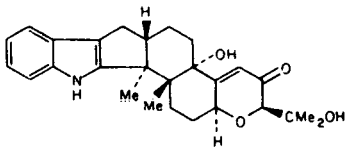

I

observed reflections. The CD spectrum of I showed positive Cotton effects for the first 2 bands and a negative Cotton effect for a third band.

THE STRUCTURE OF SAXITOXIN
E. J. Schantz, V. E. Ghazarossian, H. K. Schnoes, F. M. Strong, J. P. Springer, John O. Pezzanite and Jon Clardy
J. Am. Chem. Soc. 97, 1238 (1975)

Abstract--Saxitoxin has structure I based on a single crystal x-ray diffraction study of saxitoxin p bromobenzenesulfonate. An equilibrium presumably exists between the ketone and ketone hydrate.

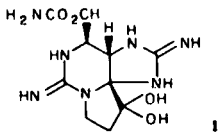

I

TRYPTOQUIVALINE AND TRYPTOQUIVALONE, TWO TREMORGENIC METABOLITES OF ASPERGILLUS CLAVATUS
Jon Clardy, James P. Springer, George Büchi, Keizo Matsuo and Richard Wightman
J. Am. Chem. Soc. 97, 663 (1975)

Abstract--Tryptoquivaline (I) and tryptoquivalone (II), two new metabolites producing severe tremors in experimental animals, were isolated from Aspergillus clavatus. Methanolysis of I gave a δ-lactone III which was transformed to the corresponding hydroxylamine-O-p-bromobenzoate IV and

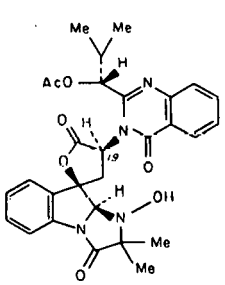

I

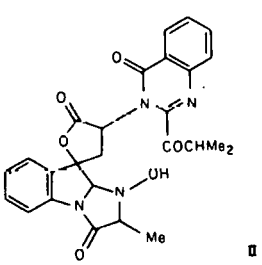

II

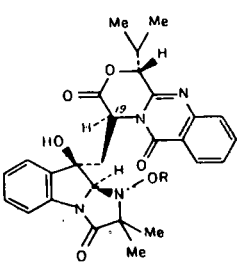

III, R = H
IV, R = p-BrC_6H_4CO
V, R = p-BrC_6H_4NHCO

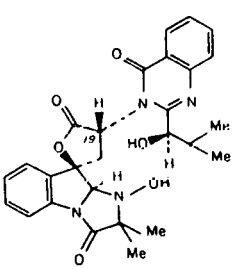

VI

the p-bromophenylurethane V. Single crystal x-ray analysis revealed the structure of V. Chemical and spectral data demand I to be the spiro γ-lactone shown rather than a δ-lactone and methanolysis is, thus, accompanied by translactonization. On exposure to base followed by relactonization both I and III gave an epi-γ-lactone VI. Spectral data only were used to derive structure II for the second metabolite.

X-RAY STRUCTURES OF PHLEBIAKAURANOL AND PHLEBIANORKAURANOL, HIGHLY OXYGENATED ANTIBACTERIAL METABOLITES OF PHLEBIA STRIGOSOZONATA
James M. Lisy, Jon Clardy, Marjorie Anchel and Steven M. Weinreb
J. C. S. Chem. Comm. 406 (1975)

Abstract--Two new antibacterial metabolites, phlebia-kauranol and phlebianorkauranol have been isolated from Phlebia strigosozonata and shown to have highly oxygenated kaurane structures.

II. Statistical Mechanics of Gaseous Systems

COLLISION INTEGRALS FOR SOFT, NONSPHERICAL MOLECULES IN TERMS OF SPHERICAL Ω^* INTEGRALS
Jerome D. Verlin, M. Keith Matzen and D. K. Hoffman
J. Chem. Phys. 62, 4146 (1975)

Abstract--A new formulation of the classical kinetic theory of dilute gases composed of molecules with rotational structure is given which closely parallels that for structureless molecules. The matrix elements of the collision operator are expressed as integral moments of a generalized collision cross section $\mathfrak{J}$. It is shown that a suitable approximation for the momentum dependence of $\mathfrak{J}$ leads to expressions for the matrix elements which can be written in terms of the familiar spherical Ω^* integrals.

TEMPERATURE DEPENDENCE OF THERMAL DIFFUSION IN CO ISOTOPIC GAS MIXTURES
Jerome D. Verlin, M. Keith Matzen and D. K. Hoffman
J. Chem. Phys. 62, 4151 (1975)

Abstract--The temperature dependence of thermal diffusion in several different isotopic gas mixtures of CO is investigated theoretically and the results are compared with experiment. The temperature range includes the inversion temperatures for all mixtures. Thermal conductivity and diffusion coefficients are also calculated. The basis of the study is a previously presented theory which provides expressions for classical collision integrals for molecules with rotational structure in terms of spherical Ω^* integrals.

THERMAL DIFFUSION IN ISOTOPIC MIXTURES OF POLYATOMIC GASES. I. THE THERMAL DIFFUSION COEFFICIENT
M. Keith Matzen and D. K. Hoffman
J. Chem. Phys. 62, 500 (1975)

Abstract--Perturbation techniques are used to derive an analytical expression for the thermal diffusion coefficient for isotopic, polyatomic gas mixtures. The expansions isolate the contributions to the thermal diffusion coefficient which are subject to isotopic variation and elucidate the effect of external-fields on the phenomenon.

THERMAL DIFFUSION IN ISOTOPIC MIXTURES OF POLYATOMIC GASES. II. MODEL CALCULATIONS
M. Keith Matzen and D. K. Hoffman
J. Chem. Phys. 62, 509 (1975)

Abstract--Model calculations are used to study the dependence of the thermal diffusion coefficient on the molecular kinematic parameters for binary, isotopic mixtures of diatomic gases. The effects of a static magnetic field on thermal diffusion are also investigated. The basis of these studies is an analytic expression for $D_{\underline{a}}^{T}$ previously derived by perturbation techniques.

III. Atomic, Molecular, and Free Radical Crossed Beams Kinetics

THE A+$B_{\underline{x}}$ CONDENSATION REACTION: CROSSED NOZZLE BEAMS OF Br_2 AND $(Cl_2)_{\underline{x}}$ OR $(NH_3)_{\underline{x}}$ CLUSTERS

Richard Behrens, Jr., Andrew Freedman, Ronald R. Herm and Timothy P. Parr

J. Chem. Phys. 63, 4622 (1975)

Abstract--Nozzle beams of Br_2 and Cl_2 or NH_3 have been crossed in a molecular beam scattering apparatus; the Cl_2 or NH_3 beam contained $(Cl_2)_{\underline{x}}$ or $(NH_3)_{\underline{x}}$ clusters distributed such that the intensity of a given cluster, $F_{\underline{x}}$, decreased with increasing $\underline{x}$ for $1 \leq \underline{x} \leq \sim 50$. Mass, angular, and time-of-flight spectra of the scattered neutral species all establish that the $A + B_{\underline{x}} \rightarrow AB_{\underline{x}}^*$ bimolecular condensation reaction is being observed. However, working from the data, it is not possible to distinguish between detection of a long-lived $AB_{\underline{x}}^*$ metastable complex or of a decomposition product formed with low recoil velocity. Product angular distributions are confined to a small region of laboratory scattering angle Θ and peak at small but positive Θ ($\Theta = 0°$ and 90° defined by cluster and Br_2 beam directions, respectively). It is pointed out that this sharp peaking at small Θ is due to a number of experimental factors, including a Jacobian factor varying as $\sin^{-2}\Theta$, and should be a universal characteristic of such condensation reactions in crossed beams. In the data it is indicated that there will be a high probability of fragmentation into small daughter ions upon electron bombardment (EB) ionization of an $AB_{\underline{x}}$ or $B_{\underline{x}}$ cluster for the range in $\underline{x}$ most sensitive to the measurements ($\sim 10 \leq \underline{x} \leq \sim 50$). This in turn implies that the concentration of neutral clusters in the beam can be seriously underestimated if the cluster ion mass spectra produced by EB ionization of the nozzle beam are assigned assuming that fragmentation is inconsequential.

ELASTIC DIFFERENTIAL CROSS SECTIONS AND INTERMOLECULAR POTENTIALS FOR Ar+CH_4 AND Ar+NH_3

Richard Behrens, Jr., Andrew Freedman, Ronald R. Herm and Timothy P. Parr

Chem. Phys. Lett. 36, 446 (1975)

Abstract--Differential elastic cross sections are reported for CH_4 + Ar ($\underline{E} = \mu \underline{g}^2/2$ = 8.43 kJ/mole) and NH_3 + Ar ($\underline{E}$ = 8.31 kJ/mole) in the region of the rainbow angles. Quantum interference undulations are apparently observed as well for CH_4 + Ar and, possibly, NH_3 + Ar. The measurements are fit to spherically symmetric intermolecular potentials yielding well depths and equilibrium intermolecular separations of 1.32 kJ/mole and 3.82 Å for CH_4 + Ar and 1.32 kJ/mole and 3.92 Å for NH_3 + Ar.

SENSITIZED FLUORESCENCE IN CROSSED ATOMIC BEAMS: Hg($6^3\underline{P}_{0,2}$) + Tl($6^2\underline{P}_{1/2}$)

Lambert C.-H. Loh, Charlotte M. Sholeen, Ronald R. Herm and David D. Parrish

J. Chem. Phys. 63, 1980 (1975)

Abstract--A velocity selected Tl beam has been crossed by an electron-bombarded Hg beam which contains a small percentage of the Hg($6^3\underline{P}$) metastable levels (an approximate 5:1 ratio of $^3\underline{P}_2$:$^3\underline{P}_0$). By means of an interference filter-photomultiplier combination beneath the collision zone, the cross section for excitation of the 5350 Å ($7^2\underline{S}_{1/2} \rightarrow 6^2\underline{P}_{3/2}$)Tl fluorescence has been determined to increase monotonically with decreasing relative collision speed, $\underline{g}$, approximately as $\underline{g}^{-\underline{s}}$ for $\underline{s}$ = 2.0 ± 0.5. Implications of these results for the sensitized fluorescence phenomenon in vapor mixtures of metallic elements are briefly discussed.

IV. Mass Spectroscopy, Ion Source Chemistry

PHYSICAL INORGANIC ASPECTS OF MASS SPECTROMETRY
G. D. Flesch and H. J. Svec
M. Maccall, Ed. Int. Rev. of Science Physical Chemistry Series 2, Vol. 5, Chapter 2. (Lancaster, Great Britain: Medical and Technical Publishing Co., Ltd., 1975) pp. 47-88

Abstract--In a review which covers as broad a subject as indicated by the title, it is necessary to limit the scope of the survey and to avoid discussion of many, albeit interesting points. Our aim has been to survey examples of the various kinds of current research in the determination of physico-chemical parameters. To be included in this review the reports must have indicated that a mass spectrometer was an important experimental tool and that the research concerned some aspect of inorganic chemistry. We have surveyed reports appearing in research journals during the years 1971, 1972 and 1973. The instrumentation and techniques involved in obtaining the experimental data are emphasized rather than the data itself or the results of manipulation and/or interpretation of the data. Readers interested in the latter can take advantage of the extensive bibliographic references.

The various reports are grouped according to the physico-chemical quantity being determined. Although these various groupings are indicated well in the accompanying table of contents, nearly every grouping includes some studies of ion-molecule reactions. Thorough and authoritative discussions of every aspect of this subject have been presented in two recent books. Both are entitled "Ion-Molecule Reactions" and both are highly recommended to anyone seeking more detailed information about the subject.

THERMOCHEMISTRY OF VANADIUM OXYTRICHLORIDE AND VANADIUM OXYTRIFLUORIDE BY MASS SPECTROMETRY
Gerald D. Flesch and Harry J. Svec
Inorg. Chem. 14, 1817 (1975)

Abstract--Mass spectral and ionization efficiency data have been obtained for the positive and negative ions produced from $VOCl_3$ and VOF_3 by electron impact. From these data values have been calculated for several thermochemical parameters (eV): $IP_v(VOCl_3) = 11.90 \pm 0.05$, $IP_v(VOF_3) = 13.88 \pm 0.05$, $EA(VOCl_3) \geq 3.6$, $EA(VOF_3) = 3.1 \pm 0.3$, and $\Delta H_{f298}(VOF_3(g)) = -12.8 \pm 0.3$. Less precise values for these same parameters have been calculated for the observed positive and negative ion fragments and for the neutral fragments inferred to be produced in the mass spectrometer ion source. Bond energies (eV) are estimated to be $\overline{D}(V-O)_{VOCl_3} = 5.5$, $\overline{D}(V-Cl)_{VOCl_3} = 4.4$, $\overline{D}(V-F)_{VOF_3} = 5.8$. Bond energy values are also reported for the positive ion and neutral fragments.

USE OF OXYGEN ISOTOPE RATIOS IN CORRELATION OF TUFFS, EAST RUDOLF BASIN, NORTHERN KENYA
Thure E. Cerling, Donald L. Biggs and Harry J. Svec
Earth and Planetary Sci. Lett. 25, 291 (1975)

Abstract--Oxygen isotope determinations were made using CoF_3 to extract oxygen from 27 volcanic glass samples from the East Rudolf Basin, northern Kenya. Results show that the older tuffs are progressively enriched in ^{18}O and that this index can be used in the correlation of volcanic ash units. This method could not distinguish individual samples from the youngest units studied because their ranges of $\delta^{18}O$ overlap. The $\delta^{18}O$ values for the shards in the Tulu Bor Tuff, the KBS Tuff, the Koobi Fora Tuff and the Chari Tuff range from 14.5 to 16.4, from 8.9 to 9.5, from 6.6 to 7.0

to 7.2, respectively, in decreasing age. Determinations from pumice cobbles are consistently higher than the above values.

V. Molecular Bonding Theory

THE LMO DESCRIPTION OF MULTIPLE BONDING AND MULTIPLE LONE PAIRS
Walter England
J. Chem. Educ. 52, 427 (1975)

Abstract--The LMO valence description for multiple lone pairs and multiple bonding was presented due to its variance with classical valence orbital hybridization.

LOCALIZED CHARGE DISTRIBUTIONS. VII. TRANSFERABLE LOCALIZED MOLECULAR ORBITALS FOR ACYCLIC HYDROCARBONS
Walter England, Mark S. Gordon and Klaus Ruedenborg
Theoret. Chim. Acta 37, 177 (1975)

Abstract--A localized molecular orbital has been found to extend slightly and regularly into regions away from the chemical bond which contains most of its charge cloud. This was made the basis for a method of transferring localized orbitals among similar molecules. Each localized orbital induces a set of so-called molecule invariant fragments consisting of one bond fragment and collections of geminal fragments, vicinal fragments, and third and fourth neighbor fragments. Localized orbital expansion coefficients in a hybrid basis can be calculated for these molecule invariant fragments without solving any equations or performing any laborious computations.

The present work is an application to acylic hydrocarbons. The result are based on the analysis of 33 INDO-SCF molecular orbital wavefunctions

in the localized representation. Computational methods for obtaining close approximations to localized orbitals are also discussed. The application of a suggested pseudo-eigenvalue localization method and its accompanying self-consistent iteration process are found to not converge.

THE NATURE OF THE CHEMICAL BOND, AN ENERGETIC VIEW
Klaus Ruedenberg
Localization and Delocalization in Quantum Chemistry Vol. 1, O. Chalvet et al. (eds) D. Reidel Publishing Company; Dordrecht, Holland (1975) pp. 223-245

Abstract--The energy of the hydrogen molecule ion system is analyzed for all internuclear distances in order to understand why it is lower at the distance of two Bohr radii (the equilibrium distance) than at infinite separation. The peculiar behavior of the kinetic and potential binding energies as functions of the internuclear distance is elucidated by resolving these curves into additive superpositions of five contributions which are simple functions of the internuclear distance. The quantitative behavior of these contributions is straightforwardly explained in terms of physical interactions and through an examination of the variational process. The analysis leads to the interpretative concepts of Promotion, Interference and Quasiclassical Electrostatic Interactions, and it identifies those effects which are essential for the formation of the chemical bond in H_2^+. The covalent bond is shown to arise from delocalization through electron sharing.

Analysis

I. Analytical Spectroscopy

INDUCTIVELY COUPLED PLASMA-OPTICAL EMISSION SPECTROMETRY: APPLICATION TO THE DETERMINATION OF ALLOYING AND IMPURITY ELEMENTS IN LOW AND HIGH ALLOY STEELS

Constance C. Butler, Richard N. Kniseley and Velmer A. Fassel
Anal. Chem. 47, 825 (1975)

Abstract--Three different inductively coupled plasma-optical emission spectrometry (ICP-OES) systems have been used for the determination of residual impurities and alloying constituents in solutions of high and low alloy steels of widely varying composition. The results of these studies show that the presence of an iron matrix does not influence the detection limits for the 12 elements studied and that these elements can be determined at fractional ppm levels without prior chemical concentration. The analytical calibrations were established with synthetic reference solutions and the resulting analytical curves exhibited linearity over three to four orders of magnitude. The relative standard deviations determined over an extended period of time ranged from ~0.01 to ~0.07.

SPECTROSCOPIC FLAME TEMPERATURE MEASUREMENTS AND THEIR PHYSICAL SIGNIFICANCE—III. EXISTENCE OF ISOTHERMAL ZONES IN SOME LABORATORY FLAMES

Isaac Reif, Velmer A. Fassel and Richard N. Kniseley
Spectrochim. Acta 30B, 163 (1975)

Abstract--For the accurate measurement of certain atomic and molecular properties, such as absolute or relative transition probabilities,

dissociation energies and optical cross sections, it is desirable to form and observe atoms and molecules in an isothermal environment whose temperature can be measured precisely. In this paper it is shown that a premixed N_2O-C_2H_2 flame burning on a long path, slot burner can provide not only a relatively high temperature (~3000 K) but also an isothermal environment as well. In this flame, well developed atomic emission spectra of all the metallic elements may be readily observed. This flame and burner system should therefore be useful for the determination of more accurate relative transition probabilities for many elements.

INDUCTIVELY COUPLED PLASMA-OPTICAL EMISSION SPECTROSCOPY. EXCITATION TEMPERATURES EXPERIENCED BY ANALYTE SPECIES
Dennis J. Kalnicky, Richard N. Kniseley and Velmer A. Fassel
Spectrochim. Acta 30B, 511 (1975)

Abstract--Spatially resolved, radical excitation temperature distributions experienced by analyte species injected into the axial channel of a toroidally shaped, inductively coupled argon plasma are presented. Typical axial temperatures experienced by the thermometric species (FeI) ranged from 6500 K to 5500 K in the analytical zone of 15-25 mm above the load coil. A comparison of temperatures calculated with different sets of transition probabilities is also given.

X-RAY EXCITED-OPTICAL LUMINESCENCE OF LANTHANIDES IN PHOSPHORS PREPARED FROM YTTRIUM OXIDE AND IRON TRANSITION-GROUP OXIDES: APPLICATION TO THE DETERMINATION OF LANTHANIDES IN IRON AND ITS ALLOYS
Edward L. DeKalb and Velmer A. Fassel
Anal. Chem. 47, 2354 (1975)

Abstract--A series of new phosphors has been prepared using yttrium oxide and the oxides of the iron transition group elements. These phosphors

when excited by x-ray radiation are strongly luminescent in the visible spectral region if the oxides of the iron-group oxides contain lanthanide elements. These phosphors have been used for the determination of several lanthanides at the ppm level in iron and several of its alloys.

INDUCTIVELY COUPLED PLASMA-OPTICAL EMISSION ANALYTICAL SPECTROMETRY. A STUDY OF SOME INTERELEMENT EFFECTS
George F. Larson, Velmer A. Fassel, Robert H. Scott and Richard N. Kniseley
Anal. Chem. 47, 238 (1975)

Abstract--Investigations of the extent to which certain interelement or interference effects occur in an inductively-coupled plasma are reported. Under conditions normally employed for analytical purposes, it is shown that: a) two solute vaporization interferences often observed in flames are eliminated or reduced to negligible proportions in the plasma; b) increasing concentrations of an easily ionizable element (Na) up to concentrations of 6900 μg/ml exerted an unusually low influence on the observed emission intensities of three selected elements (Ca, Cr, and Cd) of widely differing degrees of ionization. The high degree of freedom from interelement effects of this analytical technique is further documented by the observation that a variety of matrices did not affect the emission intensity of Mo to a significant extent.

THE RARE EARTH ELEMENTS
Richard N. Kniseley, Constance C. Butler and Velmer A. Fassel
John A. Dean and Theodore C. Rains, eds., Flame Emission and Atomic Absorption Spectrometry Vol. 3--Elements and Matrices (New York: Marcel Dekker, Inc., 1975) pp. 116-135

Abstract-- The unique similarity in the chemical properties of the rare earth group of elements has led to reliance on measurements of physical properties in order to obtain analytical data on mixtures of these elements.

Various spectroscopic techniques have proven to be very useful, and among these optical emission spectroscopy has been the most widely used. However, the arc and spark emission spectra of many of the rare earth elements are very complex and often consist of thousands of lines. As a result, line interferences are frequent and, even when high-dispersion instruments are used, interference-free lines are often difficult to find. As a result, investigators were led to explore the analytical capabilities of conventional flames because the less energetic excitation conditions found in these sources generally produce spectra which are much less complex.

II. Analytical Separations

CHROMATOGRAPHIC DETERMINATION OF PHENOLS IN WATER
Colin D. Chriswell, Richard C. Chang and James S. Fritz
Anal. Chem. 47, 1325 (1975)

Abstract--Phenols in natural waters and treated drinking water are determined by sorption on macroporous anion-exchange resin, elution with acetone, and measurement by gas chromatography. Techniques are given for preventing phenol losses caused by chlorination, oxidation, and other reactions during their determination. Common inorganic ions and many organic substances cause no interference; neutral organics that are retained by the resin can be removed by a methanol wash. The method gives accurate results for phenol, alkyl-, and chloro-substituted phenols in the ppb to ppm concentration range.

CONCENTRATING ORGANIC IMPURITIES FROM TRACE LEVELS
James S. Fritz
Industrial & Engineering Chemistry Product Research & Development 14, 94 (1975)

Abstract--Macroporous resins are used to concentrate low concentrations of organic impurities from water. Applications of macroporous resins in the sorption and gas chromatographic separation of inorganic gases and organic vapors are described. The effect of the chemical structure of a resin on its sorption affinity for various organic compounds is defined.

EXTRACTION OF METAL IONS WITH N,N-DISUBSTITUTED AMIDES
James S. Fritz and Gene M. Orf
Anal. Chem. 47, 2043 (1975)

Abstract--In this paper, liquid alkyl amides are studied as solvents for liquid-liquid extraction of metal ions. Feder first showed that N,N-dibutylacetamide is roughly comparable to tributylphosphate as an extractant for uranyl nitrate. Siddall extended the work of Feder and studied the effects of altering the hydrocarbon substituents of the amide molecule on the extraction of U(VI), Pu(IV), Pu(VI), Np(VI), Th(IV), Zr(IV), and HNO_3 from nitric acid solution. The thermal stability of amides was shown to be comparable to that of tributylphosphate and the hydrolytic stability of amides on solvent extraction about the same as TBP. Several other brief reports deal with substituent effects of amides on solvent extraction of several metal ions.

All of the previous work with amides as extractants has been on the extraction of actinide metal nitrates, zirconium nitrate, and on the extraction of nitric acid itself. The purpose of the present work is to extend the study of the extracting power of amides to several other metal ions from nitrate

solution, to study the extracting power of amides on several metal ions from perchlorate solution where the mechanism of extraction is entirely different from that in nitrate solution, and to examine the possible use of amides as reagents for analytical separations.

ULTRAVIOLET SPECTRA OF METAL IONS IN 6M HYDROCHLORIC ACID
Louise Goodkin, Mark D. Seymour and James S. Fritz
Talanta 22, 245 (1975)

Abstract--Ultraviolet absorption spectra of 66 metal ions in aqueous 6M hydrochloric acid were recorded and the spectra of 36 metal ions that absorb appreciably are reported. The absorption of these metal ions is sufficient to permit their detection in liquid chromatography.

ANALYSIS OF VARIOUS IOWA WATERS FOR SELECTED PESTICIDES: ATRIZINE, DDE, AND DIELDRIN--1974
John J. Richard, Gregor A. Junk, Michael J. Avery, Nancy L. Nehring, James S. Fritz and Harry J. Svec
Pesticides Monitoring J. 9, 117 (1975)

Abstract--Atrazine, DDE, and dieldrin were extracted and concentrated from various surface, subsurface, and finished waters using the macroreticular resin method. Organic components in the concentrates from these waters were separated by gas chromatography; the amounts of the three pesticides in the waters ranged from 0.5 to 42,000 parts per trillion by weight. Every major watershed in the State of Iowa revealed some degree of pesticide contamination and seasonal variations were consistent with agricultural runoff models. Atrazine concentrations were highest of the three pesticides, a symptom of its widespread use in the corn belt. DDE also appeared in substantial quantities, providing further evidence of the persistence of DDT and its metabolites. Water from several shallow wells and finished water from

many water treatment plants were also contaminated. Current treatment processes do not effectively remove these pesticides.

THERMOCHEMISTRY OF VANADIUM OXYTRICHLORIDE AND VANADIUM OXYTRIFLUORIDE BY MASS SPECTROMETRY
Gerald D. Flesch and Harry J. Svec
Inorg. Chem. 14, 1817 (1975)

Abstract--Mass spectral and ionization efficiency data have been obtained for the positive and negative ions produced from $VOCl_3$ and VOF_3 by electron impact. From these, data values have been calculated for several thermochemical parameters (eV): $IP_v(VOCl_3) = 11.90 \pm 0.05$, $IP_v(VOF_3) = 13.88 \pm 0.05$, $EA(VOCl_3) \geq 3.6$, $EA(VOF_3) = 3.1 \pm 0.3$, and $\Delta H_{f298}(VOF_3(g)) = -12.8 \pm 0.3$. Less precise values for these same parameters have been calculated for the observed positive and negative ion fragments and for the neutral fragments inferred to be produced in the mass spectrometer ion source. Bond energies (eV) are estimated to be $\overline{D}(V-O)_{VOCl_3} = 5.5$, $\overline{D}(V-Cl)VOCl_3 = 4.4$, $\overline{D}(V-O)_{VOF_3} = 5.9$, and $\overline{D}(V=F)_{VOF_3} = 6.8$. Bond energy values are also reported for the positive ion and neutral fragments.

III. Activation Analysis

COUNTING ALPHA PARTICLES FROM THE ^6Li+n REACTION BY TRACK-ETCH METHODS
Paul B. Hahn, Margaret A. Wechter and Adolf F. Voigt
Nucl. Instruments and Methods 123, 111 (1975)

Abstract--The track etch-spark counting technique using thin cellulose nitrate films has been demonstrated to be successful for measuring approxim

2 MeV alpha particles from a ^{210}Po alpha source and from the $^{6}Li(n,\alpha)^{3}H$ reaction. Precision of measurement was found to approach that of counting statistics and the linearity of response extended to approximately 2000 spark counts/cm^2 of detector film. The potential application of the technique to a surface activation analysis by the (n,α) reaction was investigated by irradiating ^{6}LiF thermoluminescence detector crystals in a neutron flux using an evacuated irradiation chamber.

IV. Lasers in Analytical Chemistry

ANALYTICAL LINES FOR LONG-PATH INFRARED ABSORPTION SPECTROMETRY OF AIR POLLUTANTS
Bruce M. Golden and Edward S. Yeung
Anal. Chem. 47, 2132 (1975)

Abstract--A scheme for selecting resonant frequencies for the analysis of gaseous air pollutants using long-path absorption of narrow-band infrared sources is presented. A computer search is conducted using existing spectrometric data to determine lines with minimum interference and maximum sensitivity. Results are given for the pollutants O_3, N_2O, CO, CH_4, and the nonpolluting species, H_2O and CO_2.

NON-ADIABATIC VIBRONIC INTERACTIONS AND THE RAMAN EFFECT
Gerald J. Small and E. S. Yeung
Chem. Phys. 9, 379 (1975)

Abstract--The role of non-adiabatic interactions in vibronically induced Raman scattering processes is examined for both the pre-resonance and resonance regimes. Attention is focused on the class of molecules whose

linear electron-vibration coupling strengths are characteristic of the larger poly-atomics, e.g., the benzenoid aromatics. Various approximations are introduced to simplify the general theory and the applicability of each is discussed. It is shown that for randomly oriented scatterers the non-adiabatic contribution to induced scattering in the pre-resonance regime is of minor importance relative to the adiabatic contribution. For oriented scatterers, e.g., molecular crystals, some control over the non-adiabatic contribution can be achieved through choice of polarization conditions. For resonance Raman scattering it is shown that the non-adiabaticity can play an important role in vibronically induced scattering processes.

PRE-RESONANCE RAMAN INTENSITIES
Edward S. Yeung, Michael Heiling and Gerald J. Small
Spectrochim. Acta 31A, 1921 (1975)

Abstract--A series expansion for the sum over the vibrational levels of an intermediate electronic state, which occurs in the dispersion theory of the Raman effect, is presented. The convergence properties of the series, as a function of electron-vibration coupling strength and exciting photon energy, have been studied for many model systems which span the range between rigid and diatomic-like molecules. Both Condon type fundamental and overtone transitions and vibronically induced transitions are considered. The single most important result is that the leading term of the above series represents a good approximation to the exact sum up to ca. 3000 cm^{-1} from resonance with the intermediate electronic state for Raman fundamentals. It should be possible, therefore, to study excited state geometries by pre-resonance Raman spectroscopy. The theory also shows that the Condon and vibronic

coupling mechanisms exhibit very different dependences on the exciting photon frequency. The corresponding series for Raman overtones has poorer convergence properties. In particular, it is shown that for the general case, frequency changes in excited states are as important as geometry changes in inducing overtone intensities.

PRESSURE-BROADENED LINEWIDTHS OF NITROGEN DIOXIDE
G. D. T. Tejwani and Edward S. Yeung
J. Chem. Phys. 63, 4562 (1975)

Abstract--N_2-, O_2-, and self-broadened linewidths of nitrogen dioxide for a wide range of quantum numbers N and K_a, for both type A and type B bands, have been calculated using the Anderson-Tsao-Curnutte theory of line broadening. For self-broadened linewidths of NO_2, dipole-dipole, dipole-quadrupole, quadrupole-dipole, and quadrupole-quadrupole interactions have been taken into account. Dipole-quadrupole and quadrupole-quadrupole interactions were included in foreign-gas (N_2 and O_2) broadened linewidth computations. The molecular quadrupole moment tensor of NO_2 was taken from Rothenberg and Schaefer. Air-broadened linewidths of NO_2 at 200 K have also been calculated, so that the temperature dependence can be established.

PRESSURE-BROADENED LINEWIDTHS OF OZONE
G. D. T. Tejwani and Edward S. Yeung
J. Chem. Phys. 63, 1513 (1975)

Abstract--Self-broadened and foreign-gas (N_2 and O_2) broadened linewidths of O_3 at 300°K for a wide range of quantum numbers J and K_a, for both type A and type B bands, have been calculated using the Anderson-Tsao-Curnutte theory of line broadening. In the case of O_3-O_3 collisions, dipole-dipole, dipole-quadrupole, quadrupole-dipole, and quadrupole-quadrupole

interactions were taken into account. Good agreement was obtained between the available measured linewidths and the computed values for corresponding transitions on using the molecular quadrupole moments of O_3 given by Rothenberg and Schaefer. Air-broadened linewidths of O_3 at 200°K have also been computed, so that the temperature dependence can be established.

EC-04-04

Mathematical and Computer Sciences

EC-04-04-01

Mathematical Sciences

APPELL'S FUNCTION $\underline{F}_4$ AS A DOUBLE AVERAGE
B. C. Carlson
SIAM J. Math. Anal. 6, 960 (1975)

Abstract--A quadratic transformation of a double hypergeometric series of order two (Appell's $\underline{F}_4$ with equal denominator parameters) into a series of order three revives longstanding doubts about the accepted classification by order. Both series can be represented as double Dirichlet averages of $\underline{x}^{\underline{t}}$. Appell's $\underline{F}_4$ with unrestricted parameters can be represented as such an average with two rows and three columns. There are six cases in which a restriction on the parameters reduces the number of columns to two.

INVARIANCE OF AN INTEGRAL AVERAGE OF A LOGARITHM
B. C. Carlson
Am. Math. Monthly 82, 379 (1975)

No abstract available.

INTERNAL DISTRIBUTION

E. W. Anderson
R. J. Angelici
R. G. Barnes
R. G. Bautista
M. F. Berard
L. E. Burkhart
G. Burnet
B. C. Carlson
O. N. Carlson
O. L. Chapman
C. W. Chen
P. Chiotti
J. C. Clardy
J. R. Clem
B. C Cook
J. D Corbett
H. B. Crawley
G. C. Danielson
N. Dean
J. H. Espenson
V. A. Fassel
D. K. Finnemore
A. Firestone
H. F. Franzen
J. S. Fritz
R. Fuchs
B. C. Gerstein
K. A. Gschneidner
C. L. Hammer
R. S. Hansen
R. R. Herm
J. C. Hill
L. Hodges
D. K. Hoffman
O. Hunter
R. A. Jacobson
F. X. Kayser
R F. Keller
W. J. Kernan
K. L. Kliewer
R. C. Lamb
R. J. Lambert
K. E. Lassila
R. A. Leacock
S. Legvold
S. H. Liu
D. W. Lynch
R. E. McCarley
C. G. Maple
D. S. Martin
J. J. O'Toole
D. Parker
D. T. Peterson
J. E. Powell
D. L. Pursey
K. Ruedenberg
W. C. Schick
T. E. Scott
H. R. Shanks
H. Skank
G. J. Small
J. F. Smith
F. H. Spedding
C. Stassis
W. Struve
H. J. Svec
C. A. Swenson
W. L. Talbert
J. G. Traylor
R. K. Trivedi
D. Ulrichson
J. Vary
J. D. Verhoeven
A. F. Voigt
M. S. Wechsler
D. R. Wilder
H. A. Wilhelm
S. A. Williams
F. K. Wohn
E. Wolf
C. T. Wright
E. S. Yeung
B.-L. Young

EXTERNAL DISTRIBUTION

Dr. Harold Agnew, Director
Los Alamos Scientific Laboratory
P.O. Box 1663
Los Alamos, NM 87545

Dr. Stanley W. Ahrends
Deputy Director for Projects
Division of Reactor Research and
Development--USERDA
Washington, D.C. 20545

Dr. Robert F. Allnutt
Office of the Assistant Administrator
for Administration--USERDA
Washington, D.C. 20545

Dr. Edward Alpen
Pacific Northwest Laboratory
P.O. Box 999
Richland, WA 99352

Dr. David Ballantine
Division of Biomedical and
Environmental Research--ERDA
Washington, D.C. 20545

Mr. Robert W. Barber, Director
Reactor Safety Research
Coordination--USERDA
Washington, D.C. 20545

Dr. George W. Barrow, Director
Division of Administrative
Services--USERDA
Washington, D.C. 20545

Dr. Roger E. Batzel
Lawrence Livermore Laboratory
P.O. Box 808
Livermore, CA 94550

Dr. Douglas C. Bauer, Director
Division of Nuclear Research and
Applications--USERDA
Washington, D.C. 20545

Dr. Robert H. Bauer, Manager
USERDA--Chicago Operations Office
9800 South Cass Avenue
Argonne, IL 60439

Dr. Donald Beattie
Deputy Assistant Administrator for
Geothermal and Advanced Energy
USERDA
Washington, D.C. 20545

Dr. John Belding
Asst. Director for Energy
Conversion
Division of Conservation Research
and Technology--USERDA
Washington, D.C. 20545

Rep. Berkley W. Bedell
503 Cannon (HOB)
Washington, D.C. 20515

Dr. Martin B. Biles, Director
Division of Operational Safety
USERDA
Washington, D.C. 20545

Dr. Eugene R. Bissell
Chemistry Department, L-402
Lawrence Livermore Laboratory
P.O. Box 808
Livermore, CA 94550

Dr. A. Wade Blackman
Deputy Assistant Administrator
Planning and Analysis--USERDA
Washington, D.C. 20545

Dr. H. Richard Blieden
Asst. Director for Solar Electric Application
Division of Solar Energy--ERDA
Washington, D.C. 20545

Rep. Michael T. Blouin
1118 Longworth (HOB)
Washington, D.C. 20515

Mr. D. E. Bost
USERDA--TIC
P.O. Box 62
Oak Ridge, TN 37830

Mr. Marion A. Bowden, Director
Office of Equal Opportunity
USERDA
Washington, D.C. 20545

Maj. Gen. Joseph K. Bratton
Director, Division of Military Application--USERDA
Washington, D.C. 20545

Mr. John J. Brogan, Acting Director
Division of Transportation Energy Conservation--USERDA
Washington, D.C. 20545

Col. T. W. Buttery
Mathematics and Analysis Branch
Division of Physical Research--ERDA
Washington, D.C. 20545

Mr. H. Hollister Cantus, Director
Office of Congressional Relations
USERDA
Washington, D.C. 20545

Mr. A. A. Churm, Director
Patent Division--USERDA
Chicago Operations Office
9800 South Cass Avenue
Argonne, Il. 60439

Senator Dick Clark
404 Russell (SOB)
Washington, D.C. 20510

Dr. J. S. Coleman
Asst. Director for Program Planning
Division of Physical Research--ERDA
Washington, D.C. 20545

Dr. John W. Crawford
Assistant Director of Reactor Research and Development--ERDA
Washington, D.C. 20545

Senator John C. Culver
1327 Dirksen (SOB)
Washington, D.C. 20510

Dr. H. Neal Dunning, Acting Director
Division of Oil, Gas and Shale Technology--USERDA
Washington, D.C. 20545

Dr. Charles W. Edington
Deputy Associate Director for Research and Development Programs
Division of Biomedical and Environmental Research--USERDA
Washington, D.C. 20545

Dr. S. G. English, Assoc. Director
Division of Physical Research--ERDA
Washington, D.C. 20545

Dr. Robert P. Epple
Solid State Physics & Materials Chemistry Branch
Division of Physical Research--ERDA
Washington, D.C. 20545

ERDA Library
20 Massachusetts Avenue
Washington, D.C. 20545

Mr. John Fallon, Special Assistant
Office of the Asst. Administrator for Planning and Analysis--USERDA
Washington, D.C. 20545

Dr. R. Franklin
Division of Biomedical and Environmental Research--USERDA
Washington, D.C. 20545

Mr. Jack Frazer
Lawrence Livermore Laboratory
P.O. Box 808--Mail Stop L-401
Livermore, CA 94550

Dr. Steven I. Freedman
Asst. Director for Power and Combustion
Division of Coal Conversion and Utilization--USERDA
Washington, D.C. 20545

Dr. Robert W. Fri
Deputy Administrator
USERDA
Washington, D.C. 20545

Mr. D. M. Gardiner, Director
Technical Services--USERDA
Chicago Operations Office
9800 South Cass Avenue
Argonne, IL 60439

Mr. A. Giambusso
Deputy Assistant Administrator
Office of the Asst. Adm. for International Affairs--USERDA
Washington, D.C. 20545

Dr. Edward B. Giller
Deputy Assistant Administrator for National Security--USERDA
Washington, D.C. 20545

Dr. Neal Goldenberg, Chief
Division of Space Nuclear Systems--USERDA
Washington, D.C. 20545

Dr. S. William Gouse
Deputy Assistant Administrator for Fossil Energy--USERDA
Washington, D.C. 20545

Mr. Lloyd W. Grable
Director of Personnel
USERDA
Washington, D.C. 20545

Rep. Charles Grassley
2434 Rayburn (HOB)
Washington, D.C. 20515

Mr. M. C. Greer, Controller
Office of the Controller
USERDA
Washington, D.C. 20545

Mr. Samuel L. Hack, Director
Division of Facilities and Construction Management--USERDA
Washington, D.C. 20545

Mr. Ernest C. Hardin, Jr.
Director, Internal Review
USERDA
Washington, D.C. 20545

Rep. Thomas Harkin
514 Cannon (HOB)
Washington, D.C. 20515

Dr. Walter J. Haubach
Molecular Sciences
Division of Physical Research--ERDA
Washington, D.C. 20545

Mr. Austin N. Heller
Assistant Administrator of Conservation--USERDA
Washington, D.C. 20545

Dr. H. T. Herrick, Director
Division of Labor Relations--ERDA
Washington, D.C. 20545

Dr. Bernard Hildebrand, Chief
Physics Research Branch
Division of Physical Research--ERDA
Washington, D.C. 20545

Dr. Robert L. Hirsch, Director
Division of Controlled Thermonuclear Research--USERDA
Washington, D.C. 20545

Mr. Hal Hollister, Director
Division of Environmental Control Technology--USERDA
Washington, D.C. 20545

Dr. Louis C. Ianniello, Chief
Metallurgy and Ceramics Branch
Division of Physical Research--ERDA
Washington, D.C. 20545

Dr. William D. Jackson
Acting Director, MHD
USERDA
Washington, D.C. 20545

Mr. Harry R. Johnson, Director
Office of Program Planning and Analysis--USERDA
Washington, D.C. 20001

Mr. R. Tenney Johnson
General Counsel
Office of the General Counsel--ERDA
Washington, D.C. 20545

Dr. R. J. Kandel
Office for Molecular Sciences
Division of Physical Research--ERDA
Washington, D.C. 20545

Dr. James S. Kane
Deputy Assistant Administrator for Conservation--USERDA
Washington, D.C. 20545

Mr. John W. King
Director of Public Affairs
USERDA
Washington, D.C. 20545

Dr. H. L. Kinney
Special Assistant to the Director
Division of Physical Research--ERDA
Washington, D.C. 20545

Dr. Edwin E. Kintner
Deputy Director
Division of Controlled Thermonuclear Research--USERDA
Washington, D.C. 20545

Dr. John Kirby-Smith
Division of Biomedical and Environmental Research--USERDA
Washington, D.C. 20545

Dr. Chalmer Kirkbride
Science Advisor to the Administrator
USERDA
Washington, D.C. 20545

Mr. Martin A. Langsam
Senior Contract Administrator
USERDA--Chicago Operations Office
9800 South Cass Avenue
Argonne, IL 60439

Dr. Roger W. A. LeGassie
Assistant Administrator for Planning and Analysis--USERDA
Washington, D.C. 20545

Dr. James L. Liverman
Assistant Administrator for Environment and Safety--USERDA
Washington, D.C. 20545

Miss Elizabeth Lockridge
Division of Biomedical and Environmental Research--ERDA
Washington, D.C. 20545

Mr. Harvey E. Lyon, Director
Safeguards and Security--ERDA
Washington, D.C. 20545

Dr. Sidney Marks, Director
Division of Biology and Environmental Research--USERDA
Washington, D.C. 20545

Dr. Joseph V. Martinez
Molecular Sciences
Division of Physical Research--ERDA
Washington, D.C. 20545

Mr. H. H. Marvin
Director of Solar Energy--ERDA
Washington, D.C. 20545

Dr. Daniel R. Miller, Acting Director
Division of Physical Research--ERDA
Washington, D.C. 20545

Mr. Harold Miller
Chicago Operations Office-ERDA
9800 South Cass Avenue
Argonne, IL 60439

Dr. G. Alexander Mills, Director
Division of Fossil Energy Research
USERDA
Washington, D.C. 20545

Mr. George F. Murphy, Jr.
Executive Director
Joint Committee on Atomic Energy
Room H403, U.S. Capitol Building
Washington, D.C. 20515

Dr. Walter Nervik
Chemistry Department
Lawrence Livermore Laboratory
P.O. Box 808
Livermore, CA 94550

Dr. Glen A Newby, Acting Director
Division of Space Nuclear Systems
USERDA
Washington, D.C. 20545

General Edmund F. O'Connor
Deputy Assistant Administrator for Nuclear Energy--USERDA
Washington, D.C. 20545

Dr. Charles L. Osterberg
Manager of Environmental Problems
Division of Biomedical and Environmental Research--USERDA
Washington, D.C. 20545

Mr. Francis F. Parry, Director
Division of Electric Energy Systems
USERDA
Washington, D.C. 20545

Dr. Picha, Director
Division of University and Manpower Development Programs--ERDA
400 First Street N.W.
Washington, D.C. 20545

Dr. Elliott S. Pierce
Assistant Director for Molecular Sciences
Division of Physical Research--ERDA
Washington, D.C. 20545

Dr. Herman Postma, Director
Holifield National Laboratory
P.O. Box X
Oak Ridge, TN 37830

Mr. Hudson B. Ragan
Deputy General Counsel
Office of the General Counsel--ERDA
Washington, D.C. 20545

Mr. Leonard Rawicz
Deputy General Counsel
Office of the General Counsel--ERDA
Washington, D.C. 20545

Dr. Dennis W. Readey
Metallurgy and Ceramics Branch
Division of Physical Research--ERD,
Washington, D.C. 20545

Mr. George Rial, Director
Fossil Demonstration Plants
USERDA
Washington, D.C. 20545

Mr. David M. Richman
Molecular Sciences
Division of Physical Research--ERDA
Washington, D.C. 20545

Adm. H. G. Rickover, USN
Director, Naval Reactors
USERDA
Washington, D.C. 20545

Dr. E. T. Ritter
Division of Physical Research--ERDA
Washington, D.C. 20545

Dr. Harry F. Rizzo
Chemistry Department, L-402
Lawrence Livermore Laboratory
P.O. Box 808
Livermore, CA 94550

Dr. Richard Roberts
Assistant Administrator for
Nuclear Energy--USERDA
Washington, D.C. 20545

Dr. George L. Rogosa
Assistant Director for
Nuclear Sciences
Division of Physical Research--ERDA
Washington, D.C. 20545

Mr. R. G. Romatowski
Assistant Administrator for
Administration--USERDA
Washington, D.C. 20545

Dr. Milton E. Rose, Chief
Mathematics & Analysis Branch
Division of Physical Research--ERDA
Washington, D.C. 20545

Dr. Donald Ross, Chief
Health Protection Branch
Division of Operational Safety--ERDA
Washington, D.C. 20545

Dr. Barney Rubin
Chemistry Department
Lawrence Livermore Laboratory
P.O. Box 808
Livermore, CA 94550

Dr. Robert G. Sachs, Director
Argonne National Laboratory
9700 South Cass Avenue
Argonne, IL 60439

Dr. Maxine L. Savitz, Director
Division of Buildings & Industry--ERDA
Washington, D.C. 20545

Mr. M. H. Schwartz, Director
Division of Management Information
and Telecommunications--USERDA
Washington, D.C. 20545

Mr. N. F. Seivering, Jr.
Assistant Administrator for
International Affairs--USERDA
Washington, D.C. 20545

Dr. Andrew M. Sessler, Director
University of California
Lawrence Berkeley Laboratory
Berkeley, CA 94720

Mr. D. W. Short
Schenectady Naval Reactor Office
USERDA
Schenectady, NY 12301

Dr. Farwell Smith, Director
Office of Industry and State and Local
Government Relations--USERDA
Washington, D.C. 20545

Dr. Joseph L. Smith, Director
Division of Procurement--USERDA
Washington, D.C. 20545

Rep. Neal Smith
2373 Rayburn (HOB)
Washington, D.C. 20515

Dr. Alfred D. Starbird
Assistant Administrator for
National Security--USERDA
Washington, D.C. 20545

Dr. Richard Stephens
Office of University Programs--
USERDA
400 1st Street, N.W.
Washington, D.C. 20545

Mrs. Virginia Sternberg, Librarian
Westinghouse Electric Corporation
Bettis Atomic Power Laboratory
Box 79
West Mifflin, PA 15122

Dr. D. K. Stevens
Assistant Director for
Materials Sciences
Division of Physical Research--ERDA
Washington, D.C. 20545

Dr. F. D. Stevenson
Chemical & Atomic Physics Branch
Division of Physical Research--ERDA
Washington, D.C. 20545

Dr. P. Stevenson, L-232
Lawrence Livermore Laboratory
University of California
P.O. Box 808
Livermore, CA 94550

USERDA--TIC
P.O. Box 62
Oak Ridge, TN 37830

USERDA
Pittsburgh Naval Reactors Office
P.O. Box 1069
Schenectady, NY 12301

Mr. J. Vanderryn, Director
International Research and Development Programs
Office of Asst. Adm. for International Affairs--USERDA
Washington, D.C. 20545

Dr. George H. Vineyard, Director
Brookhaven National Laboratory
Upton, Long Island, NY 11973

Dr. W. A. Wallenmeyer
Assistant Director for High Energy Physics
Division of Physical Research--ERDA
Washington, D.C. 20545

Dr. H. R. Wasson
Physical and Technological Programs
Division of Biomedical and Environmental Research--ERDA
Washington, D.C. 20545

Dr. J. Wade Watkins
Acting Director
Division of Oil, Gas and Shale Technology--USERDA
Washington, D. C. 20545

Dr. Philip White
Assistant Administrator of
Fossil Energy--USERDA
Washington, D.C. 20545

Dr. Eric H. Willis, Director
Division of Geothermal Energy
USERDA
Washington, D.C. 20545

Dr. Robert R. Wilson, Director
Fermilab
P.O. Box 500
Batavia, IL 60510

Dr. Mark Wittels, Chief
Solid State Physics and Materials
Chemistry
Division of Physical Research--ERDA
Washington, D.C. 20545

Dr. Michael I. Yarymovych
Assistant Administrator of
Laboratory & Field Coordination
USERDA
Washington, D C. 20545

Dr. Raymond L. Zahradnik, Director
Division of Coal Conversion and
Utilization--USERDA
Washington, D.C. 20001

Mr. Robert L. Zanetell
Acting Deputy Controller
Office of the Controller--ERDA
Washington, D.C. 20545